

RETURNING MATERIALS:
Place in book drop to remove this checkout from your record. FINES will be charged if book is returned after the date stamped below.

GALLERY AND SURFACE PROPERTIES OF LAYERED DOUBLE HYDROXIDES

Ву

Kevin Julius Martin

A DISSERTATION

Submitted to

Michigan State University

in partial fulfillment of the requirements

for the degree of

DOCTOR OF PHILOSOPHY

Department of Chemistry

1986

ABSTRACT

MOLKIN

GALLERY AND SURFACE PROPERTIES OF LAYERED DOUBLE HYDROXIDES

By

Kevin Julius Martin

Layered double hydroxides (LDHs) are a class of compounds of general formula [M(II)_{1-x}M(III)_x(OH)₂] [x/zY⁻ 'nH₂O], where x ranges from Ø.16-Ø.33. The gallery anions are exchangeable, making LDHs negative analogs to clay minerals. The structural properties of LDHs are well documented. Very little has been done to characterize the properties of the gallery anions or the surface properties. Most LDHs that are synthesized are dehydroxylated to form oxide catalysts. No reactions have been reported for LDHs in their pristine form. This dissertation will describe the investigations into the properties of the gallery anions of LDHs.

LDHs containing a paramagnetic anion as a spin probe were synthesized. Because the $-SO_3$ groups of the spin probe $K_2(SO_3)_2NO$ bind to surface hydroxyl groups, no spin probe was intercalated even when it was added to the synthetic mixture. Therefore, no information about the mobility of gallery anions was obtained from EPR studies.

The availability of gallery anions of $[Zn_2Cr(OH)_6]$ [Y'nH₂O], where Y⁻=I, Cl, F, for nucleophilic displacement reactions was investigated. The reaction rate of iodide substitution of alkyl bromides under solution-solid conditions was independent of the alkyl chain length. The

reaction rate depended on the surface properties of the LDH. The rates also depended on the nature of the solvent in which the reaction occurred. From adsorption studies it was deduced that the more tightly a solvent was bound to the solid, the slower the reaction.

Chloride substitution reactions did not occur under solution-solid conditions, but did occur under gas-solid conditions. Fluoride substitution did not occur under either conditions. A detailed mechanism is proposed in which the bromo group of the reactant molecule must insert into the gallery of the reactant LDH. The mechanism is consistent with all observations regarding the kinetics behavior and adsorptive properties of the Zn-Cr LDH.

TO JOHN CLIFFORD MARTIN

1944 - 1974

ACKNOWLEDGMENTS

I would like to thank Dr. T.J. Pinnavaia for patience and guidance down the long road of graduate school. I look forward to future interactions.

I also wish to thank Dr. C.H. Brubaker for careful editing of this manuscript. I hope we got all the typos and grammar mistakes.

I would like to express my gratitude to all past and present group members with whom I have come in contact. Your support and questions have helped a lot.

I would like to thank my mother, siblings and nephews for emotional and financial support. You helped me keep my sense of humor through it all.

Finally, thanks to my mother-in-law Norma Donovan for use of the word processor, and to Susan and Elizabeth, words alone cannot express what I owe to you in the completion of this work. Maybe now we can live like normal people.

TABLE OF CONTENTS

		page
LIST OF	TABLES	.vi
LIST OF	FIGURES	.viii
CHAPTER	1. INTRODUCTION	. 1
Α.	Synthesis and properties of layered double hydroxides	. 1
в.	Supported reagents	. 23
c.	Objectives of current research	. 34
CHAPTER	2. EXPERIMENTAL SECTION	. 35
A.	Synthesis of materials	. 35
	1. [Zn ₂ Cr (OH) ₆] [C1·nH ₂ O]	. 35
	2. [Ca ₂ Al (OH) ₆] [Cl·nH ₂ O]	. 36
	3. [LiAl ₂ (OH) ₆][Ø.5SO ₄ ·nH ₂ O]	. 36
	3a. Spin-labelled [LiAl ₂ (OH) ₆][0.5SO ₄ *nH ₂ O]	. 37
	4. Ion exchange reactions	. 38
В.	Displacement reactions over [Zn ₂ Cr(OH) ₆] [Y'nH ₂ O]	. 38
	1. Reactions under triphase catalytic conditions	. 38
	2. Reactions under stoichiometric conditions	. 39
	3. Gas-solid reactions	. 40
c.	Physical methods	.41
	1. X-ray diffraction	.41
	2. EPR studies	. 42
	3. IR studies	.42

		4.	Gas chromatography	page 12
		5.	Surface areas	13
		6.	Adsorption studies	13
CHAPI	ER	3.	RESULTS AND DISCUSSION4	16
	A.	Pro	perties of LDHs	16
		1.	Exchange and swelling properties	16
		2.	EPR studies	55
	В.	Nuc	leophilic displacement reactions	56
			Reactions under triphase catalytic conditions	56
			Stoichiometric biphase reactions in toluene	70
		3.	Adsorption properties of Zn-Cr LDHs	36
			Reaction and sdsorption studies in other solvents	102
		5.	Thermodynamics of reaction	109
		6.	Proposed detailed mechanism	112
	c.	Con	clusions	124
r. r.sm	OF	PFF	PRENCES	127

LIST OF TABLES

Table	Page Some Natural LDH Minerals3
2	Phases Formed Upon Aging Ni-Al LDHs12
3	Variation of Basal Spacing In [Ca ₂ Al(OH) ₆] [Y·2H ₂ O] and [Zn ₂ Cr(OH) ₆] [Y·nH ₂ O] For Various Y Species13
4	Dependence of Lattice Parameters on Octahedral Layer Composition for Some LDH Species
5	Dehydration Temperatures ^a for Some Mg-Al and Ni-Al LDHs18
6	Dehydroxylation Temperatures ^{a,b} For Some LDH Carbonates
7	Swelling of [Zn ₂ Cr(OH) ₆][C ₁₂ H ₂₅ OSO ₃] in Alcohols and Amines21
8	Reactions Utilizing Polymer-Bound Nucleophiles of the Form PSCH ₂ N ⁺ Me ₃ X ⁻
9	EPR Correlation Times for PADS-doped Li-Al LDH Materials61
10	Conversion of Alkyl Halides by the Reaction RX + Y> RY + X Under Triphase Consitions67
11	Results of Blank Reactions for Halide Exchange69
12	Conversions of Nucleophilic Displacement Reactions of C ₄ H ₉ Br Under Modified Conditions71
13	Calculated Pseudo First Order Rate Constants, k _{obs} , for Iodide Substitution of Alkyl Bromides over A.D. [Zn ₂ Cr(OH) ₆][I°nH ₂ O]72

<u>Table</u>	Page
14	Pseudo First Order Rate Constants, k _{obs} , for Iodide Substitution of Alkyl Bromides Over O.D. [Zn ₂ Cr(OH) ₆] [I · ØH ₂ O]
15	Activation Parameters for Some Alkyl Halide Iodide Substitutions at 90 °C76
16	Conversions of Gas-solid Iodide Substitutions of 1-Bromobutane Over [Zn ₂ Cr(OH) ₆][I]80
17	Conversions of Gas-Solid Chloride Substitutions of 1-Bromobutane Over [Zn ₂ Cr(OH) ₆][Cl]80
18	Maximum Adsorption Capacities and Desorption Experiment Results for Various Adsorbates on O.D. [Zn ₂ Cr (OH) ₆][I]
19 .	Pseudo First Order Rate Constants for Iodide Substitution of 1-Bromobutane with O.D. Zn/Cr/I LDH at 90°C in Various Solvents
20	Activation Parameters for Iodide Substitution of 1-Bromobutane at 90 °C by O.D. [Zn ₂ Cr(OH) ₆][I] in Various Solvents
21	Values of $D_{CX} - D_{CY}$ and 24.2 d_{gg1} for Various Alkyl Halide Exchange Reactions RX + LDH(Y) \longrightarrow RY + LDH(X)

LIST OF FIGURES

Figure	Page
1	Structure of layered double hydroxides (water molecules omitted for clarity)2
2	Diagram of the coordination geometry around the calcium centers in [Ca ₂ Al(OH) ₆][OH·2H ₂ O] showing the distortion caused by coordination to gallery water6
3	The structure of montmorillonite, a clay mineral of the smectite group7
4	a.) The effect of aging on the product distribution of coprecipitated Ni-Al LDH for a solution value of x=0.25. b.) The effect of the initial product distribution on the shape of x-ray powder diffraction peaks. Adapted from reference 58
5	Structure of an alkylammonium-exchanged smectite swollen with a linear alcohol. From reference 2522
6	A conceptual diagram of triphase catalysis28
7	A diagram of a smectite clay with gallery ions as a result of a.) homoionic intercalation of cations, and b.) intersalation of two equivalents of cation and one of anion. Structure b acts as an anion exchanger32
8	Powder x-ray diffractograms of (a). [Zn ₂ Cr(OH) ₆][Cl·2H ₂ O]; (b). [LiAl ₂ (OH) ₆] [Ø.5SO ₄ ·nH ₂ O]; and (c). [Ca ₂ Al(OH) ₆] [Ø.5CO ₃ ·2H ₂ O]47
9	Powder x-ray diffractograms of [Ca ₂ Al(OH) ₆][0.5CO ₃ ·2H ₂ O] (a). pressed powder; (b) oriented film49

<u>Figure</u> 10	Powder x-ray diffractograms of the dodecylsulfate-exchanged forms of (a). Zn-Cr LDH; (b).Ca-Al LDH; and (c). Li-Al LDH	Page 51
11	Powder x-ray diffractograms of n-octanol-swollen DDS-exchanged forms of (a). Ca-Al LDH; and (b). Li-Al LDH	.52
12	Infrared spectra from 4000 cm ⁻¹ to 1000 cm ⁻¹ of [Zn ₂ Cr(OH) ₆][Cl [*] nH ₂ O] (a). pristine material; and (b). exposed to 0.1 M NaDDS solution	i . 54
13	EPR spectra of K_2 PADS (a). 10^{-5} M solution in DMSO; and (b). frozen in D_2 O	. 56
14	EPR spectrum of [Zn ₂ Cr(OH) ₆][Cl·nH ₂ O]. Frequency = 9.14 GHz	. 58
15	EPR spectra of PADS-doped [LiAl ₂ (OH) ₆] [Cl*nH ₂ O] (a). damp material; (b). after 4 hr in vacuum dessicator; and (c). after 12 hr in vacuum dessicator. Frequency = 9.14 GHz	. 59
16	EPR spectra of an Li-Al LDH synthesized in the presence of NaDDS and K2PADS (a). damp material; (b). after 4 hr in vacuum dessicator; and (c). after 12 hr in vacuum dessicator. Frequency = 9.14 GHz	. 6 2
17	Powder x-ray diffractograms of unaged Li-Al LDH product (a). filter-washed; (b). dialyzed until free of electrolyte	. 64
18	Powder x-ray diffractogram of product formed by reaction of LiCl solution and gibbsite	. 6 5
19	First order kinetic plots for iodide substitution of alkyl bromides over [Zn ₂ Cr(OH) ₆][I·2.3H ₂ O]: ■1-bromobutane; ▲1-bromohexane; and ●1-bromo-3-methylbutane	
20	IR spectra from 4000 cm ⁻¹ to 1000 cm ⁻¹ of (a). [Zn ₂ Cr(OH) ₆] [I·2.3H ₂ O]; (b). [Zn ₂ Cr(OH) ₆] [I·0H ₂ O]	.75

Figure 21	Page First order plots for iodide substitution of 1-bromobutane over O.D.
	Zn/Cr/I LDH: (a). 120 $^{\circ}$ C; (b). 100 $^{\circ}$ C; (c). 90 $^{\circ}$ C; (d). 80 $^{\circ}$ C; and (e). 50 $^{\circ}$ C77
22	Arrhenius activation energy plot, ln k _{obs} vs. l/T, for iodide substi- tution of l-bromopentane over O.D. Zn/Cr/I LDH
23	First order kinetic plot for the extended iodide substitution of 1-bromobutane over O.D. Zn/Cr/I LDH82
24	First order kinetic plot for iodide substitution of 1-bromobutane by O.D. Zn/Cr/I LDH at RBr/LDH ratios of 4:1; \$\int 3:1; \$\int 2:1; \$\int 1:1, plotted as functions of (a)ln f _I -; (b) -ln f _{RBr} .84
25	Isotherms for adsorption of toluene onto: (a). A.D. Zn/Cr/I LDH at ◆0°C; • 22 °C; (b). O.D. Zn/Cr/I LDH at • 0°C; ■ 22 °C
26	Isotherms for adsorption of 1-iodo- butane onto: (a). A.D. Zn/Cr/I LDH at ◆0 °C; ●22 °C; (b). O.D. Zn/Cr/I LDH at ▲0 °C; ■ 22 °C
27	Isotherms for adsorption of 1-bromo- butane onto: (a). A.D. Zn/Cr/Br LDH at ◆0 °C; ●22 °C; (b). O.D. Zn/Cr/Br LDH at ▲0 °C; ■ 22 °C
28	An adsorption isotherm showing the location of Point B, the attainment of monolayer coverage92
29	Heat curves, q _{st} vs. V/V _m , for adsorption of toluene onto [Zn ₂ Cr(OH) ₆] [I·nH ₂ O] ▲ A.D. ● O.D93
30	Heat curves, q _{st} vs. V/V _m for adsorp- tion of 1-iodobutane onto [Zn ₂ Cr(OH) ₆] [I·nH ₂ O] ▲A.D. ● O.D94
31	Heat curves, q_{st} vs. V/V_m , for adsorption of 1-bromobutane onto $[Zn_2Cr(OH)_6]$ [I'nH ₂ O] \triangle A.D. \bigcirc O.D95

Figure 32	Page
32	Plot of the enthalpy of liquid adsorption, ΔH ¹ ads, vs. V/V _m for toluene adsorbed onto [Zn ₂ Cr(OH) ₆][I·nH ₂ O] ▲ A.D. ● O.D
33	Plots of ΔH^1 ads vs. V/V_m for adsorption of 1-iodobutane onto $[Zn_2Cr(OH)_6]$ [I'nH ₂ O] \spadesuit A.D. \spadesuit O.D.; and 1-bromobutane onto $[Zn_2Cr(OH)_6]$ [I'nH ₂ O] \blacksquare A.D. \spadesuit O.D
34	Adsorption of toluene onto O.D. [Zn ₂ Cr(OH) ₆][I nH ₂ O] as a function of pressure at ▲ Ø C ■ 22 C99
35	Plots of ∆H ¹ ads vs. V/V _m for ● octane and △carbon tetrachloride adsorption onto O.D. [Zn ₂ Cr(OH) ₆][I*nH ₂ O]103
36	Plots of ∆H ¹ ads vs. V/V _m for adsorption of ▲chlorobenzene and ● toluene onto O.D. [Zn ₂ Cr(OH) ₆][I·nH ₂ O]
37	Possible bonding interactions of hydroxyl group orbitals with an aromatic system. (a).e _{2g} + 5 + OH - no net overlap; (b). e _{2g} + H _{2p} - p-orbital too high in energy; (c). 0.5 e _{2g} + 5 OH - probable interaction.

Chapter 1. Introduction

A. Synthesis and properties of layered double hydroxides.

There are a large number of compounds that can be classified as layered double hydroxides (LDH). This class of materials, also known as hydrotalcite-like compounds (HT)² and Feitknecht compounds³, has both synthetic and naturally occurring members. Most of these species, of general formula $[M(II)_{1-x}M(III)_x(OH)_2][x/zY^{z-n}nH_2O]^1$, consist of brucite-like octahedral sheets with trivalent metal cations periodically substituted for the divalent metal This substitution imparts a net positive charge on the sheets which is compensated by anions intercalated between the stacked hydroxide layers together with n water molecules (Figure 1)1. These compounds will be the subject of this dissertation. Related compounds exist with only divalent cations in hydroxide-carbonate structures 3 analagous to those of malachite, Cu₂(OH)₂CO₃; hydrozincate⁵, $Zn_5(OH)_6(CO_3)_2$; and azurite⁶, $Cu_3(OH)_2(CO_3)_2$. These mixedmetal hydroxides with no trivalent cations will not be considered in this work. Also, natural minerals with more than one octahedral layer per anionic layer, such as coalingite⁷ and carrboydite⁸, will not be considered.

Only a small percentage of the known LDH species occur in nature, the most common of which is hydrotalcite,

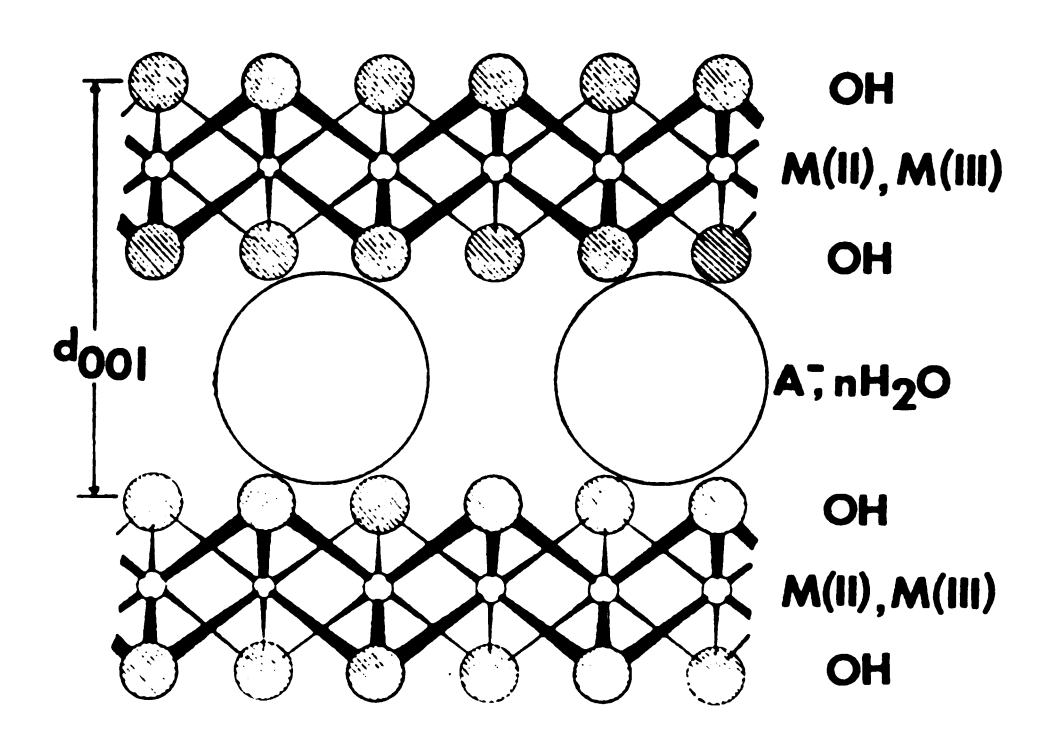


Figure 1. Structure of layered double hydroxides (water molecules omitted for clarity).

Table 1. Some Natural LDH Minerals.a

Name	Idealized Formula		
hydrotalcite, mannasseite	[Mg ₆ Al ₂ (OH) ₁₆][CO ₃ ·4H ₂ O]		
<pre>pyroaurite, sjogrenite</pre>	$[Mg_6Fe_2(OH)_{16}][CO_3^{4}H_2O]$		
stichtite, barbertonite	$[Mg_6Cr_2(OH)_{16}][CO_3^{4}H_2O]$		
reevesite	$ \begin{array}{l} \text{[Ni}_6\text{Fe}_2\text{(OH)}_{16}\text{][CO}_3\text{`$^4\text{H}_2\text{O}$]} \\ \text{[Ni}_6\text{Al}_2\text{(OH)}_{16}\text{][CO}_3\text{`$^4\text{H}_2\text{O}$]} \\ \text{[Mg}_6\text{Al}_2\text{(OH)}_{16}\text{][(OH)}_2\text{`$^4\text{H}_2\text{O}$]} \\ \text{[Ni}_6\text{Al}_2\text{(OH)}_{16}\text{][(OH)}_2\text{`$^4\text{H}_2\text{O}$]} \\ \text{[Ca}_2\text{Al}\text{(OH)}_6\text{][OH$^2\text{H}_2\text{O}$]} \end{array} $		
eardleyite	[NisAl2(OH)16] [CO3.4H20]		
meixnerite	[MGAI2 (OH) 16] [(OH) 2.4H2O]		
takovite	[Nisăla (OH) 16] [(OH) 2.4H20]		
hydrocalumite	[Ca2A[(OH) 6] [OH·2H2O]		

^aFrom reference 9.

 $[Mg_6Al_2(OH)_{16}][CO_3\cdot 4H_2O]^9$. The other formulae in Table 1 with two entries in the name column exist in two polymorphic forms⁹. The most extensively studied natural LDHs from a structural standpoint are the pyroaurite/sjogrenite polymorphs, [Mg₆Fe₂(OH)₁₆][CO₃·4H₂O]. Early powder diffraction work 10 showed that sjogrenite is hexagonal with a=3.13 A and c=15.65 A. Pyroaurite is rhombohedral with a=3.13 A and c=23.47 A. Single crystal studies of sjogrenite and pyroaurite confirmed these data 11-13. The hydroxyl groups of neighboring octahedral layers stack on top of each other. The rhombohedral pyroaurite has three octahedral layers per unit cell stacked in the sequence BC-CA-AB^{12,13}. The AB-BA-AB stacking sequence of sjogrenite leads to a hexagonal unit cell with two octahedral layers per unit cell. 11,12 In the samples examined, there was no order to the cation site distribution, i.e., the Mg(II) and Fe(III) centers were statistically distributed throughout the octahedral sites 12.

Much of the early attention focused upon synthetic LDHs resulted because a calcium-aluminum compound formed as an intermediate in the setting of Portland cement was in fact a Ca-Al LDH¹⁴. A report from 1929¹⁵ showed that two metastable compounds of "calcium sulphoaluminate" were formed by interaction of calcium aluminate and calcium sulfate. The formula of one of them, given as 3CaO·Al₂O₃·CaSO₄·12H₂O, can be rewritten as [Ca₂Al(OH)₆][1/2SO₄·3H₂O]. No structural data were given, but the formula falls into the category of a LDH. Later studies¹⁶ of the Ca-Al system confirmed that it was an LDH.

In the following years, many reports appeared on the synthesis of these basic double salts, as they were called before the structure was known¹⁷. From x-ray powder diffraction data came the knowledge that the 001 parameter of the materials varied as the size of the anion used in the synthesis or exchanged into the structure 18. A double layer structure was proposed 19 in which the divalent metal formed a hydroxide layer, like brucite, with the trivalent metal and anions intercalated between these sheets. One group 20 has used infrared spectroscopy results to support this structural argument. Specifically, the ${\rm CO_3}^{2-}$ vibrations were consistent with Al-OCO2-Al bridges in the galleries between brucite-like sheets. This structure is today not generally accepted today because of the single crystal work reported more recently. Synthetic analogues

of the natural mineral hydrocalumite, [Ca₂Al(OH)₆] [OH-2H₂O]⁹, have been investigated by single crystal x-ray diffraction²¹⁻²⁴. The results of these investigations are in essential agreement with the reported structures of pyroaurite and sjogrenite in that the metal cations are contained in octahedral hydroxide layers with anions intercalated between them^{21,22}. Because of the large size of Ca(II) compared to Al(III), the metal cations were sterically limited to an ordered arrangement 23. This result was different from the random distribution of Mg(II) and Fe(III) in pyroaurite and sjogrenite. 12 The difference in size and charge allows the more polar Al(III) centers to distort the hydroxyl groups away from the Ca(II) centers. Because of its large size and the free space created by the distortion, each calcium becomes 7-coordinate by bonding to a water molecule in the interlayer region 23,24 (Figure 2). The results from the single-crystal studies have been used to infer structural details of the many synthetic LDHs of which crystals large enough for single crystal studies cannot be grown.

The LDHs can be compared to the clay minerals²⁵. Both have a layered structure consisting of metal cations in an oxide (hydroxide) framework, as can be seen in Figures 1 and 3, with a net charge distributed through the framework due to substitutions of metal cations within the layers. Both clay minerals and LDHs have ions intercalated between these layers to balance the charge on the framework. Clay

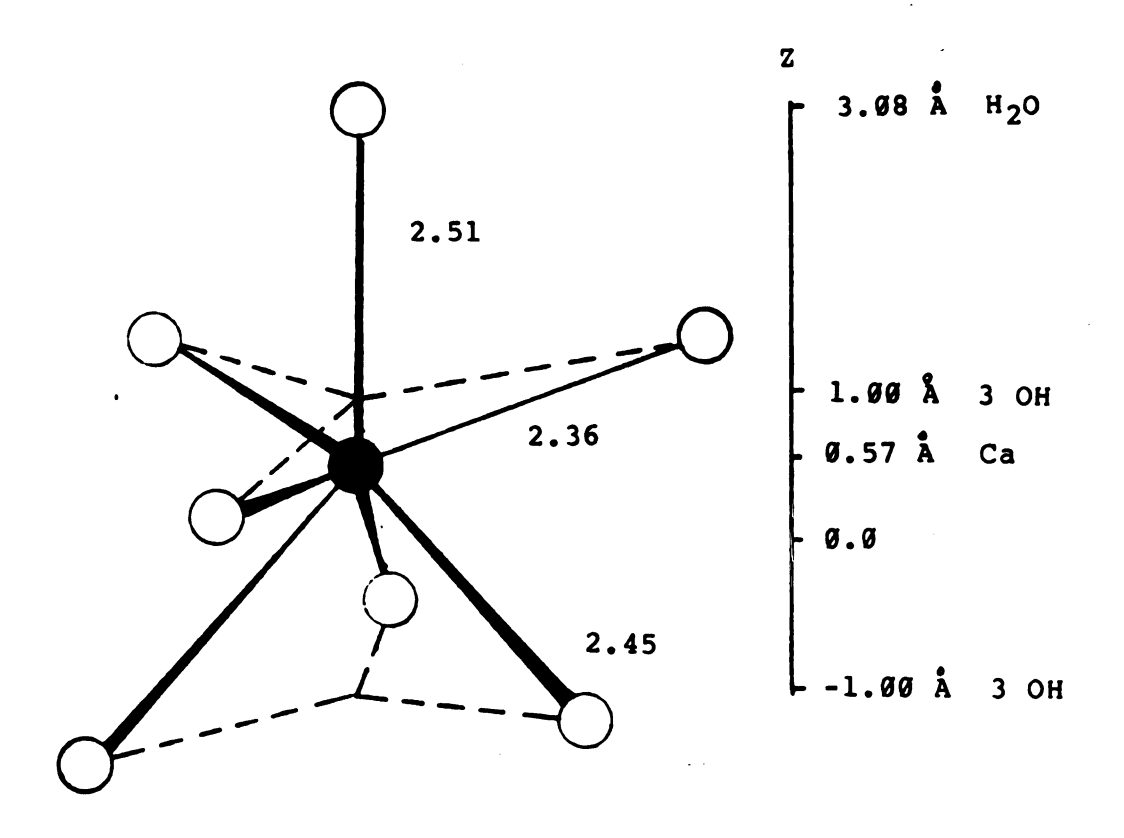


Figure 2. Diagram of the coordination geometry around the calcium centers in [Ca₂Al(OH)₆][OH·2H₂O] showing the distortion caused by coordination to gallery water. Adapted from reference 1.

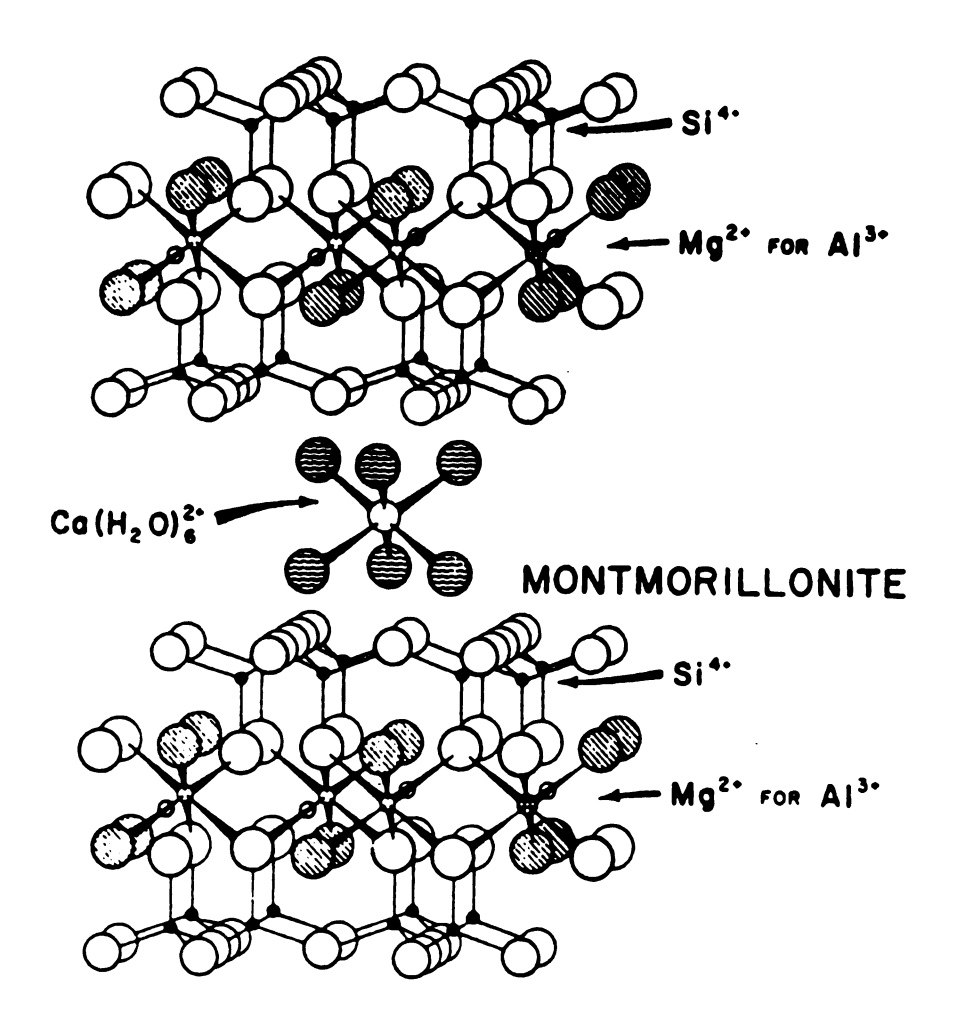


Figure 3. The layered structure of montmorillonite, a clay mineral in the smectite group.

minerals have a net negative charge on the oxide-hydroxide layers while LDH have a positive charge. The interlayer cations of many clay minerals are exchangeable, 25 as are the anions of most LDHs. Because of the possibility of substitutions in the octahedral and tetrahedral sheets of the clays, there is a greater variation in the properties of the clay minerals than is possible through substitutions in LDH compounds. Also, the swelling properties of smectite clays in various solvents cannot be duplicated in the LDH due to differences in solvation of anions vs. cations 25. The swelling of certain LDHs will be discussed in a later section.

Three general methods of synthesis have been devised. They are: 1) solid-solid reactions; 2) solid-solution reacand 3) solution-solution reactions coprecipitation. There is only one example of the first type of synthesis 26 . In this synthesis MgO and 120 3 were suspended in water and heated together at 80 °C for one week to give LDH products. This technique was especially suited for preparing carbonate-free materials 26. The second method was used in the preparation of Ca-Al LDHs for crystallographic studies 21,22. In these syntheses solid Al(OH), and Ca(OH), were suspended in an aqueous solution of the calcium salt of the desired gallery anion. After 200 hours at 150 °C, or 3 months at room temperature, crystals of [Ca2Al(OH)6][Y'nH2O] large enough for single crystal studies were produced²⁴. As another example of this synthetic approach, in studies of aluminum-containing soils and clay minerals, ²⁷ alkaline earth cations combined with various forms of hydrated alumina solids. In the case of Mg(II), these materials could be aged to give Mg-Al LDHs. The speed and extent of the reactions were dependent upon the crystallinity of the aluminum-containing material, with the "fresher", more amorphous materials reacting faster ²⁷, ²⁸. Gels of hydrated iron oxides also adsorb alkaline earth cations from solution ²⁹. Reactions of this sort have been postulated as possible routes in nature to LDH minerals and chloritic interlayers in certain clay minerals ²⁷, ²⁹.

This concept of reaction of a hydroxide gel with another cation has been extended to a general synthetic technique called induced hydrolysis 30 . A divalent metal salt solution is added to a freshly-prepared M(III) (OH) $_3$ gel at a controlled pH above that at which the M(II) (OH) $_2$ precipitates. The fresh gel seems to "induce" the divalent cation to condense into the gel structure to give the LDH product. 30

Another example of the solid-solution approach is the synthesis of $[Zn_2Cr(OH)_6][Y\cdot nH_2O]^{31,32}$. This compound was first noted in a study of the effects of chromium salt solutions upon ZnO oxidation catalysts 33 . Later workers identified the lavender products as LDHs. 31 In the synthesis of the Zn-Cr LDHs, ZnO was exposed to a 1 M solution of a Cr(III) salt until all traces of ZnO disappear from

the x-ray diffractogram of the product. It was reported that this same reaction also worked for Cr(III) and Cu0.31

The great majority of LDHs have been prepared by coprecipitation reactions. Coprecipitation is the technique of simultaneously precipitating at least two species within a solution. 34 In the original "calcium sulphoaluminate" synthesis, 15 the strongly alkaline calcium aluminate solution provided the required hydroxide ion concentration. For most other LDHs, an alkaline solution is usually added to a solution of the desired metal salts to precipitate the double hydroxide salt. This technique was exploited by Feitknecht in extensive studies of the Ca- $A1^{35-37}$ and Mg-A1^{16,17,38-40} LDH systems. Coprecipitation has been extended to hundreds of LDHs reported in a series of German $^{41-44}$ and Japanese $^{45-47}$ patents. The compounds contained these M(II) species (among others): Ba, Be, Ca, Cd, Cu, Fe, Mg, Mn, Ni, Pb, Pt, Sn and Zn, with more than one M(II) species in a single compound in many cases. These M(III) species were utilized (among others): Al, Am, Au, Bi, Ce, Co, Cr, Fe, Ga, In, La, Mn, Nd, Ni, Rh, Ti, V The LDHs were synthesized with or had exchanged into them a wide variety of simple mono-, di- and trivalent gallery anions. The range of x values reported for $[M(II)_{1-y}M(III)_{y}(OH)_{2}][x/zY^{Z-y}nH_{2}O]$ was 0.11 < x < 0.80, preferably with x between 0.24 and 0.45.41-47 The reported values of n were between 0.25 and 1.

These patents are unsurpassed in sheer numbers of

compounds presented. The properties of synthetic LDHs have been reported in detail for the Mg-Al, 48-54 Mg-Fe⁵⁵ and Ni- $A1^{50,56-58}$ systems. One of the reaction parameters studied was the effect of the variation of the value of x in the reaction systems on the identity and properties of the products. For the Mg-Al compounds, 48,50 values of x<0.17 led to the formation of brucite along with an Mg-Al LDH. Values of x>0.33 led to the formation of $Al(OH)_3$ phases along with the LDH product. Similar results have been reported for aged Ni-Al products. 57 For the Mg-Fe system, 55 pure product was formed in the range of 0.27>x>0.15. For the Mg-Al and Ni-Al compounds the values of x indicate an upper limit on the M(II)/M(III) ratio of 5 and a lower limit of 2. The limits for the Mg-Fe system appear to be 5>M(II)/M(III)>3. All these data are for materials aged either for 4-5 days at room temperature 50 , or 5 days at 60 °C.48,55,57

When freshly-precipitated Ni-Al materials were examined results different from the aged LDHs were reported. For freshly-prepared materials, single phases were found for values $0.5 \ge x \ge 0.15$, as shown in Table 2. When the compounds were aged hydrothermally for 2 days at 150 °C, the samples with x > 0.33 or x < 0.25 contained LDHs along with an additional phase, as indicated in the table. This was interpreted as evidence that the compounds formed initially when x > 0.33 or x < 0.25 were metastable, and that they changed into the more stable LDHs and either bayerite

Table 2. Phases Formed Upon Aging NiaAl LDHs.a

Solution x ^b	Before Aging	After Aging
Ø . 85	LDH	LDH, Ni(OH) ₂
Ø.8Ø	LDH	LDH, Ni(OH)2
Ø . 75	LDH	LDH
Ø.66	LDH	LDH
0.60	LDH	LDH, boehmite
Ø . 5Ø	LDH	LDH, boehmite
0.40	LDH, bayerite	<u> </u>

or Ni(OH)₂ upon hydrothermal treatment.⁵⁷ This conclusion was in accord with general observations concerning fresh precipitates of low crystallinity, 34 that they are often metastable under their conditions of preparation and that their composition is usually flexible. This points to the importance of aging coprecipitated LDHs, a step mentioned in every synthesis of this type. The importance of improving the crystallinity of the product can be seen in the Ca-Al example. 15,21-24 The material prepared by coprecipitation and unaged was metastable in its reaction mixture. 15 The same compound formed under hydrothermal conditions, 21-24 with aging built into its synthesis, was very stable. So improving crystallinity is not only important for structural studies, but also for increased stability of the precipitates.

An extensive literature exists on powder x-ray diffraction of synthetic LDHs. Almost all the patterns recorded can be indexed on the basis of either a hexagonal

aFrom reference 57. bx=[M(III)]/([M(II)]+[M(III)]).

or rhombohedral unit cell. As discussed earlier, this indexing corresponds to two layers and three layers per unit cell, respectively. 12 In the following discussion, the rhombohedral species will be discussed on the basis of hexagonal unit cell parameters \underline{a} and \underline{c}_0 . For simplicity, c', the actual layer repeat distance, will be used instead of c_0 , since c' is independent of symmetry group. Table 3 the values of c' for two LDH series of constant octahedral layer composition are given. The c' parameter varies as a direct function of the radius of the gallery anion. If the octahedral layer thickness (4.8 \mathring{A} = two layers of hydroxide⁵⁹) is subtracted from c', the result is close to the diameter of the anion. Based on this assumption, the values of c' for the CO₃²⁻ and NO₃⁻ forms of the Zn-Cr LDH should be approximately the same. For the CO_3^{2-} form, c'-4.9 Å = 2.7 Å, which is the approximate diameter of an oxide group. 59 This data agrees well with

Table 3. Variation of Basal Spacing In [Ca₂Al(OH)₆] [Y°2H₂O] and [Zn₂Cr(OH)₆][Y°nH₂O] For Various Y Species.

Metals	Y -	<u>c</u> ' (Å)	References
Ca, Al	ОН	7.4	23
Ca, Al	C1	7.9	22
Ca, Al	0.5CO ₃	7.6	8
Ca, Al	Ø.5SO ₄	8.9	21
Zn, Cr	F T	7.51	31,32
Zn, Cr	C1	7.73	31,32
Zn, Cr	Br	7.85	31,32
Zn, Cr	0.5CO ₃	7.6Ø	31,32
Zn, Cr	NO3	8.88	31,32

the single crystal results¹² that show carbonates in an orientation parallel to the hydroxide sheets. Apparently since there are twice as many nitrates per unit cell as carbonates, there is not room for them to orient in the same manner as the carbonates.³² Therefore, they must stand on end to all fit into the interlayer. This effect has been observed for other LDH.^{54,57}

Table 4 shows the dependence of <u>a</u> and <u>c'</u> on the constitution of the octahedral layers for several carbonate intercalated LDHs. There are several observations which can be made about the data presented in the table. For a given pair of metal cations, as the value of x increases, the value of <u>c'</u> decreases. This decrease was said postulated as the result of increased electrostatic attraction between the octahedral layers and anionic interlayers as the density of charge centers increases. This effect was not only observed in the Mg-Al^{49,50} and Ni-Al^{50,57}, but also in the Mg-Fe⁵⁵ LDH series.

Table 4. Dependence of Lattice Parameters on Octahedral Layer Composition for Some LDH Species.

M(II)	M(III)	_x a	<u>a</u> (Å)	<u>c</u> '(Å)	Reference
Mg	Al	Ø . 16	3.07	7.9	49
Mg	Al	Ø . 25	3.06	7.90	54
Mg	Al	0.30	3.05	7.73	50
Mg	Al	Ø.34	3.04	7.57	54
Ni	Al	Ø . 17	3.05	7.86	50
Ni	Al	0.22	3.04	7.76	50
Ni	Al	Ø.28	3.02	7.58	50

 $a_{x=[M(III)]/([M(II)]+[M(III)])}$

Observations about the <u>a</u> parameter can also be made. In the Mg-Al series, the value of <u>a</u> decreases from 3.07 Å to 3.04 Å as x increases from 0.16 to 0.34. $^{50-54}$ This trend also holds in the Ni-Al series. 57 The shrinkage of the unit cell was due to the increasing substitution of smaller Al(III) ions $(r=0.675 \text{ Å})^{59}$ into Mg(OH)₂ (Mg(II) $r=0.86 \text{ Å})^{59}$ and Ni(OH)₂ (Ni(II) $r=0.83 \text{ Å})^{59}$ lattices. This is evidence, independent of the single crystal studies, that the M(III) species was incorporated into the octahedral layer, not in the gallery as originally suggested. 19

When precipitates are hydrothermally aged, there is, in general, a narrowing of the x-ray diffraction lines. 34 This effect is usually attributed to an increase in the crystallinity of the sample. Another factor which can account for line narrowing is related to the method of synthesis. 34 In coprecipitation reactions, when an alkaline solution is added to the mixture of salt solutions, the pH begins to rise toward the final desired value. As it does, the precipitate formed first will be rich in that metal ion component of the LDH whose hydroxide forms at a lower pH. Likewise, at higher pH, the solid formed will be rich in the second component since the ratio of the two metal cations in solution has shifted in that direction during the earlier precipitation. As shown above, the xray parameters of LDHs vary with the composition of the octahedral layers. X-ray powder diffraction of the fresh materials reveals broad peaks. These could be made up of

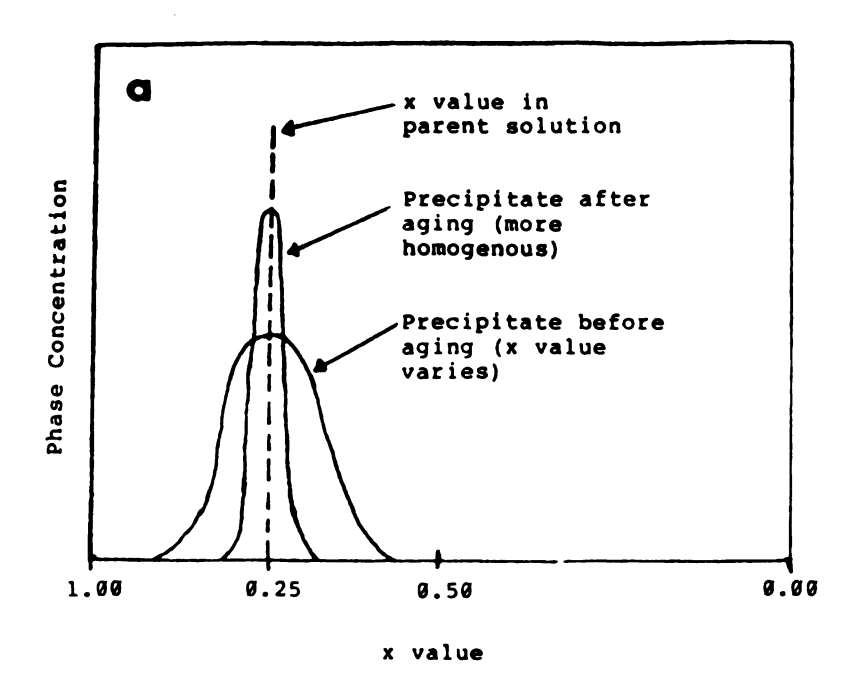
reflections from two or more different materials, overlapped to give a broad peak, as shown in Figure 4 for a Ni-Al example.⁵⁸ Upon aging the material becomes more homogeneous in composition and more crystalline, both of which serve to sharpen the x-ray peaks.

The results of thermal analysis of different LDHs are very similar. In almost all of them the first change upon heating is loss of molecular water, both from the surface of the particles and from interlayer regions, 32 followed by dehydroxylation of the octahedral layers and thermal degradation of the interlayer anions. The last two steps often occur·simultaneously.60

Differential thermal analysis (DTA) and thermogravimetric analysis (TGA) of pyroaurite and sjogrenite⁶⁰ showed that molecular water was lost below 200 °C, but that the process was reversible with no change in structure. By 450 °C, dehydroxylation and loss of CO₂ were complete. X-ray diffraction showed the formation of MgO and the spinel MgFe₂O₄. These products became more crystalline as the sample was heated to 750 °C.⁶⁰

Early stuidies of synthetic Ca-Al LDHs indicated that up to 150° C the structure of the LDHs remained intact. The \underline{c} ' distance was shortened due to loss of interlayer water. At temperatures above 150° C, the x-ray diffraction pattern grew into that of a mixed calcium-aluminum oxide.

Among the systems studied in detail were the $\rm Zn-Cr^{32}$, $\rm Mg-Al^{50-54}$ and $\rm Ni-Al^{57}$ series. In the $\rm Zn-Cr$ system, DTA



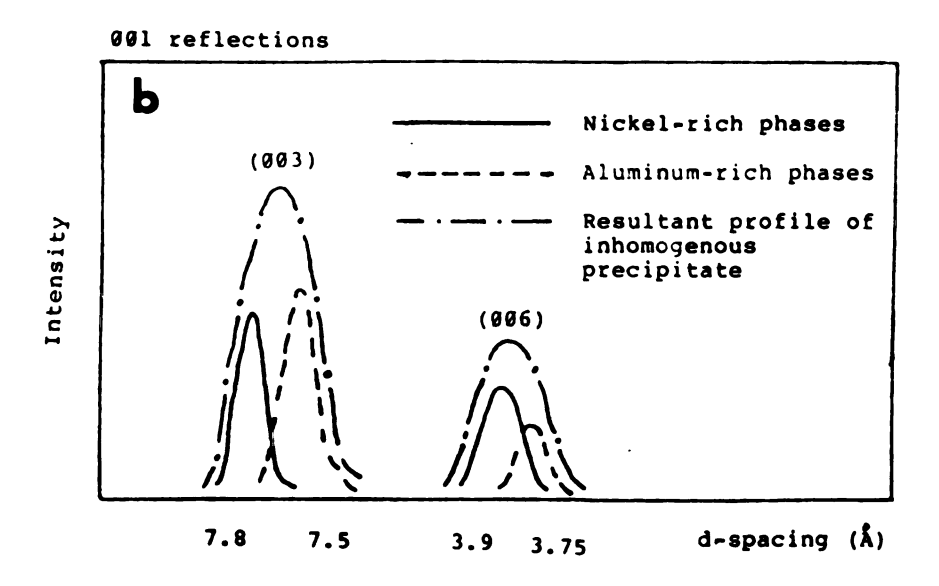


Figure 4. a.) The effect of aging on the product distribution of coprecipitated Ni-Al LDH for a solution value of x=0.25. b.) The effect of the initial product distribution on the shape of x-ray powder diffraction peaks. Adapted from reference 58.

results showed a dependence of the temperature of transition on the gallery anion. Of the halide forms, only the fluoride species showed a well-defined endothermic peak resulting from the loss of gallery and surface water from the solid. The next step, partial dehydroxylation, occurred at a lower temperature for the fluoride and iodide than for the bromide and chloride. The chloride and iodide showed another endotherm. These were interpreted as loss of halide as either HX or X₂. The final forms of the LDHs were assumed to be a mixture of ZnO and chromium oxides or a spinel, as can be formed by other LDHs.

The Ni-Al LDHs⁵⁷ also showed a dependence of dehydration peak on gallery anion. In particular, carbonate forms showed a higher first dehydration peak in DTA results (Table 5). The carbonate forms of Mg-Al LDHs show the same effect.^{51,54} This result was rationalized on the basis of single-crystal data reported for carbonate minerals.¹² The carbonate was seen to be a "good fit" in

Table 5. Dehydration Temperatures for Some Mg-Al and Ni-Al LDHs.

Metals	хp	Anion	Dehydration Temperature(^O C)	Reference
Mg, Al	Ø . 25	NO ₂ -	235	51
	Ø.25	CO32-	245	54
Mg, Al Ni, Al	Ø.25	NO3-	100	57
Ni, Al	Ø.25	NO 32 - NO 3 - CO 3 2 -	245	57

aCenter point of dehydration peak of TGA.
bx=[M(III)]/([M(II)]+[M(III)]).

the gallery. The interlayer spacing, dependent on the oxide group diameter, provided a good fit for the oxygen of water.⁹ The oxide groups of the carbonate galley anions also provided strong hydrogen-bonding to the water, further hindering dehydration of the galleries.¹

A comparison of dehydroxylation temperatures among the various LDHs in Table 6 shows trends associated with the metal centers in the octahedral layer. The species containing Zn(II) dehydroxylated at lower temperatures than the other compounds in accord with the reported dehydroxylation temperatures of the pure divalent metal hydroxides. 62

One of the interesting properties of smectite clays is their ability to undergo unidimensional swelling.²⁵ They can imbibe a number of different solvents, expanding in the contraction. In the extreme case in water and other solvents, the sheets may be completely exfoliated, expanding the contraction of the contrac

Table 6. Dehydroxylation Temperatures^{a,b} For Some LDH Carbonates.

Metals	ХC	Dehydroxylation Temperature(^O C)	Reference	
Ni, Al	Ø . 25	345	57	
Ni, Al	Ø . 33	357	57	
Mg, Al	Ø.25	440	54	
Mg, Al	Ø.33	420	54	
Zn, Cr	Ø.33	300	32	

Temperatures from center of dehydroxylation peak from TGA. bDehydroxylation temperatures ($^{\circ}$ C) for comparison: Zn(OH)₂: 125; Ni(OH)₂: 230; Mg(OH)₂: 350. Values from reference 62. $^{\circ}$ Cx=[M(III)]/([M(II)]+[M(III)]).

For LDHs, however, there have been only two reported examples of swelling behavior. The first of these was reported for a Ca-Al LDH 63. Two forms of the hydroxideexchanged LDH were reported. [Ca2Al(OH)6][OH·2H2O] had a c' parameter of 7.4 Å, reflecting the presence of one layer of water in the galleries with the hydroxide. [Ca₂Al(OH)₆] [OH·6H2O] exhibited an interlayer spacing of 10.7 Å, enough additional space for a second layer of molecular water. No other LDH has shown this ability to imbibe extra water layers. It has been suggested that the behavior of the Ca-Al LDH is related to its unique structure outlined earlier. According to the latest hypotheses, 25 smectites intercalated with monovalent cations swell due to interactions of the clay surface with the cation and its strongly-held solvation sphere. Gallery anions of LDHs lack this type of solvation sphere. Therefore, LDHs would not be expected to swell in the same manner as smectites. In Ca-Al LDHs, however, because of its large radius, the Ca(II) is exposed to the interlayer region. In the crystal structure of [Ca₂Al(OH)₆] [OH·2H₂O], a water molecule is coordinated strongly enough to the Ca(II) center to distort its geometry from octahedral. 12,13 It was suggested that this cation was exposed enough to hold an extra layer of water in the same way the cations in smectites attract extra layers. That this phenomenon was observed only when OH was the gallery anion suggests hydrogen bonding interactions as important factors in the swelling.

The other example of swelling in LDHs was reported for Zn-Cr LDHs.³¹ When an alkyl sulfate exchanged form of the material was exposed to either a linear primary alcohol or amine, the interlayer spacing was found to increase. The magnitude of the swelling was dependent upon the hydrocarbon chain length of the swelling agent, as shown in Table 7. This swelling phenomenon was said to be the result of solvation of the alkyl chains of the anion to give an approximate double layer structure.³¹ This behavior was compared to that of alkyl ammonium substituted layer silicates.²⁵ A model of this interaction is shown in Figure 5.

Among the patented uses of LDHs are applications as ion exchangers, 41 carriers for anionic pharmaceuticals, 64 inhibitors of thermal and ultraviolet degradation of thermoplastic resins 65 and scavengers of Cl $^-$ from Ziegler-Natta

Table 7. Swelling of [Zn₂Cr(OH)₆][C₁₂H₂₅OSO₃] in Alcohols and Amines.^a

Swelling Agent	Interlayer Spacing (Å)	
none ^b	26.2	
C ₄ H ₉ OH	29.2	
С ₄ н ₉ ОН С ₆ н ₁₃ ОН С ₁₀ н ₂₁ ОН	3 0. 8	
С <mark>1</mark> аĤ21ОН	38.2	
С ₁₂ Н ₂₅ ОН	41.1	
С16 Н33 ОН	44.9	
С ₁₆ H ₃₃ OH С ₁₂ H ₂₅ NH ₂	41.7	

aFrom reference 31.

bExchanged in water, air-dried.

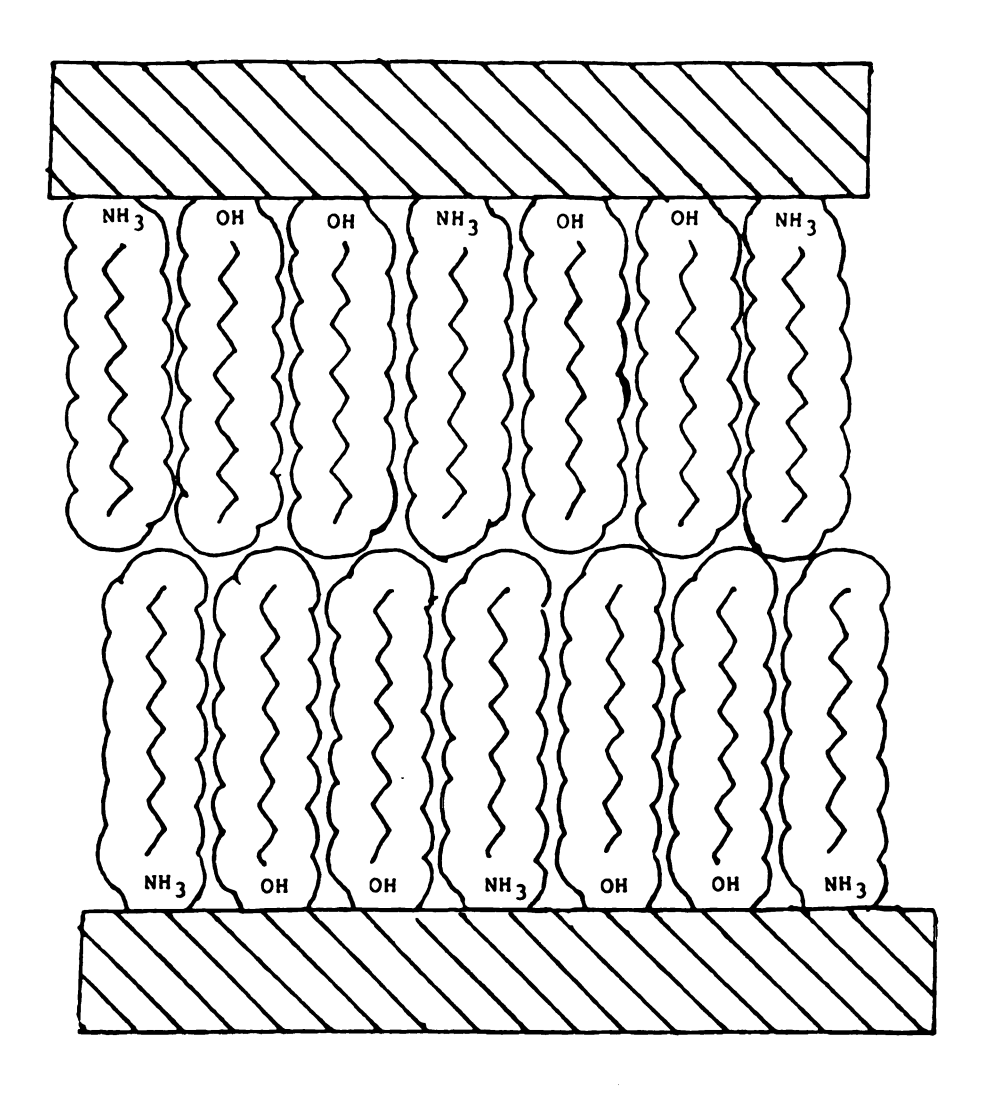


Figure 5. Structure of an alkylammonium-exchanged smectite swollen with a linear alcohol. From reference 25.

catalyst residue in plastics.⁶⁶ By far the greatest utilization of LDHs has come in the field of catalyst preparation.^{34,56-58,67-71} LDHs formed by coprecipitation have been calcined to form oxides to catalyze aldol condensations.^{70,71} Ni-Al LDHs have been calcined, then reduced, to give supported nickel catalysts for steam reforming.⁶⁷ Cu-Zn-Al LDHs have been treated in a similar manner to produce catalysts for methanol synthesis.⁶⁹ Part of the extensive literature on the preparation of these catalysts is concerned with the characterization of the catalyst precursors (LDHs), and much of the data quoted in this work comes out these reports.^{56-58,67,68} To date, however, no reactions involving uncalcined LDHs have been reported.

2. Supported reagents.

One of the major advances in organic chemistry in the recent past has been the use of supported reagents in synthesis 72. In this technique, reactants for organic reactions are bonded to a polymeric organic backbone 73, or somehow attched to an inorganic support 72,74. This can be accomplished by covalent bonding, adsorption or intercalation. These supported reagents offer several advantages 72-75. (1) The effective surface area for reaction is increased. This accelerates the reaction rate by increasing the number of reactant pairs brought together. (2) Solids always have microscopic pores on their surfaces. These pores may serve to constrain the

substrate and reactant, and therefore lower the entropy of activation of the reaction. (3) Product workup after reaction is usually simplified. This is especially true where, without a solid support, a mixture of solvents must be used to bring the reactants together. This situation can lead to complex distillation schemes or azeotrope problems. With the supported reagents the solvent for the solution-phase reactant can be chosen so that separation problems are kept to a minimum, or in some cases no solvent is needed at all. (4) In many cases the supported reagent can be easily regenerated.

Among the solid supports which have been utilized in the formulation of supported reagents are: ^{72,73} Celite, silica, alumina, graphite, activated carbon, montmorillonite, molecular seives, polymers and resins. Of the inorganic supports, Celite-supported silver carbonate was among the first to be utilized ⁷². Acid and base forms of ion exchange resins were among the first organic solid reagents to be used in synthesis ⁷⁶. Since these early uses, many other reagents supported on solids have been devised.

The range of reactions studied encompasses all classes of organic synthesis. The focus here will be on nucleophilic substitution reactions by anionic species. In general, these reactions are carried out by preparing an anion exchange resin in the form of the desired nucleophile, then mixing the substrate with the resin at the

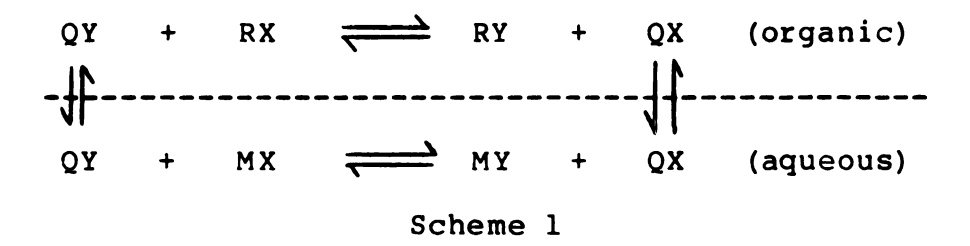
desired temperature 73. One of the first reactions to be reported using this technique was the cyanation of benzyl halides to their corresponding cyano compounds 77. Among the problems associated with this reaction in the solution phase was the formation of side products by competing elimination reactions. The polar solvent used in these reactions, usually acetonitrile, promoted these side reactions. With the supported reagent, only the substrate benzyl halide need be dissolved so that a nonpolar solvent could be utilized. The problem of elimination reactions was solved in most of the systems studied. 76 A partial listing of other nucleophilic displacement reactions which have been carried out using polymer-supported reagents is given in Table 8. As can be seen, a number of reactions have been reported. Many of the reactions shown were difficult to carry out in the solutions phase. The polymer support seemed to increase the nucleophilicity of such reactants as F^{-79} and sulfonates, 86 allowing reactions such as this to be performed simply.

One application of supported reagents is the technique of triphase catalysis ^{87,88}, which is an extension of phase transfer catalysis ^{89,90}. Phase transfer catalysis provides a way to react two mutually-insoluble reagents without the use of a cosolvent. All phase transfer reactions involve at least two steps: ⁹⁰ (1) transfer of one reagent from its "normal" phase into the second phase; and (2) reaction of the transferred reagent with the nontransferred reagent.

Table 8. Reactions Utilizing Polymer-Bound Nucleophiles of the Form PS---CH₂N+Me₃X

x -	Reaction System	References
F	conversion of sulfonyl chlorides and alkyl halides to fluorides	78,79
Cl,Br,I	halogen exchange with alkyl halides	79,80
CN	alkyl halides to nitriles	77,81
SCN	alkyl halides to thiocyanates or iso thiocyanates	£ 81,82
OCN	alkyl halides to ureas and urethanes	82
NO ₂ .	alkyl halides to nitroalkanes and nitrite esters	81,83
OCOR	alkyl halides to esters	84
ОН	condensation reactions	85
OAr	alkyl halides to ethers	83
0 ₂ SPh	synthesis of alkyl sulfones	86

Some of the species which have been found to function as phase transfer catalysts are 90,91 quaternary ammonium and phosphonium salts, crown ethers, cryptands and linear polyethers. Details of the mechanism of reaction vary with these different catalyst systems, but the simplest case involved $S_{\rm N}2$ -type nucleophilic displacement reactions as shown in Scheme 1. 89 The catalyst provides a way of ferrying the nucleophile to the organic reagent, then regenerating in the aqueous phase. More than 1000 publications and patents on phase transfer catalysis attest to its utility in these and many other reactions. 88,90



More recently, a synthetic approach has been developed that simplifies catalyst recovery and avoids the problem of emulsion formation sometimes encountered in phase transfer catalysis^{87,88}. This approach, termed triphase catalysis, is an extention of phase transfer catalysis. A conceptual diagram of triphase catalysis is given in Figure 6. Most triphase catalyst systems have involved the attachment of one of the active phase transfer species to an insoluble support. The supports utilized include polystyrenedivinylbenzene polymers⁸⁷ and silica gel^{92,93}. Smectite

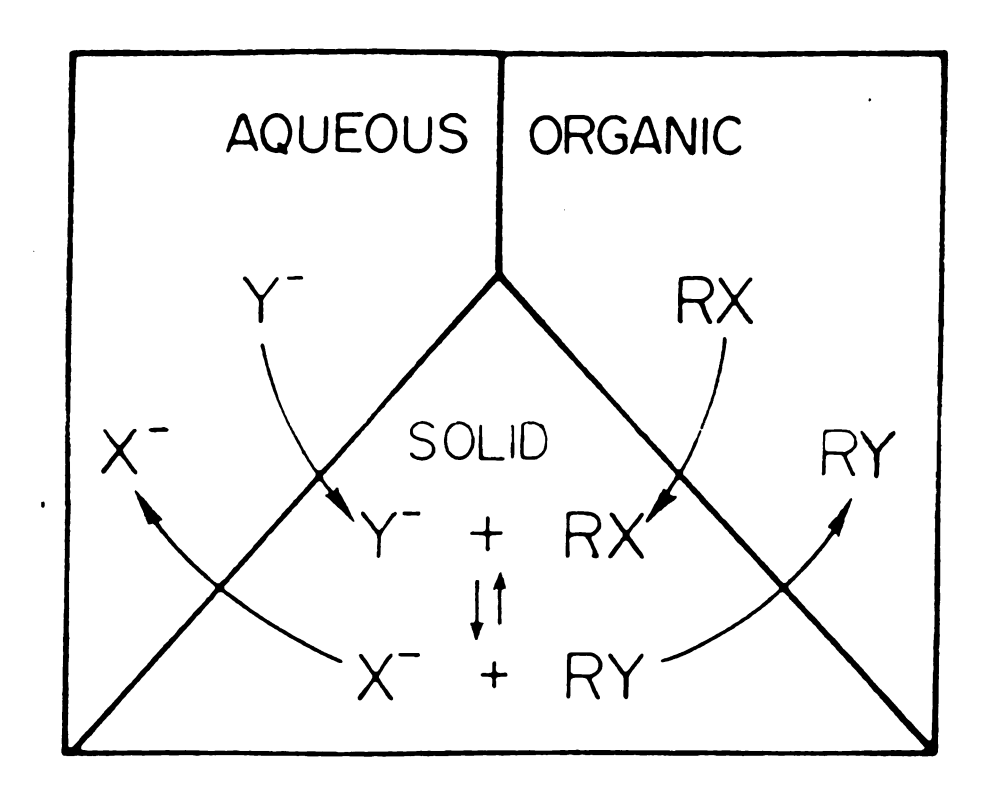


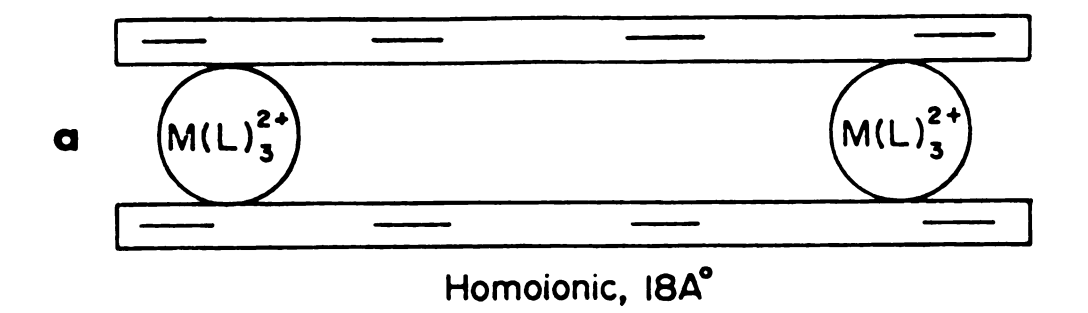
Figure 6. A conceptual diagram of triphase catalysis.

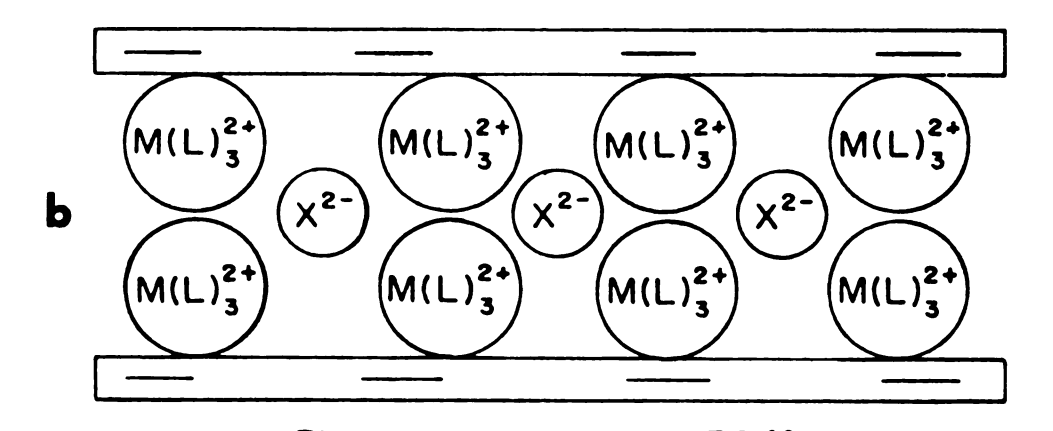
clays modified so that they became anion exchangers 94 have also been utilized In order for these materials to function as triphase catalysts, they must provide(): (1) anion exchange capacity; (2) an environment in which these aqueous anion exchanges can take place (i.e., a degree of hydrophilicity); and (3) an environment in which the organic reagent has access to the nucleophile (i.e., a degree of organophilicity). The way in which these criteria were met in the aforementioned systems will now be described.

By far the greatest number of reports have concerned themselves with polymer-based catalysts. 88 In these systems the active sites consist of quaternary ammonium or phosphonium groups bound to the polymer matrix through a hydrocarbon chain. Crown ethers and cryptands have also been effectively utilized as active species. 95 The polymer matrix employed in these studies is usually polystyrene crosslinked with 1-4% divinylbenzene. The organic matrix and hydrocarbon groups surrounding the anion exchange site make the solid organophilic enough for the organic reagent to interact with the nucleophile. At the same time the anion exchange site is exposed enough to be accessible to the aqueous solution of nucleophile that regenerates the active sites. One of the problems associated with the use of these supports is matching solvent with polymer. 90 These polymers swell to differing degrees in different solvents as a function of their percentage of crosslinking. In the cyanation of 1-bromooctane, the activity of the catalyst depends on the swelling properties of the resin support. 90 Specifically, the resins that swell more in the organic phase than in water showed greater activity. This effect can be explained on the basis of diffusion. If the resin were swelled with organic phase, there would be a large amount of reactant dispersed in the resin. Under these conditions diffusion of the organic reactant to the active site would be more favorable than if the aqueous phase predominated in the resin. Since the reaction rates were higher when the organic phase was present, the interpretation was that the rate is controlled by diffusion of the substrate to the active site on the catalyst.

Another way in which the ammonium and phosphonium salts have been supported is by attachment to silica gel.92,93 Attachment was accomplished by way of a functionalized organosilane coupling agent. These catalysts were effective in many of the same reactions as the more prevalent resin-bound materials. These solids provided access to both organic and aqueous phases in much the same way that the polystyrene-supported materials did. There was no problem with swelling in these catalysts, 96,97 as there was with the resins. Therefore, in order to simplify product workup, the reactions could be run without an organic solvent. There was a problem, however, with water adsorbed on the surface of the silica that created a hydrophilic environment around the active sites of the catalyst under certain conditions. These conditions arose if the hydrocarbon chain on the silane group was too short, or long enough to allow the active site to be bent to the silica surface. Also, with very long chains, phenyl-substituted substrates were solvated by the long chains. These solvated molecules were unavailable for reaction and consequently the rate of reaction was slower. The use of smectite clays as triphase catalyst supports has been recently reported. Montmorillonite intersalated with benzyltri-n-butylammonium bromide catalyzed the reaction of phenol with 1-bromobutane in the presense of base. The environment of the solid seems to have enhanced the nucleophilicity of the phenoxy group, as the conversion with the supported system was greater than that using an analagous homogeneous phase transfer catalyst system.

In other work that utilized clays, hectorite was intersalated with Ni(phen)₃SO₄ (phen=1,10-phenanthroline) and with cetylpyridinium bromide.^{94,99} A comparison of intercalation and intersalation is given in Figure 7. The net effect of intersalation was to induce anion exchange capacity in the smectites.⁹⁴ These materials were utilized as triphase catalysts in halide exchange reactions on alkyl halides. Apparently, the use of organometallic complexes and organic cations in the galleries of the clays provided the organophilicity that, along with the aforementioned anion exchange capacity, are the two requirements for producing a solid catalyst for triphase reactions. In the halide exchange reactions, the [Ni(phen)₃]²⁺ intersalates





Bilayer Intersalation,~30A°

Figure 7. A diagram of a smectite clay with gallery ions as a result of a.) homoionic intercalation of cations, and b.) intersalation of two equivalents of cation and one of anion. Structure b acts as an anion exchanger.

were more effective than the cetylpyridinium intersalates. 99 Also, in the case of the halide exchange reactions using the nickel-based material, the catalyst was somewhat size and shape selective. 94 The rate of conversion of 1-chloropentane to its corresponding bromide was reported to be much greater than any of the larger, more bulky alkyl chlorides. The reactions proceeded at almost identical rates under homogeneous phase transfer conditions that used tricaprylmethylammonium chloride as the catalyst. 94 Inherent differences in reactivity of these primary alkyl chlorides were apparently not responsible for the differences in conversion using the solid catalyst.

There were two possible explanations put forth for the differences in reactivity. 99 The first one stated that the differences arose from the layered structure of the clay. There was only a limited amount of space in the interlayer region of the clay, allowing the smaller, unbranched molecules to diffuse more rapidly into the interlayer region where the nucleophile was immobilized. This explanation was made with the assumption that the reaction took place within the clay layers. The other explanation started out with the hypothesis that the reactions took place in an interface between the two liquid phases on the surface of the clay. 99 Since the nucleophiles were contained within the aqueous phase, the smaller, less hydrophobic alkyl would react more quickly by virtue of their greater ability to diffuse into this aqueous phase. This still did not

explain why the branched hydrocarbons reacted so much more slowly than their straight-chain analogs. Perhaps the true mechanism was some combination of these two.

Objectives of Current Research.

As outlined above, the physical properties of layered double hydroxides have been relatively well explored. The chemical properties of gallery anions and surface properties of the materials have not been adequately addressed in the past. In this work, the goal of the research was an understanding of these properties. The properties of the gallery anions and surface were to be explored by use of LDHs as sources of nucleophile under triphase catalytic conditions and under stoichiometric conditions. The interactions of LDHs with aqueous and organic phases under these conditions would provide data about the availability of gallery anions for reaction and the relationship of surface properties to reactivity.

Chapter 2. Experimental Section.

- A. Synthesis of Materials.
- 1. [Zn₂Cr(OH)₆][Cl*nH₂O].

This compound was prepared by a modified $version^{32}$ of the original reported procedure. A slurry of 45 g (0.55 mol) ZnO was prepared by adding water to the powder with stirring. To this slurry was added 150 mL of a 1.0 M CrCl₃ solution (0.15 mol Cr(III)) in 50 mL water. This addition brought the pH of the solution to 3.4. The mixture was stirred at 60 °C until the solution became colorless, indicating that all of the Cr(III) had been consumed. clear solution was decanted from the solid, and a further 150 mL of 1 M CrCl₃ and 50 mL water added to the solid, bringing the total Zn/Cr ratio of the mixture to slightly less than 2, the small excess of Cr(III) assuring complete reaction of all ZnO. The mixture was stirred at 60°C for 5 The solid product was washed with distilled water by centrifugation until the wash water was free of Cl (AgNO3 The lavender-gray product was resuspended in water and poured onto a glass sheet to dry as a 5-10% suspension and allowed to air dry. The product was identified by xray powder diffraction $(d_{\alpha\alpha_1}=7.73\text{\AA})$. Completeness of reaction was verified by the absense of any peaks attributable to ZnO. 100

2. [Ca₂Al (OH)₆] [Cl^onH₂O].

In accord with one of the published methods for preparation²² 5.97 g (54.0 mmol) anhydrous CaCl₂ was dissolved in approx. 75 mL distilled water. To this solution was added 6.96 g (89.0 mmol) Al(OH)₃ and 10.0 g (135 mmol) Ca(OH)2, resulting in a Ca/Al ratio of 2.10, a slight excess of Ca(II). The suspension was placed in a Parr stainless steel pressure reactor equipped with a Pyrex liner and a stirrer. The mixture was heated to 150 °C. The temperature was monitored and controlled through use of a temperature controller and a built-in thermocouple. reaction was allowed to proceed for 100 h. The resulting white product was washed with distilled water by centrifugation until the wash water was free of Cl (AgNO3 test). The material was resuspended and poured onto a glass plate to dry. Identity of the product was confirmed by x-ray powder diffraction through comparison with published data $(d_{qq_1} = 7.9 \text{ Å})^{22}$ and by the absence of any peaks associated with the starting materials. 100

3. $[LiAl_2(OH)_6][SO_4^nH_2O]$.

This compound was prepared by following the procedure of Serna et. al. 101 A saturated solution of LiOH was prepared with freshly boiled deionized water to remove traces of carbonate. This solution was placed in a three-neck flask that had been purged with N₂ to remove traces of CO₂ that could be absorbed by the strongly basic (pH=13.0) solution. These precautions were necessary because of the

reported preference of LDHs for carbonate ion. As N₂ was bubbled through the solution, a $0.5 \ \underline{\text{M}}$ solution of $\text{Al}_2(\text{SO}_4)_3$ was added dropwise. The pH of the solution was monitored during the addition. When a value of pH=10 was reached, the addition was stopped. The resulting powder product and its mother liquor were placed in a Parr pressure reactor and hydrothermally treated for 3 days at 130 °C. The resulting product was washed on a Buchner funnel under N₂ until the wash water was free of Li⁺ (flame test). The identity of the product was confirmed by x-ray powder diffraction by comparison of the basal spacings with literature values $(d_{001}=10.45 \ \text{Å})^{102}$ and the absence of peaks from any other Al or Li containing phases.

3a. Synthesis of spin-labelled [LiAl2(OH)6][Cl*nH2O].

Nitroxide-doped samples of [LiAl $_2$ (OH) $_6$] [Cl*nH $_2$ O] were prepared for EPR analysis with K $_2$ NO(SO $_3$) $_2$, peroxylamine disulfonate (PADS), present in the reaction mixture. Since the PADS $^{2-}$ species was stable in basic solution and unstable in acid, 0.064 g (0.24 mmol) K $_2$ PADS was placed in 5 mL water with 1.0 g (24 mmol) LiOH·H $_2$ O. A 0.5 M solution of AlCl $_3$ was added as before. The solid was allowed to age at room temperature for 4 h and then washed under N $_2$. The hydrothermal treatment used on the sulfate sample earlier would have caused the decomposition of the spin probe. The solid was stored under Ar in a dessicator to prevent the decomposition of PADS $^{2-}$ by oxygen.

4. Ion exchange reactions.

In a typical ion exchange reaction, 1 g of solid was immersed in enough 1 \underline{M} solution of the desired exchange anion to give a 30-fold molar excess of anion. The mixture was stirred at 60 $^{\circ}$ C for 2-3 h. The solution was decanted and the process repeated. Usually, one repetition was enough to make the original LDH undetectable in the x-ray diffraction pattern. In cases where solubility problems precluded use of a 1 \underline{M} solution, as in the case of sodium dodecylsulfate exchange, or thermal instability prevented reaction at 60 $^{\circ}$ C, as in attempted exchanges with PADS, longer exchange times and repeated applications of fresh solution were used to effect complete exchange.

- B. Displacement Reactions Over [Zn₂Cr(OH)₆][Y•nH₂O].
- 1. Reactions Under Triphase Catalytic Conditions.

The conditions utilized were similar to those used by earlier workers in triphase catalysis in order to facilitate direct comparison of results. Iodide substitution reactions of alkyl halides were investigated. In these reactions the aqueous phase consisted of 0.899 g (6 mmol) NaI in 3.0 mL water. The organic phase was composed of 1 mmol alkyl halide in 2.0 mL toluene. In all cases a 20:1 molar ratio of alkyl halide:LDH was utilized. So for the reactions, 0.023 g (0.05 mmol) [Zn₂Cr(OH)₆][I·2.3 H₂O], prepared by anion exchange with the original chloride

material, was added to catalyze the reaction. A dodecylsulfate-exchanged form (DDS, C₁₂H₂₅OSO₃-) was also used in some reactions to test whether the presence of an organic species in the gallery would affect reaction yields. these cases, 0.029 g of the DDS form of the solid was used in the reaction mixtures. All of these reactions were carried out in Pyrex culture tubes sealed with a Teflonlined cap. The tubes were placed in a constant temperature (Omega Engineering model 4000 temperature controller) oil bath maintained at 90 °C. A magnetic stir plate and spin bars in the individual tubes provided agitation of the reaction mixtures. The reactions were allowed to proceed The products were analyzed by GC. reactions were also run which included all the ingredients listed except the solid LDH. These were carried out and analyzed in the same manner as the triphase reactions.

2. Reactions Under Stoichiometric Conditions.

The same reactions carried out under triphase catalytic conditions were also attempted in the absence of an aqueous phase. The iodide-exchanged form of the Zn-Cr LDH was again utilized. The air-dried (A.D.) form with n=2.3³² and a form dried at 150 °C for 2 h under Ar, the oven-dried (O.D.) form with n=0, were tested in the reactions. In both cases 1 mmol equivalent of intercalated I (0.453 g A.D. LDH or 0.412 g O.D. LDH) was added to 3.0 mL organic solvent in a pyrex culture tube with Teflon-lined cap. To this mixture were added 1 mmol alkyl halide and a magnetic

spin bar. The culture tubes were placed in the temperature controlled oil bath at the desired reaction temperature, typically 90 $^{\circ}$ C. A magnetic stir plate provided agitation of the reaction mixtures. The tubes were withdrawn from the oil bath every 10 min, cooled in an ice bath to quench the reaction and ca. 10 μ l of liquid reaction mixture withdrawn. The culture tubes were quickly resealed and returned to the oil bath after each extraction of material. The samples were analyzed by GC to calculate percentage conversions.

In some cases the RBr:I ratio was varied to study the effect on the reactions. Ratios of 2, 3, and 4 were used in addition to the typical 1:1 ratio.

3. Gas-Solid Reactions.

A vertically-mounted, fixed bed continuous flow microreactor previously used to test for catalytic activity of
clay minerals 102 was utilized to study the reactivity of
LDHs toward vapor phase alkyl halides in nucleophilic displacement reactions. The reactor consisted of 7 mm I.D.
quartz tubing encased in a tube furnace heated and controlled by a three stage temperature controller (Eurotherm
model 919A). The alkyl halide was introduced with a
syringe pump (Sage Instruments, model 341A) into a preheater zone at the top of the reactor. The vector gas, He,
was purified with BASF R3-11 catalyst to remove oxygen and
4A molecular seives to remove water. The He flow rate was
controlled through a flowmeter.

In a typical reaction, 1 mmol Zn-Cr LDH was loaded into the reactor tube. Several 2 mm glass beads were placed on top of the solid to ensure complete vaporization of the alkyl halide. The solid was pretreated at 150 °C for 2 h under a flow of He to remove water from the structure. The syringe pump delivered 1 mmol alkyl halide in 4.8 min into a He flow of 3.0 mL/min. This combination of parameters gave a contact time on the solid of 0.20 seconds. The product mixture was collected at liquid N₂ temperatures in a quartz trap at the bottom of the reactor for 30 min to ensure collection of all reaction products. The products were diluted with toluene and analyzed by GC.

- C. Physical Methods.
- 1. X-ray Diffraction.

Powder x-ray diffractograms were recorded using either a Siemens Crystalloflex-4 or Philips x-ray diffractometer. Both instruments utilized Ni-filtered Cu K_{∞} radiation. Some samples were prepared by placing approx. 1 mL of a 1-5% suspension of the solid to be examined on a microscope slide and allowing it to dry. The slide was then placed in the goniometer for examination. For samples such as DDS-exchanged species that could not be resuspended or would not form a film which adhered to the slide, a different technique was used. Double sided tape was placed on the microscope slide. The powder was applied to the tape and then pressed on with another slide. The second slide was

removed, leaving a pressed powder sample. The first technique, which gave films with the LDH platelets preferentially oriented parallel to the slide, was the preferred method of preparation since the d_{001} reflections were accentuated in these diffractograms. Typically, the samples were scanned from a 2-value of 2° to 30° . The intensity of the signal was recorded on a strip chart recorder. The 2-values were converted to d-spacings using a standard chart based on Bragg's equation for Cu K₄ radiation (λ =1.5405 Å).

2. EPR Studies.

EPR spectra were recorded using a Varian E-4 X-band spectrometer. The synthesized materials containing the PADS spin probe were placed in a quartz tube while damp and forced to the bottom of the tube by a Teflon rod. EPR spectra were recorded while the sample was damp and after drying for various periods of time. Standard pitch served as a reference material (g=2.0023).

Infrared Studies.

Infrared spectra were recorded by use of a Perkin Elmer model 457 or model 533 spectrophotometers. Both were double beam instruments with diffraction gratings for wavelength selection. The spectra were recorded from 4000 cm $^{-1}$ to 250 cm $^{-1}$ on samples prepared as KBr pellets.

4. Gas Chromatography.

Reaction product mixtures were analyzed by using gas liquid chromatography (GC). Some samples were analyzed by

use of a Varian Associates model 920 GC with thermal conductivity detection. A 10' x 0.25" 5% SE-30 on Chromosorb-W column separated the components of the sample. The chromatograms were recorded by use of a Linear Instruments model 252A recorder-integrator which was calibrated with standard mixtures to insure accuracy of integration. All reaction mixtures involved in kinetic studies were analyzed by use of a Hewlett-Packard model 5890A capillary GC using a 60 m x 0.25 mm dimethyl polysiloxane (Supelco SPB-1) column and flame ionization detection. The chromatograms were recorded and analyzed by a Hewlett-Packard model 3392A programmable plotter/integrator which was capable of customized data handling. All peaks were identified by comparison of retention times with authentic samples of reaction mixture components.

5. Surface Areas.

Surface areas were determined using a Perkin-Elmer-Shell model 212B sorptometer with N_2 as the adsorbing gas. These surface areas are referred to as B.E.T. surface areas, in honor of the developers of the technique, Brunauer, Emmett, and Teller. The samples were either outgassed for 1 h at room temperature under dry Ar or at 150 $^{\rm o}$ C for 2 h under Ar.

6. Adsorption Studies.

The adsortion capacities of Zn-Cr LDHs were measured by using a McBain balance arrangemen 103 of quartz springs in a vacuum system. The vacuum line was constructed of quartz.

Teflon stopcocks and valves were used to keep the system grease-free. Vacuum was achieved with rotary pumps and a CVC model PVMS-31 diffusion pump. Pressure was measured with a Datametrics model 1400 electronic manometer.

In a typical experiment, 75 mg of an LDH was placed in a quartz bucket and suspended from a pre-calibrated quartz spring. The position of the bucket was measured using a telescope on a height-calibrated mount. The portion of the vacuum system containing the solid was then evacuated. Samples were either evacuated to 1×10^{-3} torr at room temperature before adsorption, or heated to 100° for 90° min under vacuum to remove water from the structure. While the samples were being treated, the solvent to be used as adsorbate was degassed in a vacuum isolated from the solid samples. Heat treated samples were allowed to equilibrate for 1 h before adsorption studies began. The position was noted so that the final weight of the solid material could be calculated and used in subsequent data treatment.

The adsorptions were carried out at 2 temperatures, 22°C and 0°C . An ice bath was employed to cool the samples to 0°C . These samples were allowed to equilibrate for 1 h before beginning adsorption. The adsorbate was also maintained at 0°C to minimize condensation on th solid at high values of p/p_{0} . After all temperatures were equilibrated the system was isolated from the vacuum pumps. A small quantity of adsorbate was leaked into the system from a smaller manifold. The system was allowed to

equilibrate approx. 5 min, by which time the sample had stopped adsorbing. The position of the bucket was recorded to a precision of 0.05 mm by using the telescope. The pressure was also recorded. The procedure was continued up to a value of $p=p_0$ for the adsorbate at 0 $^{\circ}$ C.

Chapter 3. Results and Discussion.

- A. Properties of LDHs.
- 1. Exchange and Swelling Properties.

The compounds $[Zn_2Cr(OH)_6][Cl^2H_2O]$, $[Ca_2Al(OH)_6]$ $[1/2CO_3^2H_2O]$ and $[LiAl_2(OH)_6][0.5SO_4^2H_2O]$ were synthesized. The carbonate form of the Ca-Al LDH was formed in the initial synthesis due to improper precautions against CO2 absorption. Proper precautions were taken in subsequent syntheses. The powder x-ray diffractograms of these materials are shown in Figure 8. As can be seen, the patterns are nearly identical, as the structural components of these species were very similar. When anion exchange reactions were attempted with these species, the Zn-Cr LDH exchanged more readily than the other two species. difference may have been due to some adventitious carbonate in the structure of the Ca-Al and Li-Al LDHs, even when precautions against CO2 adsorption were taken. It has been reported that carbonate forms of LDHs are difficult, if not impossible to exchange. This difficulty is due to the good fit of carbonate in the gallery and the -2 charge. acidic conditions under which the Zn-Cr LDH was formed preclude the uptake of CO2 by the reaction mixture.

As can be seen from the diffractograms in Figure 8 the

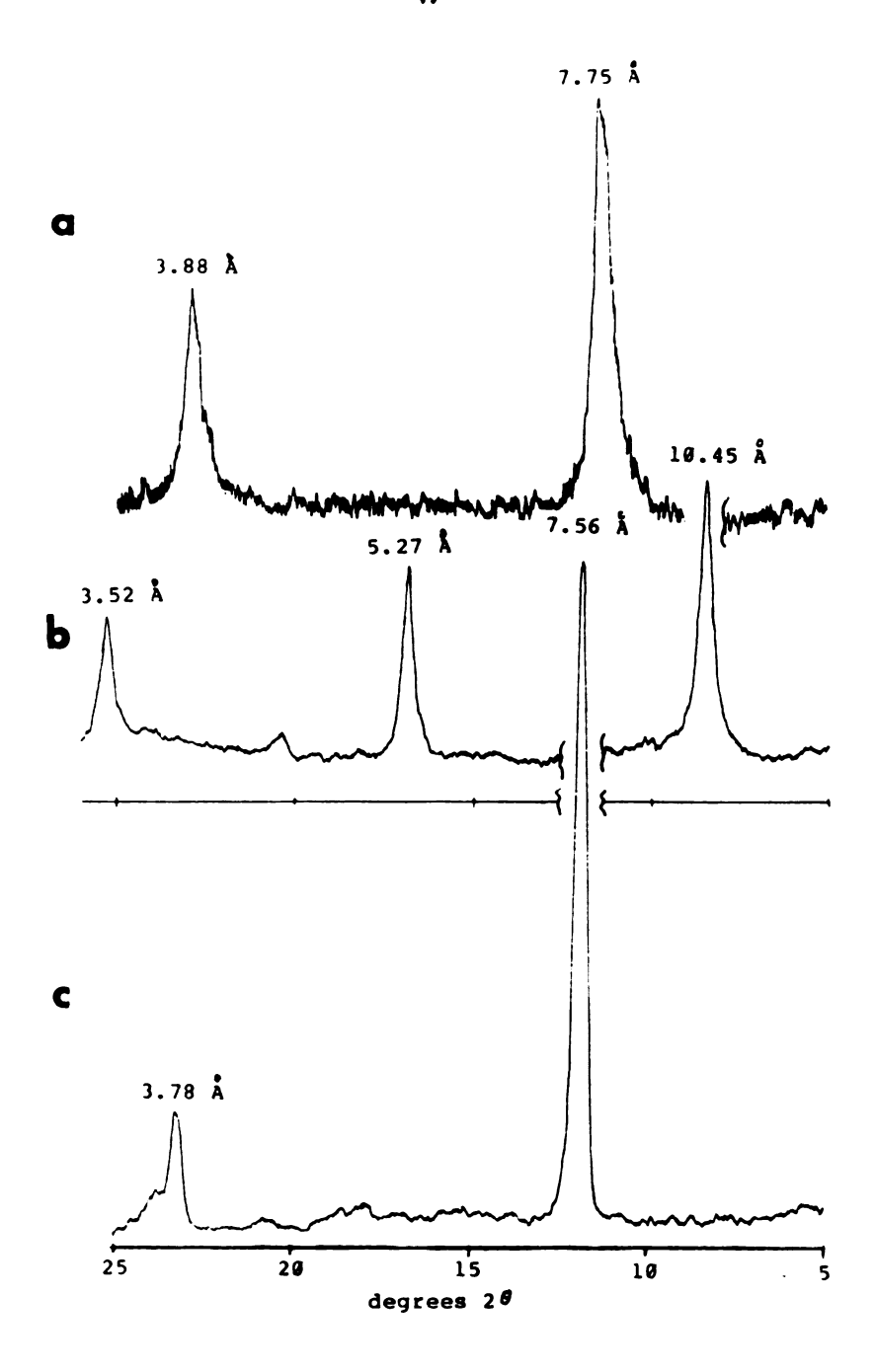


Figure 8. Powder x-ray diffractograms of (a). $[2n_2Cr(OH)_6]$ $[Cl^2H_2O]$; (b). $[LiAl_2(OH)_6]$ [0.5SO₄*nH₂O]; and (c). $[Ca_2Al(OH)_6]$ [0.5CO₃*2H₂O].

peaks from Zn-Cr LDH were broader than those of the other species and was partially due to the method of sample preparation for x-ray examination. The Ca-Al and Li-Al species formed oriented films on microscope slides. This preparation tends to minimize layer disorder that can broaden diffraction peaks. An x-ray diffractogram of a Ca-Al sample prepared by the pressed powder method is shown in Figure 9 along with that of the oriented film sample. Some broadening of the d_{ggl} peak is observed in the pressed powder sample. The Zn-Cr LDH did not form oriented films and therefore was examined in the diffractometer as a pressed powder sample. This random orientation of platelets probably helped broaden its peaks.

Another factor which determines diffraction peak width is particle size. The synthesis of the Ca-Al and Li-Al LDHs featured a hydrothermal aging step. Aging increased particle size and in turn lead to sharper diffraction lines. The synthesis of the Zn-Cr LDH included no such aging step. Indeed, other workers 31,32 have found that the particles of this compound cannot be made larger through aging. The small particle size, along with the absence of carbonate, probably contributes to making Zn-Cr LDHs the most facile anion exchangers.

In a previous section the swelling behavior of alkyl sulfate intercalates of Zn-Cr LDH was discussed. The swelling behavior is a general property of the LDHs tested. Anion exchange reactions were carried out by using a 0.5 M

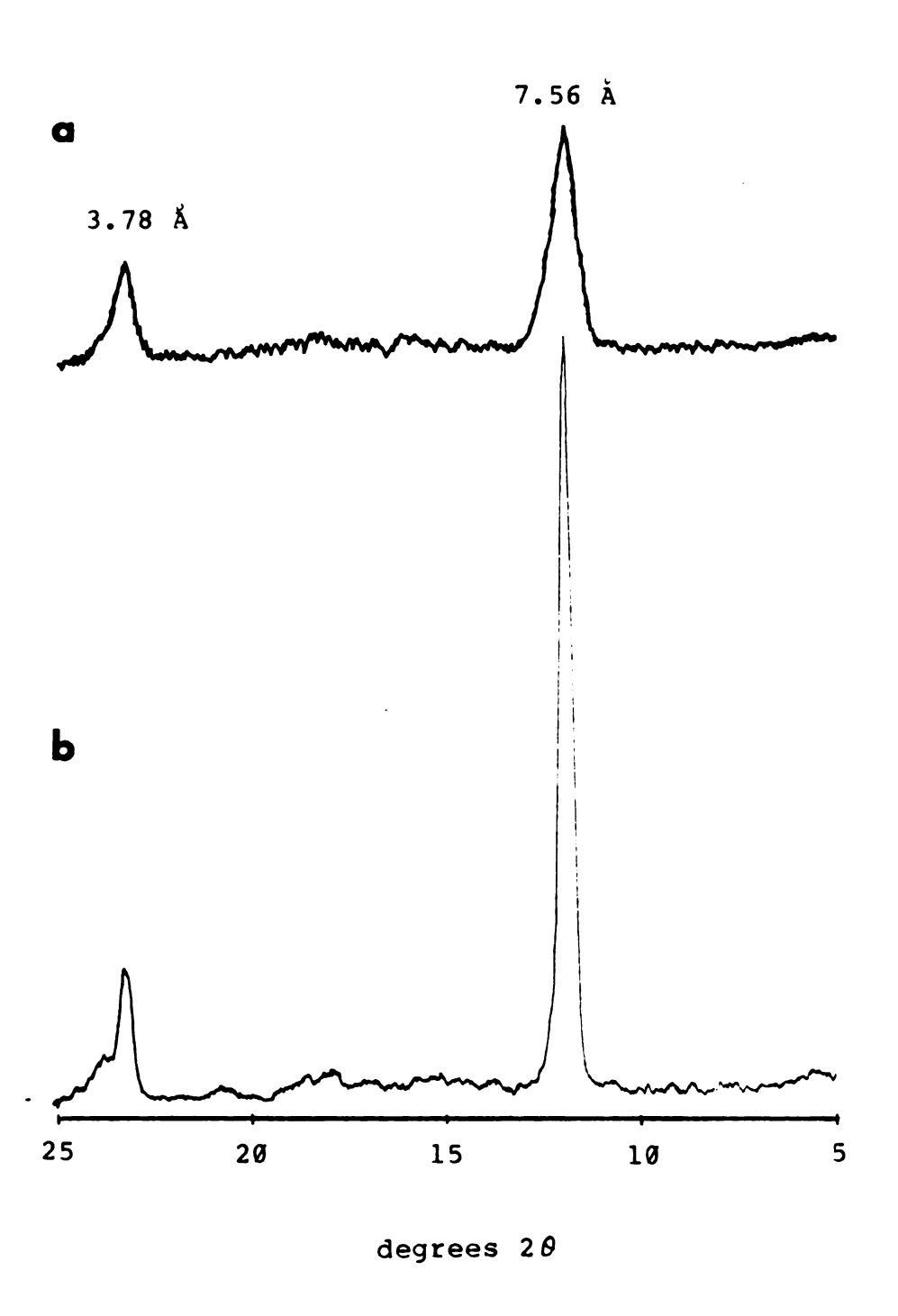


Figure 9. Powder x-ray diffractograms of [Ca₂Al(OH)₆] [0.5CO₃·2H₂O] (a). pressed powder; (b) oriented film.

solution of NaDDS with the three LDHs. X-ray diffractograms of the three intercalates are shown in Figure 10. Again the diffractograms of different LDHs with the same gallery anion are practically identical. The small differences (dgg1=22.6-24.5 Å; gallery heights=17.6-19.5 Å) were probably due to instrumental uncertainties at low angles and to so-called kink block structures. These result from differences in the carbon chain arrangement when long chain hydrocarbon species are intercalated in layer structures. When the three DDS-LDHs were immersed in n-octanol, all were swollen as had been previously reported for the Zn-Cr LDH. The gallery heights ranged from 30.4 to 33.9 Å. The x-ray diffractograms for the swollen species are given in Figure 11.

There was a dramatic change in surface properties of the three LDHs upon exposure to NaDDS solutions. The DDS seemed to have a strong affinity for the surfaces of the LDHs. The affinity was first indicated in washing the materials after exchange of DDS into the galleries. Removal of the excess electrolyte by centrifugation normally required 5-10 washings of the material after exchange. After exposure to DDS, however, 15-20 washings were required before foaming of the wash solutions ceased, indicating that excess NaDDS had been removed from the system. Upon drying, the DDS-exchanged materials were found to be hydrophobic to the extent that they floated on water. This behavior was completely opposite that of

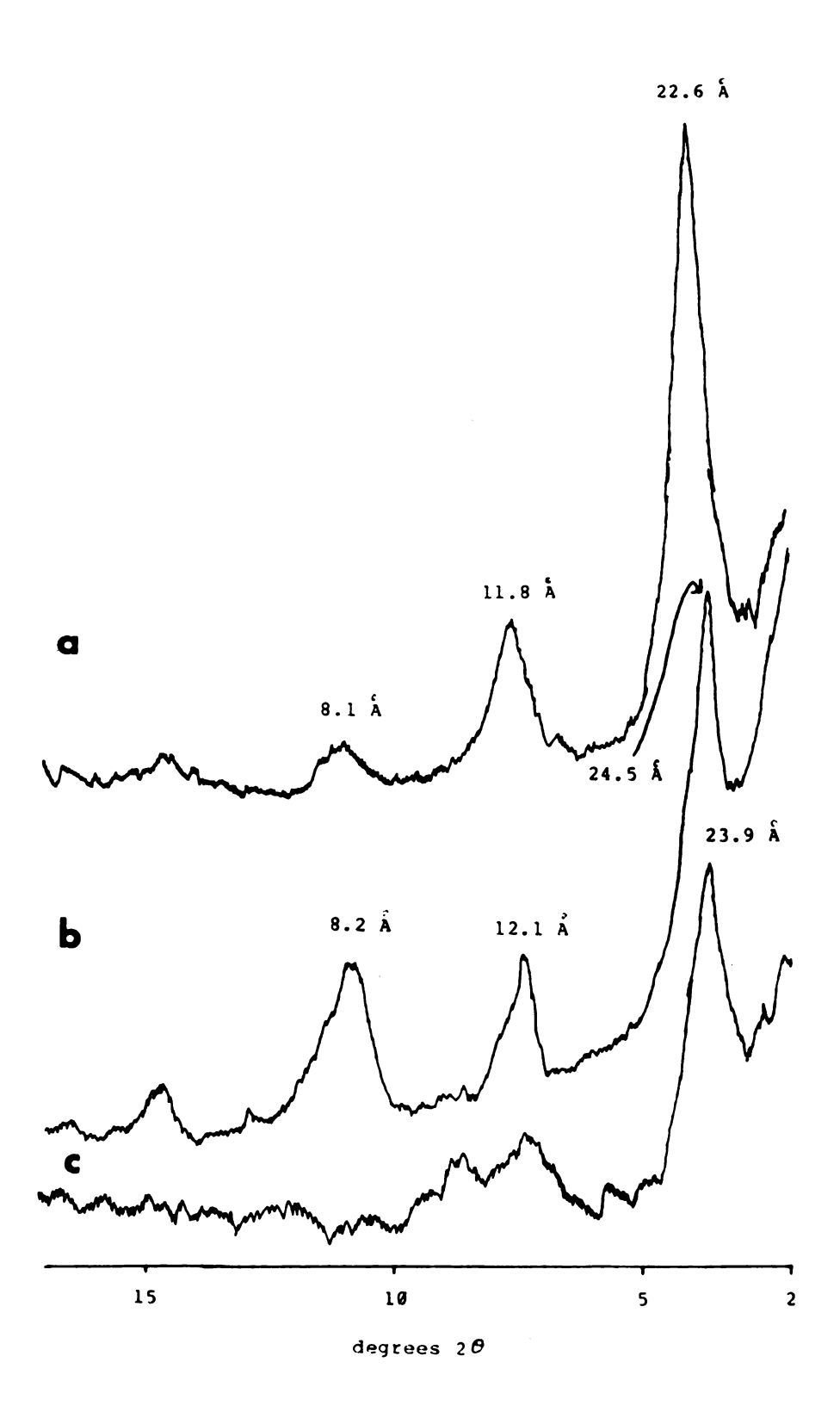


Figure 10. Powder x-ray diffractograms of the dodecyl-sulfate-exchanged forms of (a). Zn-Cr LDH; (b). Ca-Al LDH; and (c). Li-Al LDH.

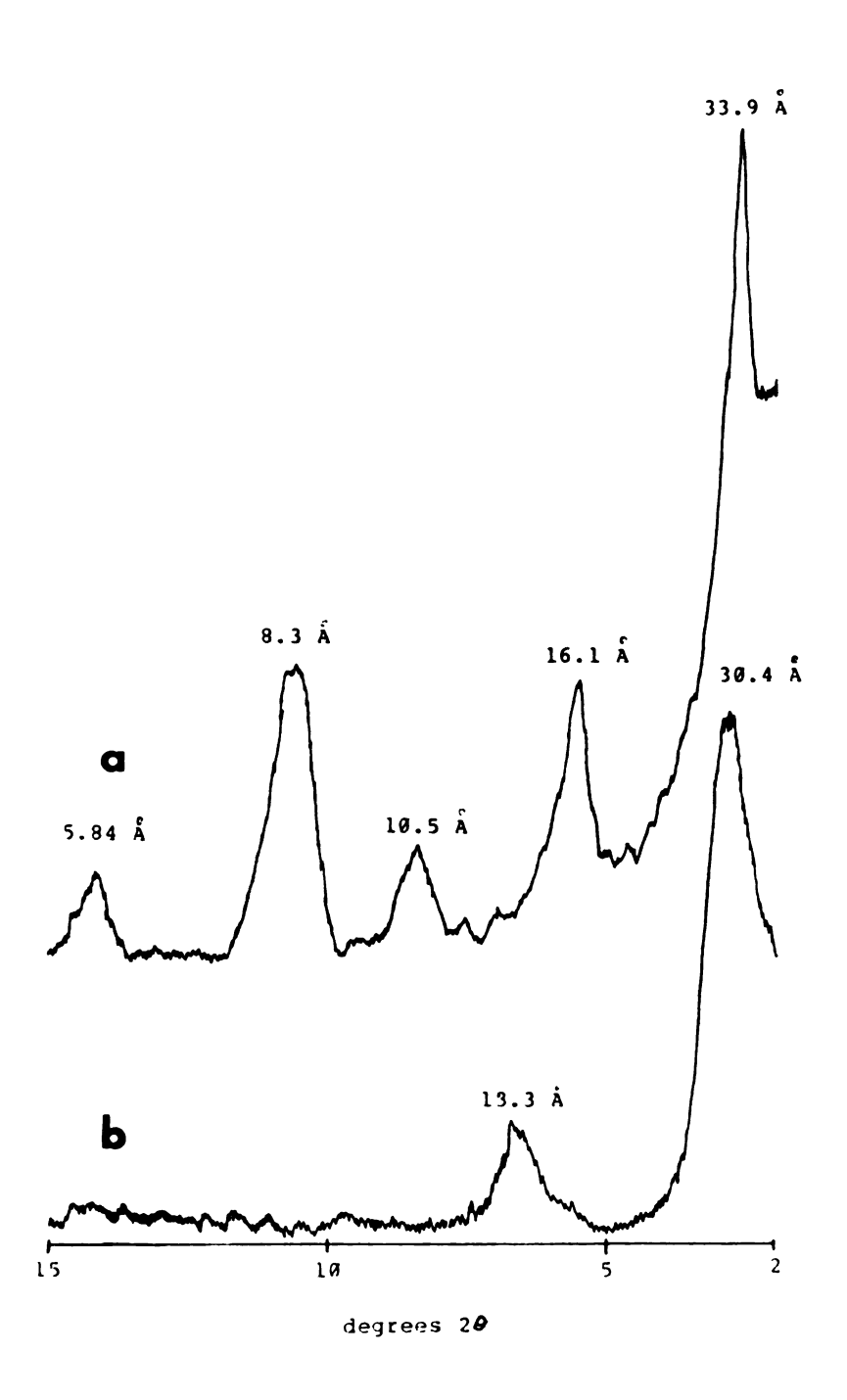


Figure 11. Powder x-ray diffractograms of n-octanol-swollen DDS-exchanged forms of (a). Ca-Al LDH; and (b). Li-Al LDH.

inorganic-anion exchanged LDHs. The pristine materials were all found to disperse in water, and also to be wetted by toluene and alcohols. When placed in the presence of both toluene and water, the water was preferred. The DDS materials dispersed in organic solvents but not in water. This behavior persisted even upon repeated washing in ethanol and acetone, sonification and repeated washing to remove the DDS from the surface.

The tenacity with which the DDS anion was attached to the surface of the LDHs is not unprecedented. It has been reported 104 that DDS $^-$ was strongly bound to $^-$ alumina through interaction of the -SO₃ tail of the anion with the hydroxide surface. The "fit" of the -SO₃ group to the surface groups was found to be very good, encouraging a strong electrostatic interaction. LDHs have a similar arrangement of hydroxide groups on the surface, plus a net positive charge in the layers not completely compensated by the gallery anions. Therefore, an even stronger attraction for DDS probably exists here than in the alumina. Additionally, $[Zn_2Cr(OH)_6][Cl^2H_2O]$ was exposed to a 0.1 \underline{M} solution of NaDDS for 30 seconds, then removed and washed as if an exchange had taken place. X-ray diffraction indicated that no exchange had occurred, but the material exhibited the same hydrophobic properties as the exchanged material had, indicating that the source of the change in properties was due to surface interactions. The IR spectra of pristine and DDS-exposed materials shown in Figure 12.

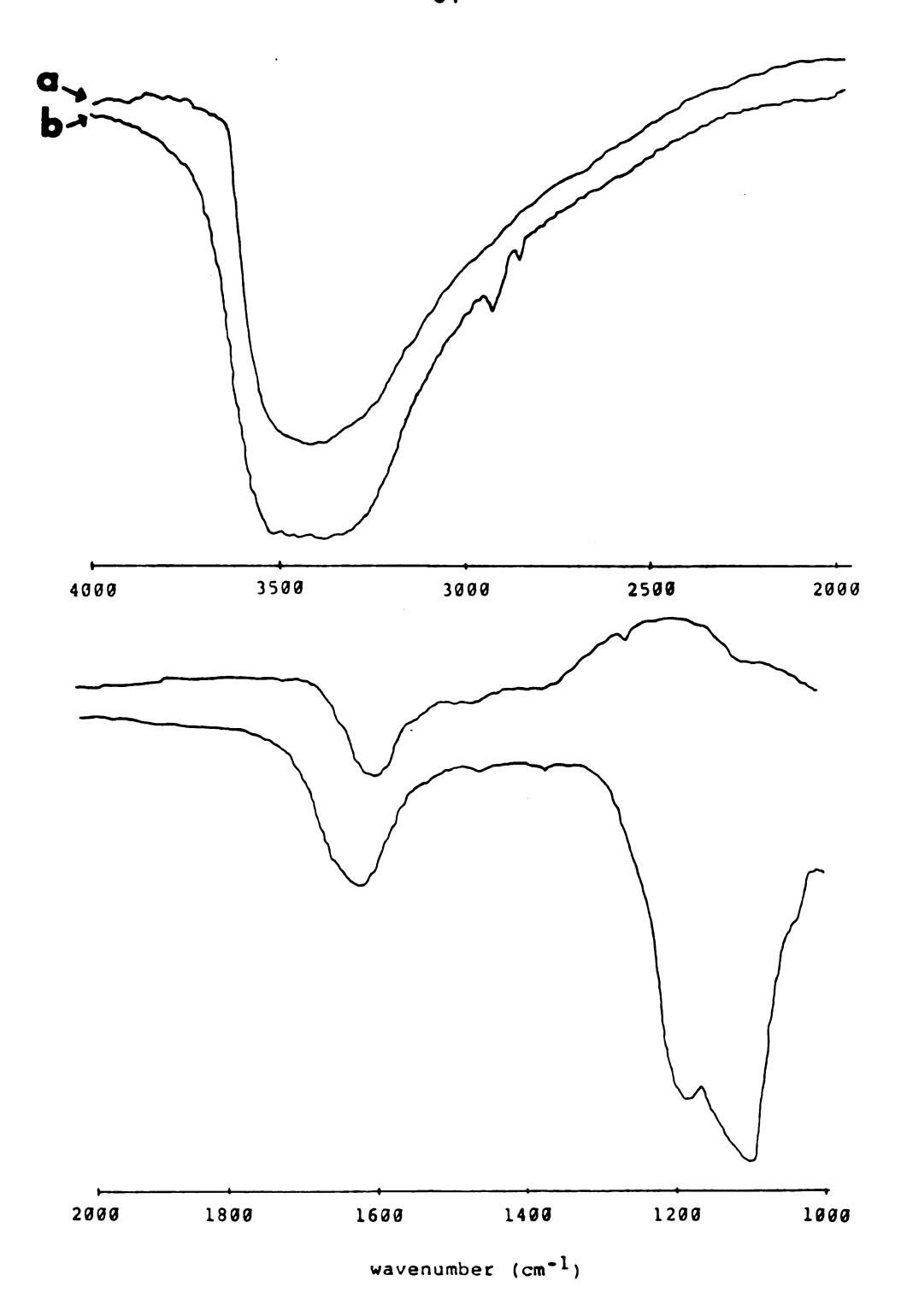


Figure 12. Infrared spectra from 4000 cm⁻¹ to 1000 cm⁻¹ of $[Zn_2Cr(OH)_6][Cl^*nH_2O]$ (a). pristine material; and (b). exposed to 0.1 \underline{M} NaDDS solution.

The presence of DDS is indicated by the C-H stretching bands near 3000 cm⁻¹ and bands at 1100 cm⁻¹ and 1175 cm⁻¹ due to S-O stretches of bound DDS. These IR data compare with those given for DDS on alumina, with S-O bands at 1200 cm⁻¹ and 1240 cm⁻¹. 104 The shift to lower energy of the S-O stretch in the present study is probably an indication of stronger binding of the -SO₃ group to LDHs. The authors also stated that after the first layer of DDS⁻ was attached to the surface, additional layers were adsorbed by cosolvation of the alkyl groups of bound and unbound anions. This phenomenon could account for the large number of washings required to remove excess NaDDS from an exchange mixture. The implications of this type of interaction will play a role in the interpretation of EPR data to be presented.

2. EPR Studies.

EPR spectroscopy has provided a probe into the mobility of gallery cations and anions of layered compounds. For smectite clays, paramagnetic metal cations such as Cu(II) and Mn(II) have been used as probes, 105,106 as well as the protonated form of the radical 4-amino-2,2,6,6-tetramethyl-piperidine-N-oxide (H+TEMPO).107 The PADS dianion has been used as a probe for intersalated smectites. The mobilities of these species in the galleries has led to work in which gallery cations in clays were used as catalysts, 108 and the triphase catalysis using intersalated clays outlined earlier.

In the present work, attempts were made to use the PADS dianion as a spin probe in LDHs. If LDHs were to be effective as solid reagents or solid phase transfer catalysts for nucleophilic displacement, freedom of movement of the gallery anions would be necessary. The nitroxide spin probes in general have been observed to tumble rapidly enough at 25 °C to completely average the anisotropies in g tensors and hyperfine values. As the tumbling of the anion in solution is restricted, the spectrum becomes increasingly anisotropic. The two limits of anion mobility give the two spectra shown in Figure 13.

The spectra obtained in this study were analyzed following an approach used by biophysicists studying mobility of spin probes in muscle tissue under conditions of varying water content. The relationships for the spin correlation times are shown in Equations 1 and 2. In these

$$\gamma_{i} = -2211W_{g}R_{-}/H_{g} \tag{1}$$

$$\gamma_{\lambda} = \emptyset.65W_{\emptyset}(R_{+}-2) \tag{2}$$

$$R_{+} = [(h_{g}/h_{+1})^{1/2}] + [(h_{g}/h_{-1})^{1/2}]$$
 (3)

equations, and are tumbling times in nanoseconds, W_g is the linewidth of the central peak in G and H_g is the magnetic field in G of the central peak. The symbols h_g , h_{+1} and h_{-1} represent the heights of the middle, low and high field peaks, respectively. The correlation time, $_C$, was the average of the two values from Equations 1 and 2. The equations used to obtain the correlation times are strictly valid only for isotropic rotation, but they are useful for

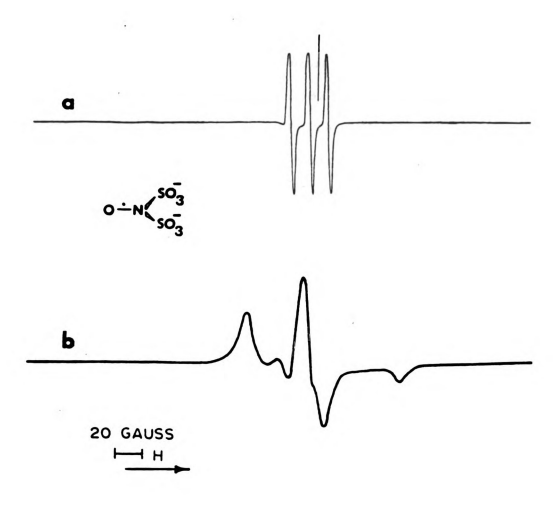


Figure 13. EPR spectra of K₂PADS (a). 10 $^{+5}$ M solution in DMSO; and (b). frozen in D₂O.

comparative purposes for studying anisotropic rotation at surfaces.

The first attempt to prepare samples for EPR analysis was made by trying an anion exchange reaction of a 0.1 M solution of K₂PADS into [Zn₂Cr(OH)₆][Cl·2H₂O]. The EPR spectrum of the resulting material is shown in Figure 14. As can be seen, if any PADS²⁻ were present, its signal was swamped out by the huge peak due to Cr(III). This spectrum is identical to one of the pristine Zn-Cr LDH. It was obvious from this experiment that an LDH with only diamagnetic constituents in the octahedral layers was need for EPR experiments.

The [LiAl2(OH)6][Cl'nH2O] synthesis with the PADS-doped LiOH solution was undertaken to provide just such a The EPR spectra of the material obtained are material. shown on Figure 15. Analysis of the top spectrum taken while the material was still damp gave a correlation time of 1.8 ns. This value was essentially the same as that observed in the doped hectorite intersalates maintained a 98% humidity. Drying the LDH material in a vacuum dessicator for 4 h and overnight produced more anisotropic EPR signals and correspondingly longer correlation times of 12.0 and 40.1 ns respectively. That the figures for damp material compared favorably with those of intersalated hectorite seemed to be a good sign that reaction of the gallery anions could take place in the LDHs as they had in the intersalates.

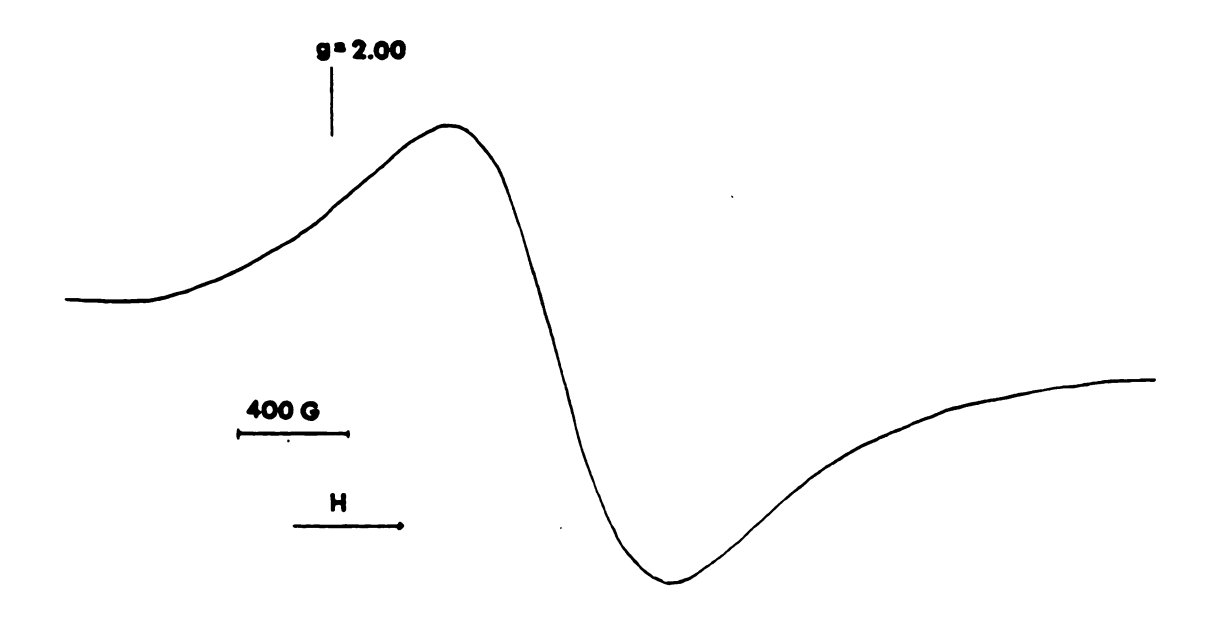


Figure 14. EPR spectrum of $[2n_2Cr(OH)_6][Cl^*nH_2O]$. Frequency = 9.14 GHz.

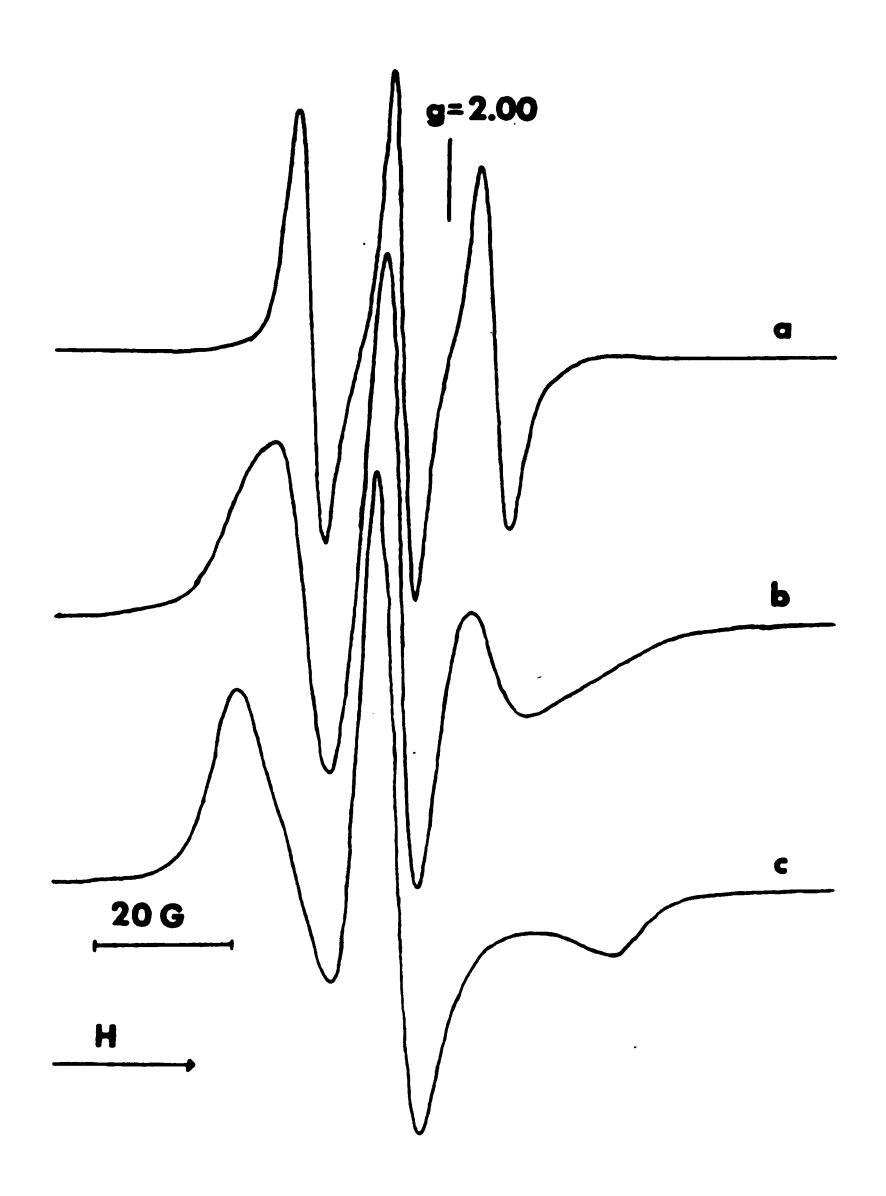


Figure 15. EPR spectra of PADS-doped [LiAl₂(OH)₆] [Cl^onH₂O] (a). damp material; (b). after 4 hr in vacuum dessicator; and (c). after 12 hr in vacuum dessicator. Frequency = 9.14 GHz.

The numbers were not reasonable, however, when the basal spacings of the species involved were considered. The $d_{\alpha\alpha 1}$ spacing of the intersalated hectorite was 31.5 Å, which corresponded to a gallery height of 6 Å when the thicknesses of the main clay layer and two layers of complex cation were subtracted. That a material with a basal spacing of 7.7 \hat{A} (gallery height= 2.9 \hat{A}) could exhibit the same degree of tumbling freedom seemed unreasonable. There was no doubt that the PADS species was present in the Li-Al LDH system since the blue color persisted through numerous washings and the material gave an EPR spectrum. The answer to the problem lies in the structure of PADS, shown in Figure 13. It contains -SO₃ groups of the same orientation as those found in DDS. The PADS dianion would bind more strongly than the DDS due to greater electostatic attraction. As the material was dried, surface water was removed, restricting the freedom of movement of the PADS on the surface. Even if some of the spin probe made it into the galleries, its signal was overpowered by that of the surface species.

To try to alleviate this adsorption problem, another synthesis of the Li-Al material was attempted. In this case, the LiOH solution was not only doped with PADS but also was 0.1 M in NaDDS. It was hoped that the greater concentration of DDS would block adsorption of PADS on the surface by blocking edge sites. In this way any PADS present in the product would be in the galleries. The EPR

spectra of the resulting materials are given in Figure 16, and a comparison of the correlation times obtained for this sample and the previously-prepared sample is given in Table As can be seen the correlation times for the two similarly treated products were practically identical. x-ray diffraction of the samples showed that Cl from the AlCl₂ solution had been intercalated in both cases. DDS concentration was not high enough for the larger DDS anion to be favored over the smaller Cl. The dianionic PADS should have been preferred over Cl-, since dianions have been found to possess a higher affinity for LDHs than monoanions. 1 Even with the surface of the LDH covered with DDS the surface concentration of PADS was larger than that of the gallery, if any were exchanged at all.

Later experiments cast further doubt on the validity of the interpretation of this work with Li-Al LDHs.

EPR Correlation Times for PADS-doped Li-Al LDH Table 9. Materials.

Material ^a	Drying Time ^b	c(nanoseconds)	
Li+Al+Cl	damp	1.8	
Li-Al-Cl	4 hr	12.0	
Li-Al-Cl	12 hr ^C	40.1	
Li-Al÷DDS	damp	1.8	
Li#AlaDDS	4 hr	11.8	
Li-Al-DDS	12 hr ^C	43.0	

^aPrepared by coprecipitation. Li-Al + DDS material had LiOH synthesis solution 0.1 M in NaDDS.

In vacuum dessicator.

Covernight.

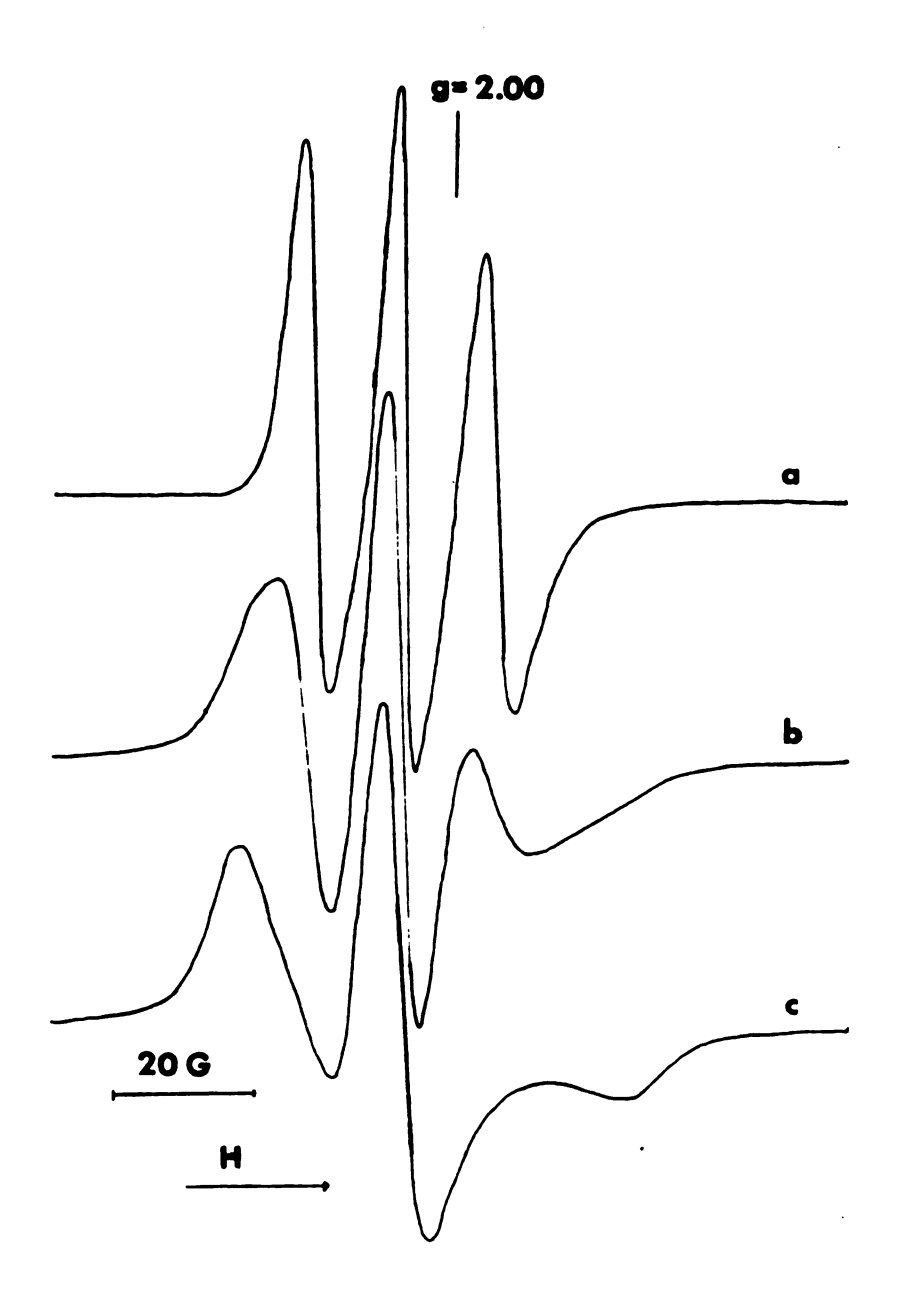


Figure 16. EPR spectra of an Li-Al LDH synthesized in the presence of NaDDS and K2PADS (a). damp material; (b). after 4 hr in vacuum dessicator; and (c). after 12 hr in vacuum dessicator. Frequency = 9.14 GHz.

		,	

freshly-prepared Li-Al LDH was placed in dialysis tubing to be washed free of excess electrolyte, only Al(OH), remained, as shown by the x-ray diffraction patterns in Figure 17. The diffractogram of fresh material shows the expected LDH pattern. When this material was dialysed, the second diffractogram results. Elemental analysis confirms that >98% of the Li⁺ had been removed. Material which had been hydrothermally treated after synthesis did not lose Li tupon dialysis. Gibbsite intercalated with lithium salts have been prepared 110 by heating LiX solutions with gibbsite. A powder x-ray diffractogram of a material prepared in this manner from gibbsite and LiCl is shown in Figure 18. It looks very much like the patterns obtained from LDHs. The Li⁺ in such species is removeable by washing with fresh water. From this data it was concluded that upon coprecipitation of Al(III) and Li(I) salts, an intercalated aluminum hydroxide is formed. When this material is treated hydrothermally, the Li⁺ ion is driven into the octahedral sheet. Reactions of this sort 111 also occur in montmorillonite, a smectite clay mineral with an empty site in its octahedral layer (Figure 3). These later results would have raised doubts as to the validity of any correlation times obtained had the PADS been successfully intercalated.

In summary, the reactions with PADS did not provide a mechanism to examine anion mobility in LDHs. A majority of the spin probe was apparently adsorbed on the surface of

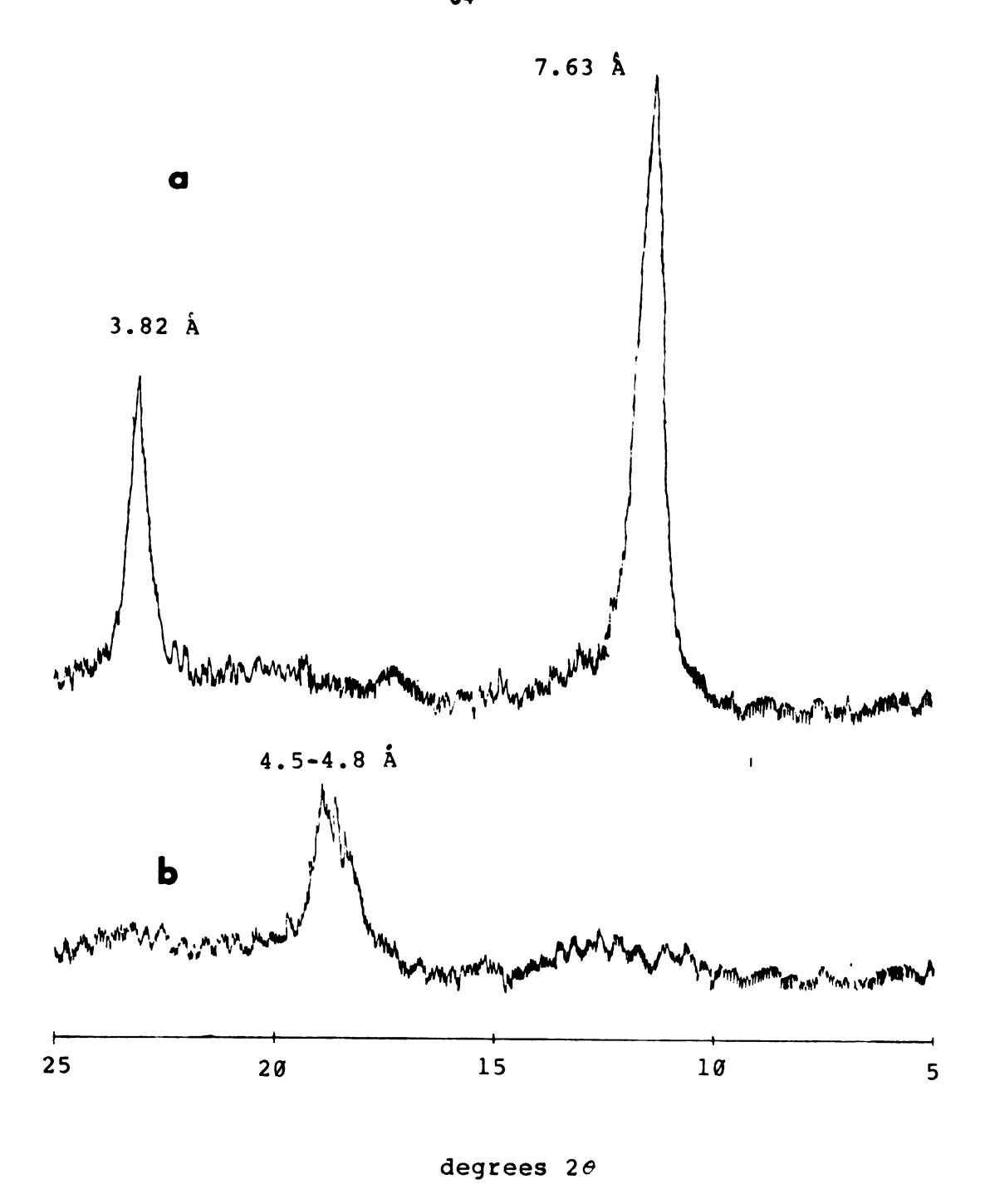


Figure 17. Powder x-ray diffractograms of unaged Li-Al LDH product (a). filter-washed; (b). dialyzed until free of electrolyte.

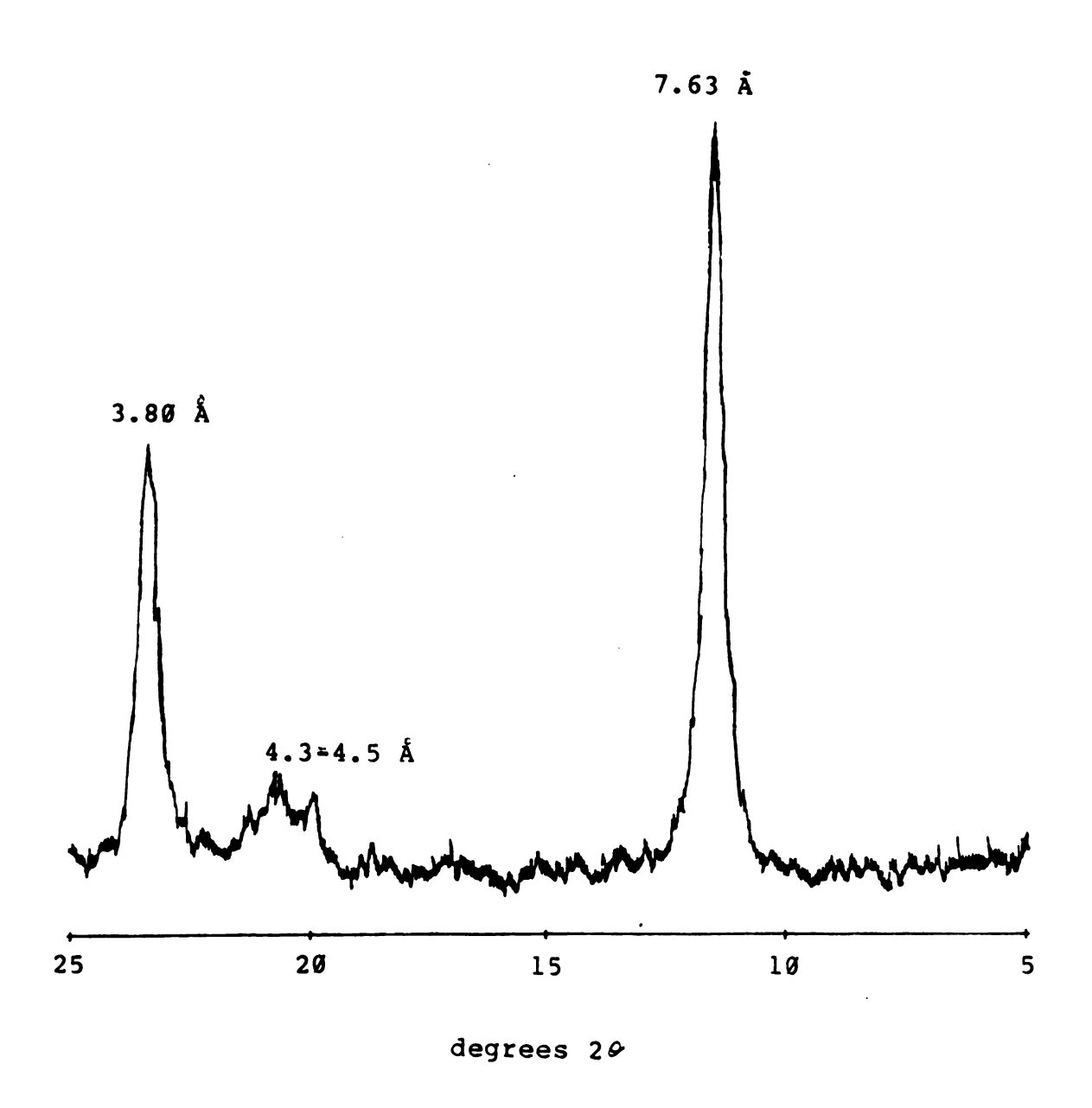


Figure 18. Powder x-ray diffractogram of product formed by reaction of LiCl solution and gibbsite.

the LDH in a manner analogous. As a result of the attempts to synthesize samples of an Li-Al LDH with PADS present, the variable structure of unaged Li-Al LDHs was discovered. EPR analysis could be helpful in studying the gallery if a different probe could be used, one which did no interact appreciably with the surface, such as an anionic complex of a paramagnetic transition metal.

- B. Nucleophilic Displacement Reactions.
- 1. Reactions Under Triphase Catalytic Conditions.

One of the main interests in developing the chemistry of anion exchangers was working toward an effective system for triphase catalysis. As outlined earlier, the requirements for a successful system include anion exchange capacity and sturdiness under reaction conditions. materials seemed to fit these two requirements. Questions remained as to the availability of the anions for nucleophilic attack under reaction conditions and about the ability of the solid to be regenerated under these con-Also, since the nucleophile for the reaction would be in a restricted environment, the possibility of size and/or shape selectivity existed. It was postulated that access to the anions might be more restricted for larger, bulkier alkyl halides than for smaller ones. these thoughts in mind the triphase reactions were carried out.

The choice of reactions to study was very large, as outlined earlier. Halide substitution reactions were chosen for study because of their simplicity and because of expertise developed in the group in previous work of this type. 99 Iodide substitution reactions of alkyl halides were chosen as the most likely to succeed because a). the nucleophilicity of the I species is greater than that of Cl and Br; and b). I substituted Zn-Cr LDH provides a larger basal spacing than Br or Cl forms and conceivably more space for a reaction to take place.

The results of the reactions are shown in Table These reactions were carried out for 24 h at 90°C and were vigorously stirred. The data seemed to indicate that some of the predicted behaviors were occurring. The larger

Conversion of Alkyl Halides by the Reaction RX + Table 10. Y → RY + X Under Triphase Consitions.a

RX	Y -	Solid ^b	% Conversion
1-C ₄ H ₉ Br	I	1 .	85.4
-C ₅ H ₁₁ Br	I	1	54.9
1-CcH ₁₂ Br	I	1	40.7
CH3CH(CH3)CH2CH2Br	I	1	30.4
-C ₄ H ₉ Br	Cl	1	9.2
IPC6H13Br	Cl	1	1.6
1-C4H9Br	I	2	88.6
ı÷C4HoCl	I	2	18.0
+C4H9Cl -C5H11Br	I	2	56.3

^aReaction conditions: reaction time: 24 hr; temperature: 90 °C; Y -/RX mole ratio: 6.0; RX/solid mole ration: 20.0; [Y⁻]_{aq}: 2.0 M; 2.0 mL toluene; 3.0 mL H₂O. bSolid 1: $[Z\bar{n}_2Cr(OH)_6][I^2.3H_2O]$ when Y = I; $[Zn_2Cr(OH)_6][Cl^2.2H_2O]$ when Y = Cl. Solid 2: $[Zn_2Cr(OH)_6][DDS^nH_2O]$.

alkyl halides were reacting more slowly than the smaller 1-bromobutane. Also, the branched alkyl halide, 1-bromo-3-methylbutane reacted more slowly than the straight-chain counterparts. The conversion of RBr to RCl was slower than conversion of RBr to RI. The low conversion for the chloride substitution reactions could be attributed to the energetic requirements for the replacement of intercalated C1 by Br, a process requiring lattice expansion of the LDH. All of these observations were interpreted as evidence that anions for reaction were coming from the galleries of the LDH.

However, the above data were open to another interpretation, one that was shown to be correct when blank experiments were carried out. The same reactions were performed with no solid in the mixture, but otherwise duplicating the conditions of the triphase reactions. Table 11 gives the results of the blanks. A comparison of the numbers in Tables 10 and 11 shows that the conversions are virtually identical. The conclusion drawn from these data was that the reactions were taking place much more rapidly at the organic-aqueous interface than at the solid. The selectivity toward smaller alkyl groups can be explained on the basis of decreased miscibility of longer alkyl groups with the aqueous phase. The observed selectivity toward iodide substitution reactions over chloride substitutions apparently arises from the greater miscibility with organic solvents of iodide over chloride.

Table 11. Results of Blank Reactions for Halide Exchange.

RX	ı -	% Conversion
n-C ₄ H _o Br	I	86.2
1+C5H11Br	I	57.9
CH2CH(CH2)CH2CH2Br	I	31.2
n=C ₄ H ₉ Br n=C ₅ H ₁₁ Br CH ₃ CH (CH ₃)CH ₂ CH ₂ Br n=C ₄ H ₉ Br	Cl	8.9

aReaction conditions: reaction time: 24 hr; temperature: 90 °C; Y /RX molar ratio: 6.0; [Y] aq: 2.0 M; 2.0 mL toluene; 3.0 mL H₂O.

The interpretation of these results was that the surface of the LDH was too hydrophilic to allow interaction of the organic reagent with the gallery anion under the reaction conditions. Since it was known that exposure to NaDDS solution made the surface more hydrophobic, some of the Cl form of Zn-Cr LDH that had been so treated was used in a series of triphase reactions. It was thought that the I would quickly displace the Cl under reaction conditions and that iodide substitution would proceed more readily on the hydrophobic surface. The results of the reactions are given in Table 10. The conversions with the DDS-treated materials were slightly higher than those of the plain I form. However, x-ray diffraction showed that even after 24 h at 90 °C the Cl had not been displaced from the gallery. Therefore none of the reaction was taking place with the gallery anions; indeed, none of the iodide even made it into the galleries. The increase in conversion when the DDS-treated LDH was used may have been due to increased interfacial surface area. The surface area of the DDS-

treated solid was found to be $15.0 \, \text{m}^2/\text{g}$ versus $7.7 \, \text{m}^2/\text{g}$ for the pristine material under air-dried conditions. The result of this experiment was to transform a material that was too hydrophilic for access by organic reagent into one that was too hydrophobic for interaction with the aqueous phase in the reaction mixture.

Under triphase reaction conditions with the untreated LDH the anions were unavailable for reaction with alkyl halides. The surface properties of the LDH seemed to be responsible. In order to test this hypothesis, another series of reactions was undertaken. In these reactions, the components of the triphase mixture were removed one or two at a time to study the effect on conversion. conditions of reaction and conversions are listed in Table These reactions were carried out under stoiciometric conditions. A dramatic improvement in conversion was noted when the water was removed from the system (11.5% vs.76.6%). This seemed to confirm that water on the surface was blocking access of the organic substrate to the anions. A series of experiments characterizing the availability and reactivity of gallery anions in relation to the surface properties of the LDHs proceeded from this point.

2. Stoichiometric Biphase Reactions in Toluene.

The probe reactions used in this portion of the research were the same as those used in the triphase reactions. Toluene was chosen as the organic solvent to

Table 12. Conversions of Nucleophilic Displacement Reactions of C_AH_QBr Under Modified Conditions.^a

Run	н ₂ о	toluene	1 mmol NaI	1 mmol LDH	% conversion
1	yes	yes	yes	no	51.6
2	no	yes	yes	no	Ø
3	yes	yes	no	yes	11.5
4	no	yes	no	yes	76.6

^a1.0 mmol C_4H_9Br present initially in all runs. 3.0 mL H_2O , 3.0 mL toluene present where indicated. Reactions run 24 hr at 90 ^{O}C . $^{D}[Zn_2Cr(OH)_6][I^2.3H_2O]$.

keep some continuity with previous work in the triphase area. The experimental procedure was designed to allow the conversion to product to be followed over the course of the reactions. Analysis of the conversion data would provide information about the kinetics of reaction and possibly a greater understanding of the mechanism of the reactions taking place.

Data treatment was simplified by the programmable plotter/integrator from which the percent conversion could be obtained directly. A flame ionization detector was used with this particular GC and meant that all conversions reported by the integrator were weight percent values. The weight percentages were converted to molar percentages by a routine on a programmable calculator before any subsequent data treatment.

Air-dried (A.D.) [Zn₂Cr(OH)₆][I·2.3 H₂O] was used in the initial studies of displacement reactions. The data collected from these reactions fit a first order kinetic expression with a high degree of correlation. From plots

of $-\ln(f_{RBr})$ vs. time, where f_{RBr} =the fraction alkyl bromide remaining unconverted, pseudo-first order rate constants were determined. Several kinetics plots are shown in Figure 19 with the values of k_{obs} and their 90% confidence limits given in Table 13. The data in this table indicate that the the values of k_{obs} did not vary to a significant extent with the length of the alkyl chain of RBr. The branched 1-bromo-3-methylbutane was the slowest of the reactions, suggesting that there was some steric hindrance in the reaction mechanism.

In the triphase systems, reactions on the solid were seemingly inhibited by the presence of water in the system. Since A.D. Zn-Cr LDHs had water on their surfaces, ³² it seemed reasonable that removing this surface water would accelerate the biphase reactions. Previous studies ³² had indicated that all the water could be removed from both the surface and galleries of the I-Zn-Cr LDH by heating the material to 150 °C under argon. Treatment at this

Table 13. Calculated Pseudo First Order Rate Constants, k_{obs}, for Iodide Substitution of Alkyl Bromides Over A.D. [Zn₂Cr(OH)₆][I·nHH₂O].

RBr	105 k _{obs} (s-1)b		
l-bromobutane l-bromopentane l-bromo-3-methylbutane l-bromohexane l-bromooctane	3.79 + 0.28 3.66 + 0.59 2.08 + 0.14 2.89 + 0.34 3.03 + 0.21		

aReaction conditions: temperature: 90 °C; 0.453 g (1.00 mmol) [Zn₂Cr(OH)₆][I·2.3H₂O]; 1.00 mmol RBr; 3.0 mL toluene; sampled every 10 min for 1 hr. b+ 90% confidence limit based on linearity of data fit.

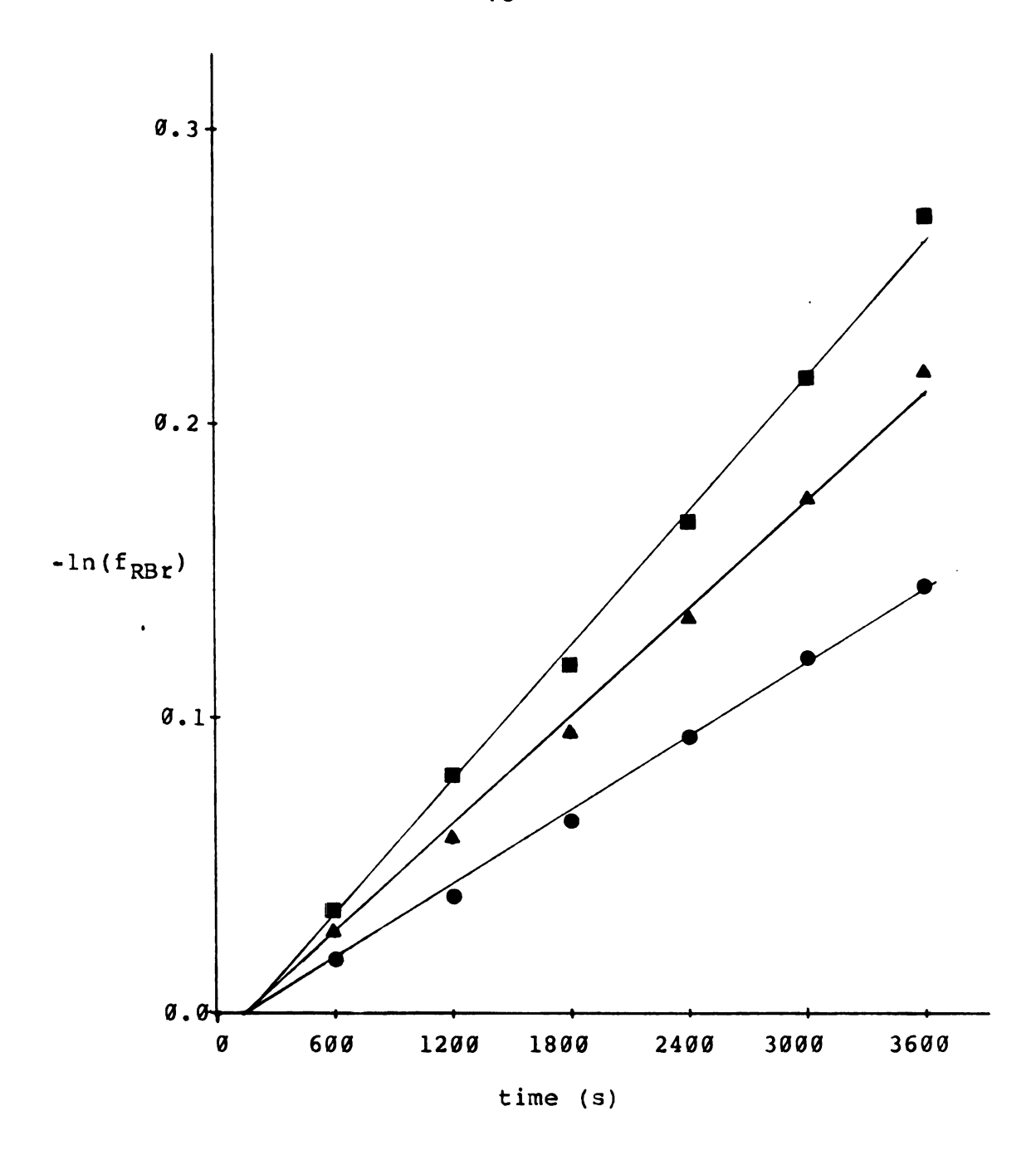


Figure 19. First order kinetic plots for iodide substitution of alkyl bromides over [Zn₂Cr(OH)₆] [I·2.3H₂O]: 1-bromobutane; 1-bromohexane; and 1-bromo-3-methylbutane.

temperature apparently did not cause any dehydroxylation of the octahedral layers. With these thoughts in mind, some of the I Zn-Cr LDH was treated at 150 °C for 2 h under Ar. Part of the IR spectrum of this material, along with that of an A.D. sample, is given in Figure 20. A comparison of the region from 4000 cm⁻¹ to 1000 cm⁻¹ shows the virtual disappearance of the bending modes of water around 1600 cm⁻¹ after heat treating. The OH-stretching region of the spectra, due mainly to the hydroxide groups of the octahedral layers, remains almost identical upon heat treatment.

When this O.D. material was used as the iodide source in the conversion of alky bromides, the kinetics results were similar to those obtained with the A.D. material. The data could be fit with a high degree of linearity to a first order rate expression. The values of for kobs obtained for O.D. materials are given in Table 14 along with their 90% confidence limits. The values obtained using O.D. LDH are approximately 3-4 times those of their A.D.

Table 14. Pseudo First Order Rate Constants, k_{obs}, for Iodide Substitution of Alkyl Bromides Over O.D. [Zn₂Cr(OH)₆][I·0H₂O].^a

RBr	10 ⁵ k _{obs} (s ⁻¹) ^b		
l-bromobutane l-bromopentane l-bromo-3-methylbutane l-bromohexane l-bromooctane	13.2 ± 0.92 12.7 ± 0.43 9.40 ± 0.26 12.1 ± 0.23 9.39 ± 0.11		

aReaction conditions: 90 °C; 1.00 mmol RBr; [Zn₂Cr(OH)₆] [I]; 3.0mL toluene; sampled every 10 min for 1 hr. b+ 90% confidence limits based on linearity of data fit.

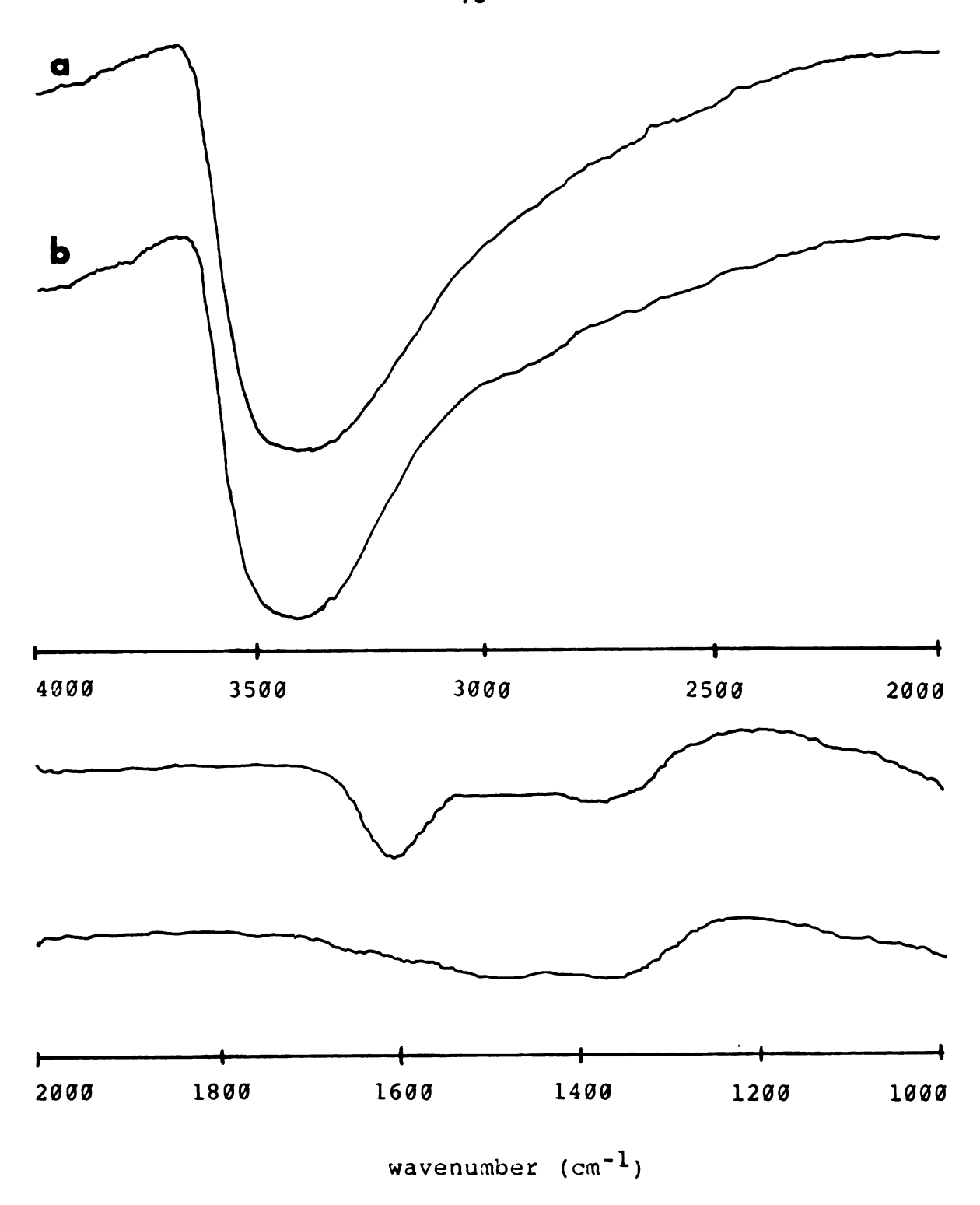


Figure 20. IR spectra from 4000 cm⁻¹ to 1000 cm⁻¹ of (a). $[2n_2Cr(OH)_6][I^*2.3H_2O]; (b). [2n_2Cr(OH)_6] [I^*\sim 0H_2O].$

counterparts. The increase in surface area upon drying the material was only approximately 25% $(7.7 \text{ m}^2/\text{g A.D. vs. 9.9} \text{ m}^2/\text{g O.D.})$, so increased surface area could not adequately account for the 3-4 fold increase in rates. This seemed to confirm the proposition that removing water from the surface did improve access to the gallery anion.

One of the experiments carried out to characterize the reactions measured the rate constants at different temperatures in order to calculate an Arrhenius activation energy and thermodynamic parameters of activation. The plots of kinetics data used to calculate activation parameters for 1-bromobutane are shown in Figure 21. The iodide substitution of 1-brompentane and 1-bromo-3-methylbutane were also carried out at different temperatures. The plot of $\ln k_{\rm obs}$ vs. 1/T for 1-bromopentane is shown in Figure 22. The values of the activation parameters for the three alkyl halides are given in Table 15, along with some values

Table 15. Activation Parameters for Some Alkyl Halide Iodide Substitutions at 90 Oc.a

RX	I' source	ΔH [‡] (kcal/mol)	4S* (cal/mol ^O K)	ref
	LDHb LDHb LDHb solution solution solution	13.1 ± 1.0 14.5 ± 1.3 15.1 ± 0.6 15.8 ± 1.0 16.3 ± 2.0 20.3	-40.6 ± 3.0 -36.8 ± 3.7 -35.7 ± 2.7 -7.6 ± 3 -16.4 ± 6 -15.4	this work this work this work 113 114

a+ 90% confidence limits for values from this work; source
of limits not stated in referenced material.
bO.D. [Zn₂Cr(OH)₆][I].

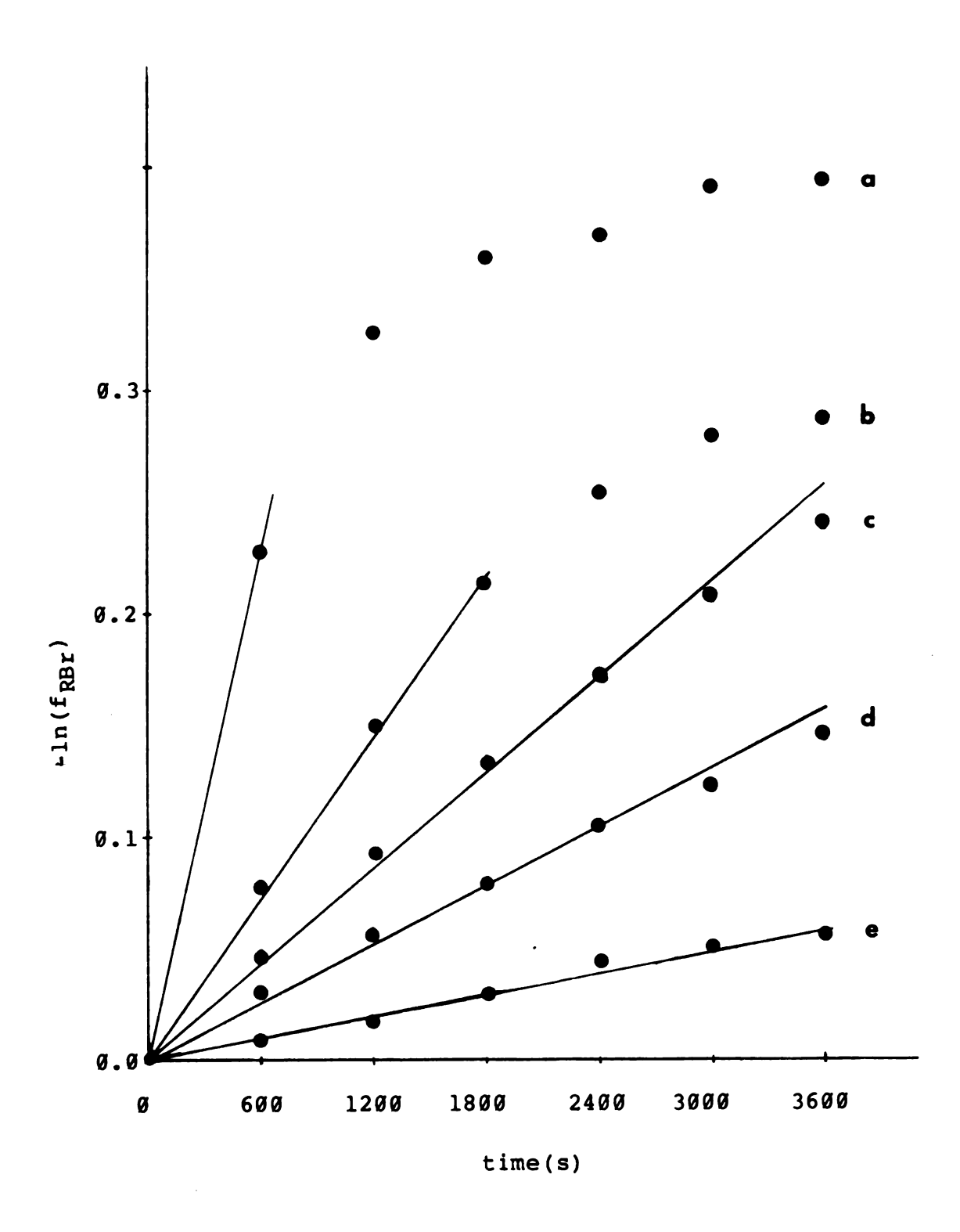


Figure 21. First order plots for iodide substitution of l*bromobutane over O.D. Zn/Cr/I LDH: (a). 120 °C; (b). 100 °C; (c). 90 °C; (d). 80 °C; and (e). 50 °C.

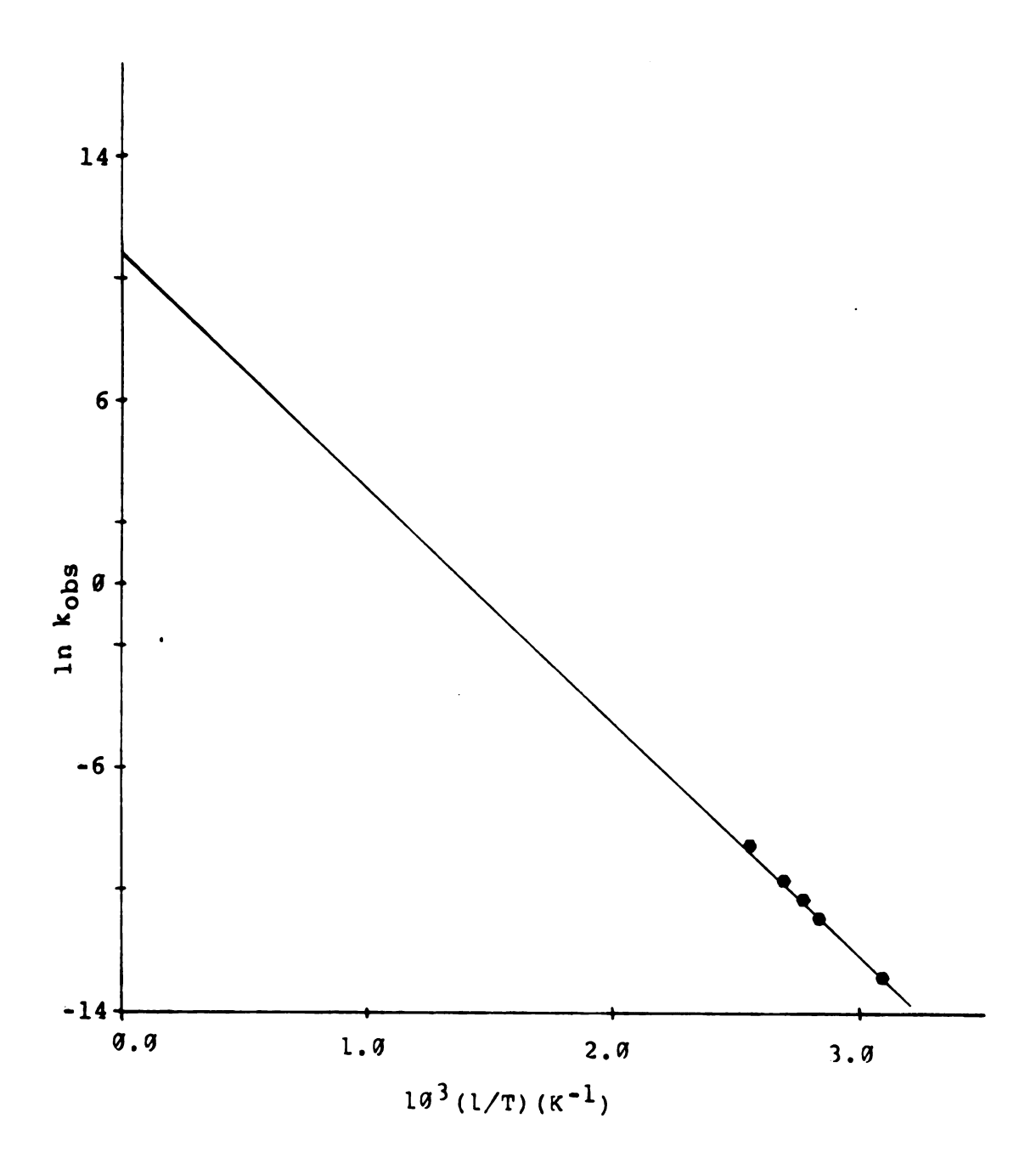


Figure 22. Arrhenius activation energy plot, $\ln k_{obs}$ vs. 1/T, for iodide substitution of 1-bromopentane over O.D. Zn/Cr/I LDH.

calculated for similar reactions in solution. 113,114

The values of ΔH^{ϕ} found for the reactions over solids and in solution were similar. This similarity was interpreted as evidence that the reactions over the solid were following a similar mechanism to that in solution, $S_N 2$ displacement. The negative values of ΔS^{ϕ} indicate a coming together of particles in the transition state, supporting the picture of a nucleophilic attack. The magnitude of entropy change was significantly larger for the reactions over solids as compared with their homogeneous cogeners. This difference was interpreted as evidence for the reaction taking place on the surface of the solid. The arranging of an adsorbed molecule into the special orientation required for reaction on the solid would conceivably be a more ordered state than the coming together of two particles in solution.

The activation data argued against another mechanism that could be postulated. That was one in which an equilibrium concentration of halide ion existed in the toluene solution and was responsible for the nucleophilic displacement reactions occurring. If this mechanism were operating, it seems that the ΔS^{\sharp} data would be approximately the same as that for the homogeneous reactions. Instead, the values are much more negative.

The data from gas-solid reactions also argue against a soluble nucleophile mechanism. As can be seen from the conversions for these reactions listed in Table 16 the

Table 16. Conversions of Gas-solid Iodide Substitutions of 1-Bromobutane Over [Zn₂Cr(OH)₆][I].^a

Temperature(OC)	% Conversion
90	38
130	64
140	74
150	80

^aReaction conditions: He folw rate: 3.0 mL/min; contact time: 0.20 s; total C_4H_9Br : 1.0 mmol; 1.0 mmol LDH treated 2 hr at 150 °C in He flow before reaction.

reaction proceeds in the gas phase from 90 $^{\rm o}$ C to 150 $^{\rm o}$ C. That the reactions proceeded in the gas phase at all where there was no solvent present suggests that the soluble nucleophile mechanism was certainly not necessary to explain the conversions in the solution phase.

Gas-solid chloride substitution reactions of 1-bromobutane were also performed. The conditions employed were identical with the iodide substitutions except that $[\mathrm{Zn_2Cr}(\mathrm{OH})_6][\mathrm{Cl}^*\mathrm{2H_2O}]$ was the solid phase in the reactor. The conversions are given in Table 17. The values are very close to the iodide substitution results. Chloride substitution of 1-bromobutane under solution-solid conditions

Table 17. Conversions of Gas-Solid Chlorinations of l-Bromobutane Over [Zn₂Cr(OH)₆][Cl].^a

Temperature(OC)	% Conversion	
90	33	
130	60	
140	71	
150	80	

aReaction conditions: He flow rate; 3.0 mL/min; contact time; 0.20 s; total C₄H₉Br: 1.0 mmol; 1.0 mmol LDH treated 2 hr at 150 °C under He before reaction.

gave a conversion of approximately 1% after 1 h, compared with 30-35% iodide substitution conversion. When fluoride substitution of 1-bromobutane with $[Zn_2Cr(OH)_6][F]$ was attempted under solution-solid and gas-solid reaction conditions, no conversion was noted. The significance of these data to the proposed mechanism of reaction mechanism will be discussed in a later section.

From this evidence, then, it appeared that the mechanism was one of adsorption of RBr onto the solid, followed by the rate determining step of nucleophilic displacement, then desorption of product. This chain of events is illustrated by Scheme 2.

The questions that remained at this point concerned the relative availability of all the anions in the solid and the importance of the adsorption properties of the solid to the course of the reaction. These problems will be addressed.

In the reactions at 90 °C of alkyl bromides with toluene as the solvent, pseudo-first order kinetics behavior was observed for the first hour of reaction. When reactions were carried out for longer periods of time, deviations from first order behavior occurred. The first order plot for extended iodide substitution of 1-bromobutane is shown in Figure 23. The graph clearly shows the

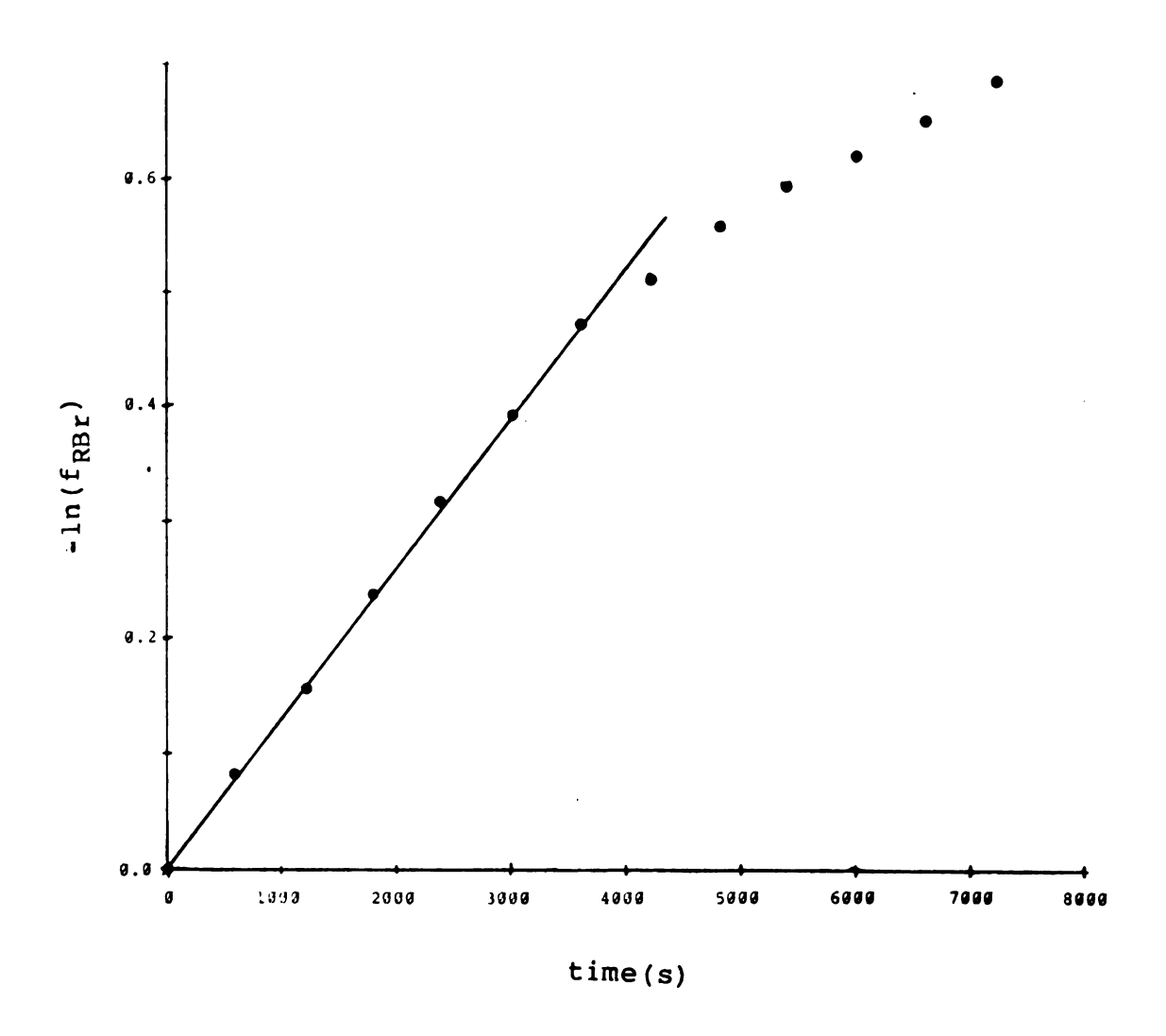


Figure 23. First order kinetic plot for the extended iodide substitution of labromobutane over O.D. Zn/Cr/I LDH.

deviation from first order behavior. The data from reactions carried out a higher temperatures also sheds some light on the situation. An examination of the data given in Figure 21 for reactions a 100 $^{\rm O}$ C and 120 $^{\rm O}$ C reveals deviation from first order behavior at values of $-\ln(f_{\rm RBr})$ of 0.35-0.40, corresponding to conversions of 30-35%. This was also the region of the plots at 90 $^{\rm O}$ C at which first order behavior was no longer observed.

Two explanations could be advanced to explain this behavior. The first has to do with the availability of gallery anions. It seemed reasonable to assume that as more of the I⁻ was consumed and replaced by Br⁻ in the galleries of the LDH, the remaining I⁻ would be relatively inaccessable compared with that near the outside edges of the particles. Perhaps 35% conversion, the point at which deviation from first-order behavior became pronounced, was the value at which access to I⁻ became the rate controlling factor of the reaction.

This hypothesis was easily tested. Reactions were run at 90 °C with excess alkyl bromide, but were otherwise identical to previous reactions. The data from the reactions run a 2-, 3-, and 4-fold excess of 1-bromobutane plotted as first order data are shown in Figure 24. The data was not very revealing until it was plotted in a different manner. Since the stoichiometry of the reaction was known, as was the initial ratio of RBr to I⁻, it was possible to calculate the fraction of the initial amount of

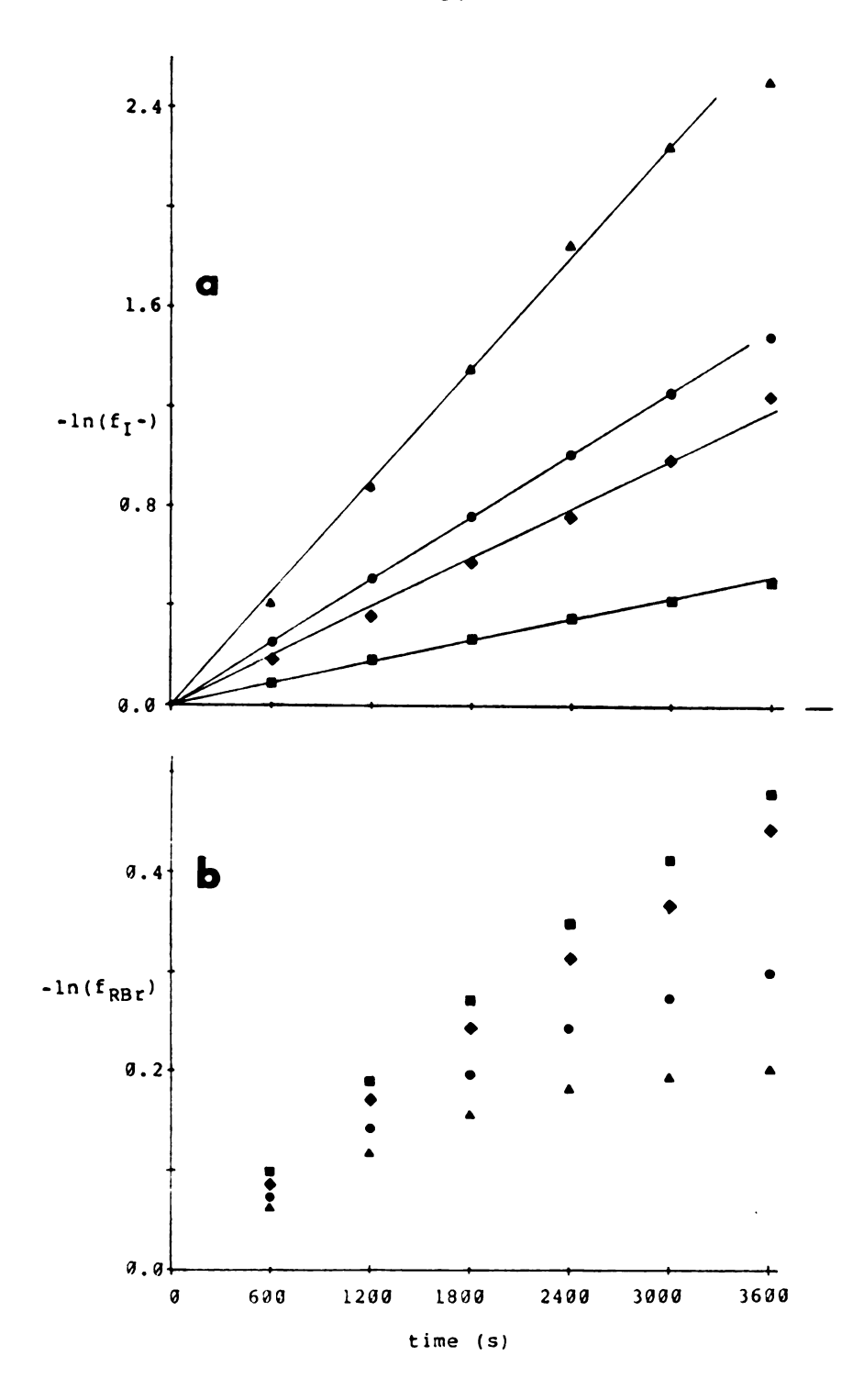


Figure 24. First order kinetic plot for iodide substitution of 1-bromobutane by 0.D. Zn/Cr/I LDH at RBr/LDH ratios of \blacksquare 4:1; \spadesuit 3:1; \spadesuit 2:1; \blacktriangle 1:1, plotted as functions of (a). \leftharpoonup 1n f_I $^{\bot}$; (b) \lnot 1n f_{RBr}.

I remaining (f_I -). When the data were plotted as $-\ln(f_I$ -) vs. time, the results shown in Figure 24a were obtained. These plots were linear out to a consumption of 85-90% of gallery iodide when a 4-fold excess of RBr was used. These data suggested that the rate of iodide substitution was not related to what was going on in the galleries of the LDH.

The linearity of the plots calculated from f_I - indicated that the proper statement of reaction kinetics was that the reaction was pseudo-first order in f_I - for the first hour of reaction. Under the original reaction conditions, where f_I - = f_{RBr} , this distinction was not made. It now seemed that the reaction would follow pseudo-first order kinetics as long as the surface concentration of RBr was kept approximately constant.

The data supported the other possible explanation for the deviation from first order behavior after 30-35% conversion. This explanation had to do with the adsorptive properties of the LDH. In the first stages of the reaction, the reactant molecules were competing for adsorption sites on the solid with the solvent. Later in the reaction, as iodide substitution product was accumulated, it would begin to compete for adsorption sites also. If the affinity of the product for the solid were comparable to that of the reactant, which seemed likely given the similarities in structure, fewer reactive sites would be available for the reactant, slowing the reaction. Knowledge of the adsorptive properties of the solids

involved would be useful in understanding the reactions taking place. Therefore, adsorption studies of the Zn-Cr LDHs were undertaken.

3. Adsorption Properties of Zn-Cr LDHs.

In general the affinities of solids for vapors can be determined by measuring adsorption isotherms for adsorption at two different temperatures. The Clausius-Clapeyron equation is then applied to calculate an isosteric heat of adsortion, $q_{\rm st}$, as shown below:

$$q_{st} = -R \left(\frac{d (\ln p)}{d (1/T)} \right)_{\theta}$$
 (4)

In this equation, Θ is the surface coverage. From adsorption isotherms, pressure and temperature data are entered into the equation for points from the two isotherms of the same surface coverage. For the isotherms described here surface coverage was expressed in mmoles adsorbed per mg of solid. Physical adsorption is a spontaneous process and as such the free energy change is negative. Since the change in entropy is always positive when a gas is changed to a more ordered adsorbed state, the enthalpy of adsorption must always be negative. The values calculated using by Equation 4 are positive for physical adsorption. The sign convention was adopted so that the numbers to be dealt with would be positive. To convert to an isosteric enthalpy of adsorption one must change the sign on q_{s+}. The adsorption of a vapor can be viewed as a two-step process, as shown in Scheme 3.

The value of ΔH^g_{ads} is the inthalpy change that is calculated from the two adsorption isotherms by using the Clausius-Clapeyron equation. The value which has bearing

on the reactions under study that are carried out under solution-solid conditions is ΔH^1_{ads} , the enthalpy of adsorption of a liquid phase species onto the surface of a solid. The equations in Scheme 3 may be rearranged to calculate ΔH^1_{ads} as shown in Scheme 4.

Adsorption studies of toluene and 1-iodobutane by $[Zn_2Cr(OH)_6]$ [InH2O] were undertaken. These isotherms for both the A.D. and O.D. materials are shown in Figures 25 and 26. The isotherms for 1-bromobutane shown in Figure 27 were measured for adsorption onto the Br form since adsorption onto A.D. I material resulted in reaction to form 1-iodobutane. The solvent source was maintained at 18 $^{\circ}$ C for those isotherms measured at room temperature (22 $^{\circ}$ C) and at 0 $^{\circ}$ C for isotherms recorded at 0 $^{\circ}$ C. The p_{o} in the p/p_{o} expressions refers to the saturation pressure of the adsorbate at the temperature of the adsorbent.

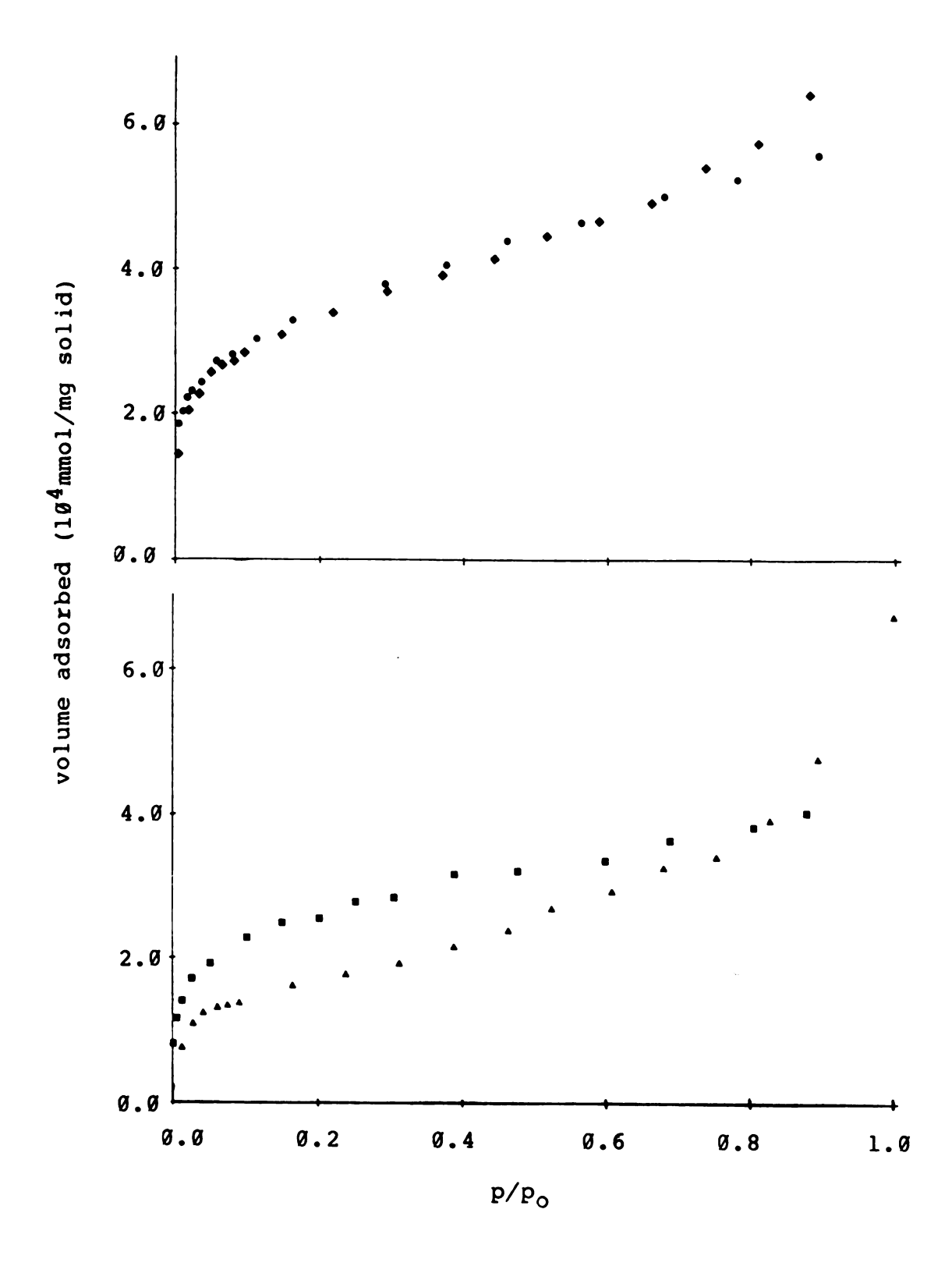


Figure 25. Isotherms for adsorption of toluene onto: (a).

A.D. Zn/Cr/I LDH at $\phi 0$ °C; $\phi 22$ °C; (b). O.D.

Zn/Cr/I LDH at $\phi 0$ °C; $\phi 22$ °C.

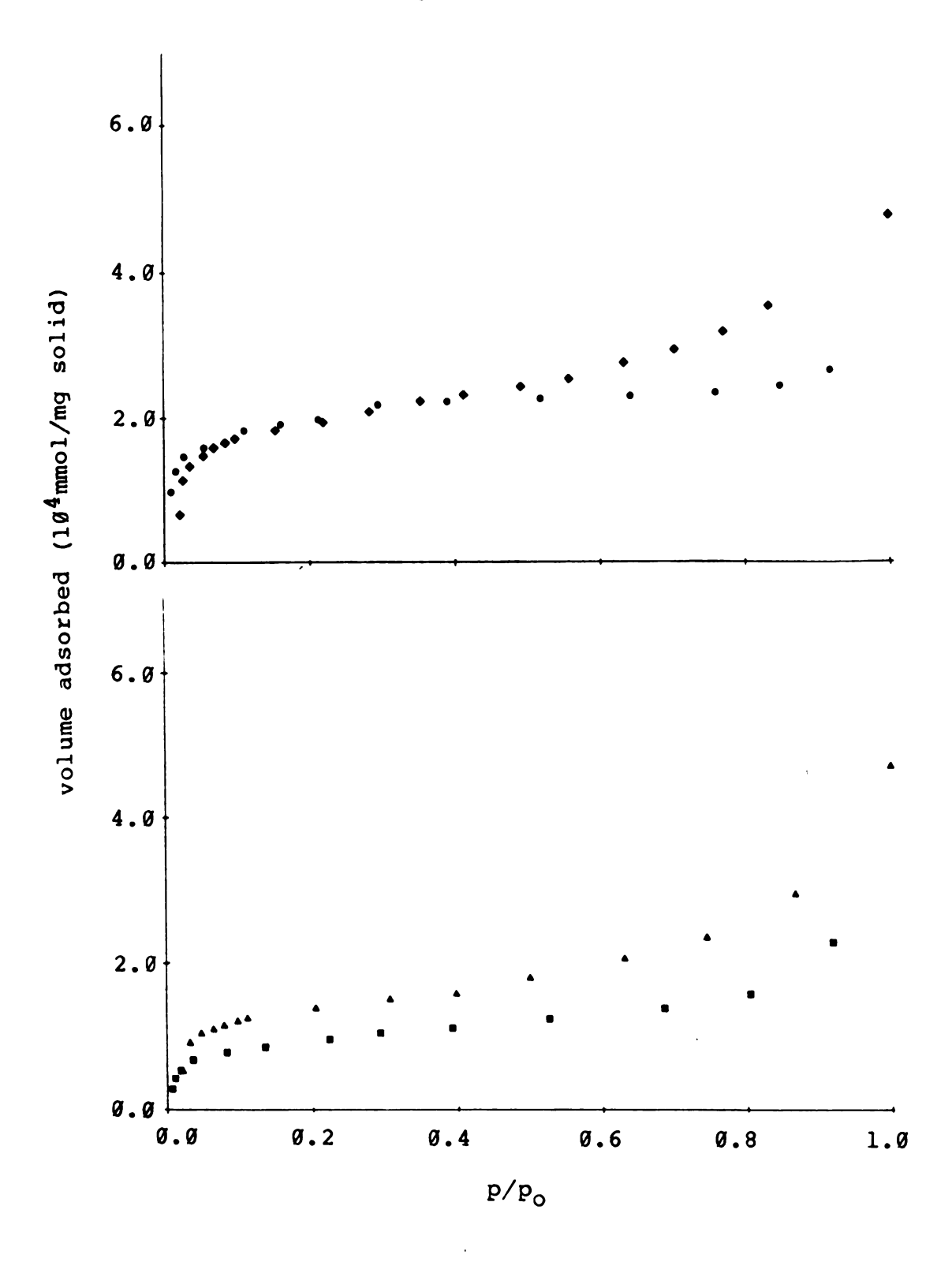


Figure 26. Isotherms for adsorption of 1-iodobutane onto:
(a). A.D. Zn/Cr/I LDH at ◆0 °C; ● 22 °C; (b).
0.D. Zn/Cr/I LDH at ▲0 °C; ■22 °C.

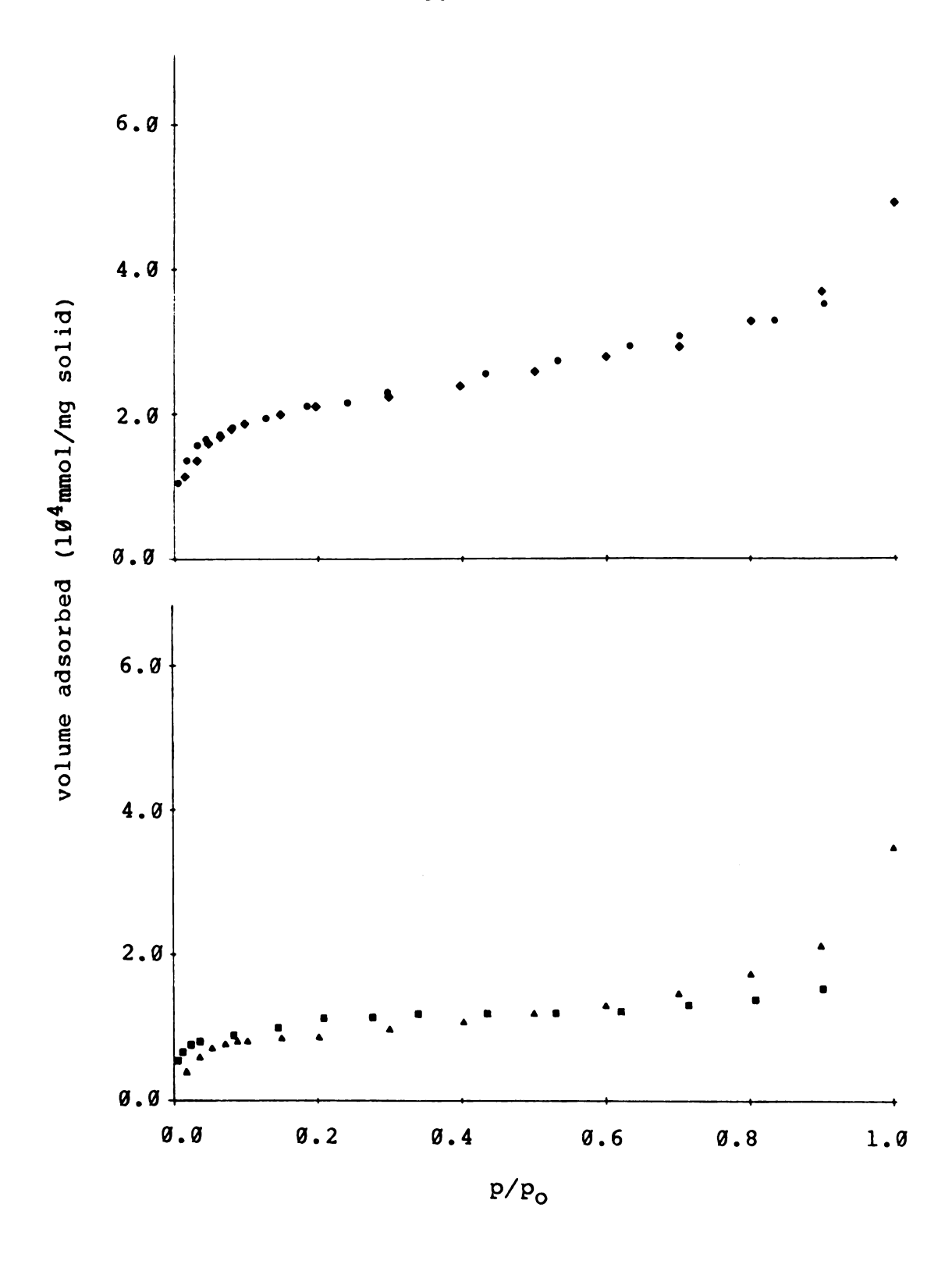


Figure 27. Isotherms for adsorption of 1-bromobutane onto:

(a). A.D. Zn/Cr/Br LDH at $\phi \emptyset$ °C; $\phi \ge 22$ °C; (b).

O.D. Zn/Cr/Br LDH at $\phi \emptyset$ °C; $\phi \ge 22$ °C.

Isosteric heats of adsorption were calculated for these systems. For a given specific adsorption volume at 0 °C, a value of pressure was interpolated from the room temperature isotherm. This procedure produced a (p,V) point from each curve so that a value of q_{s+} could be calculated at that point. The procedure was repeated for each point on both curves to generate pairs of (p,V) data. These values were plotted as so-called heat curves as function of V/V_m , the fraction of monolayer coverage. The values of $\boldsymbol{v_{m}}$, the volume of adsorbate required for monolayer coverage of the adsorbent, were calculated for each adsorbate by using the isotherms. Adsorption isotherms can generally be broken down into three regions (Figure 28): (1) a non-linear region at low values of p/p_0 ; (2) a linear region at midrange values of p/p_0 ; and (3) another non-linear region at high partial pressures. The transition point between the first two regions, the so-called Point B, has been $postulated^{117}$ to be the point at which monolayer coverage is completed since the uptake of adsorbate is changing in character most rapidly at this point. Point B analysis has proved successful in calculating monolayer coverages, yielding good agreement in surface area measurements with N_2 B.E.T. measurements. 115,117 The agreement was good for a variety of adsorbates on different adsorbents. values for the present study were estimated from the isotherms at the two temperatures studied and averaged. heat curves are given in Figures 29-31. Plots of AH ads

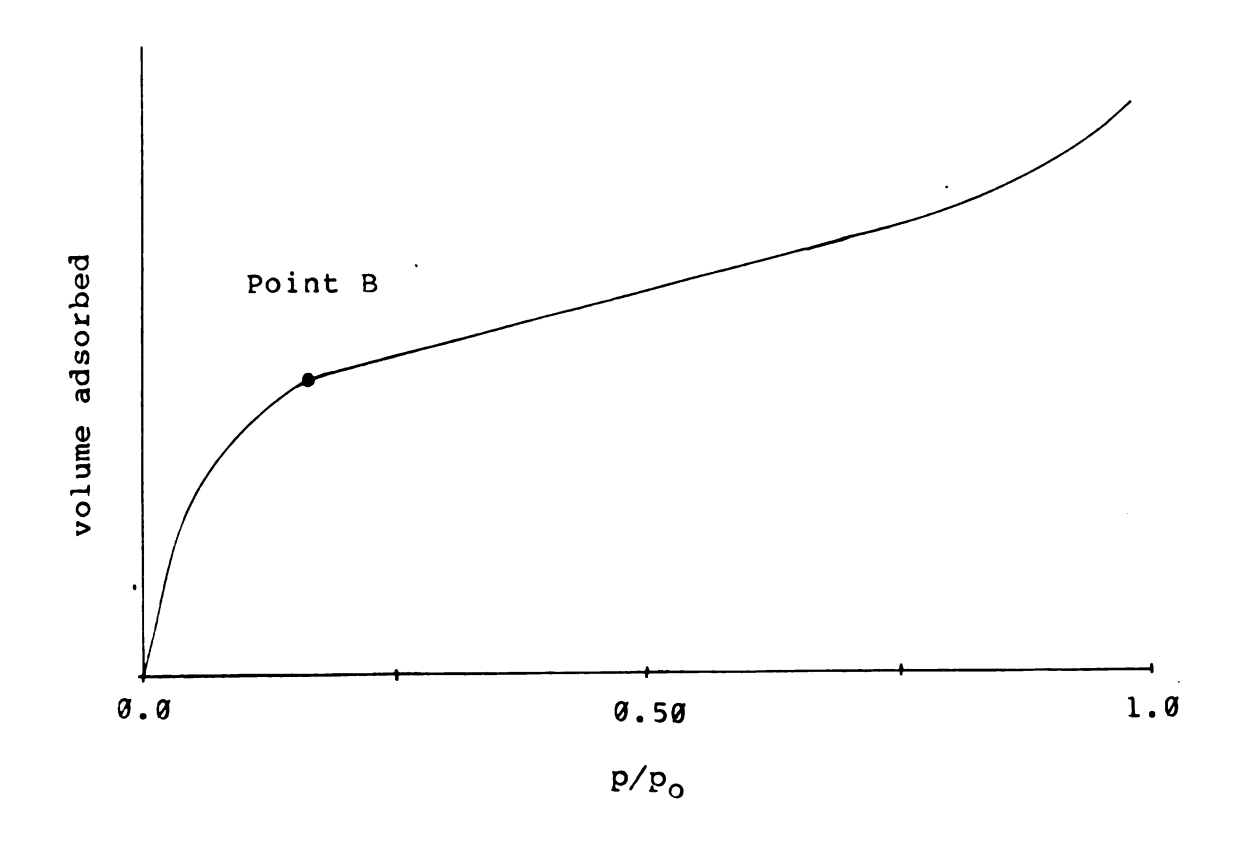


Figure 28. An adsorption isotherm showing the location of Point B, the attainment of monolayer coverage.

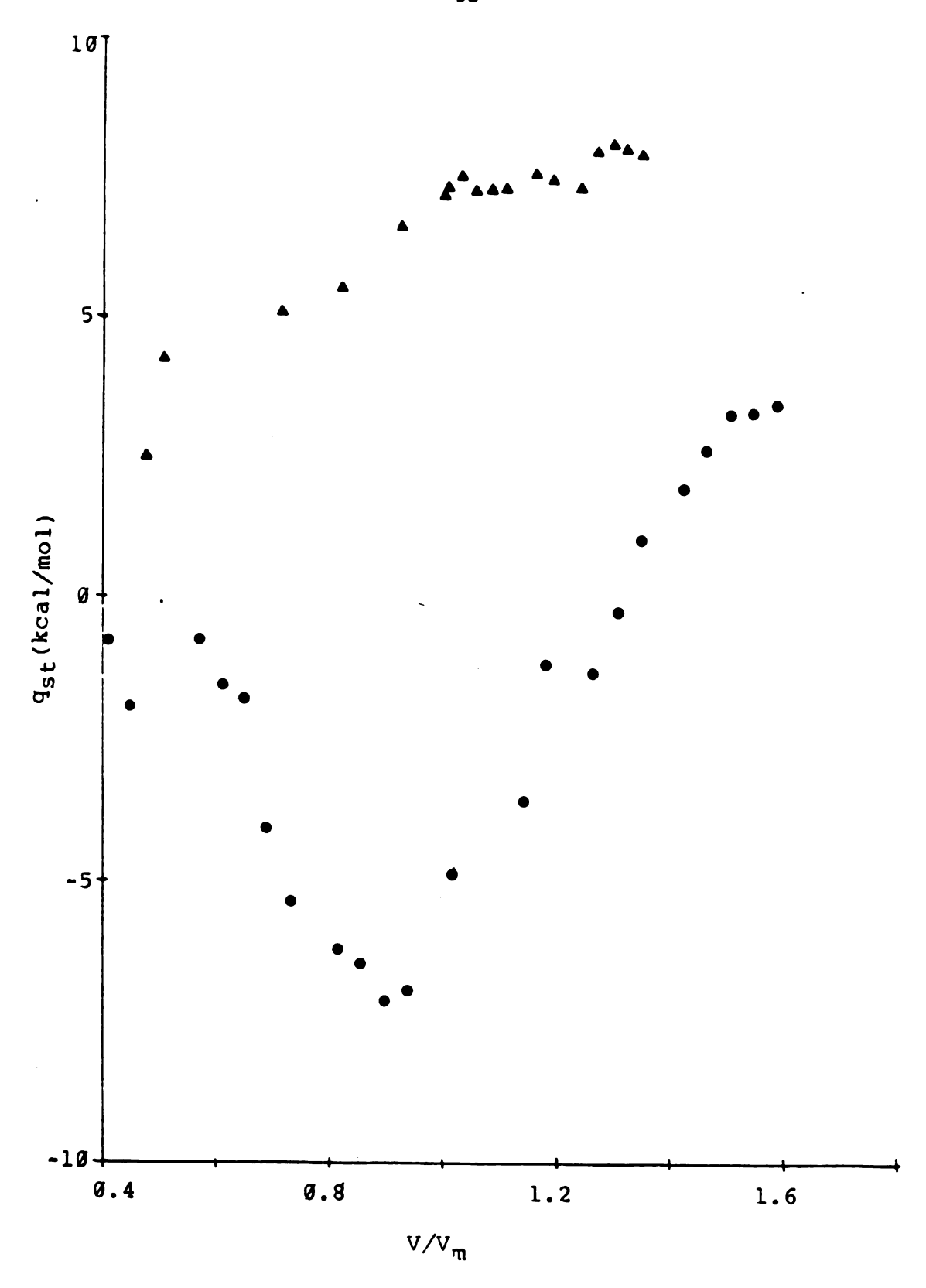


Figure 29. Heat curves, q_{st} vs. V/V_m, for adsorption of toluene onto [Zn₂Cr(OH)₆][I·nH₂O] ▲A.D. ●O.D.

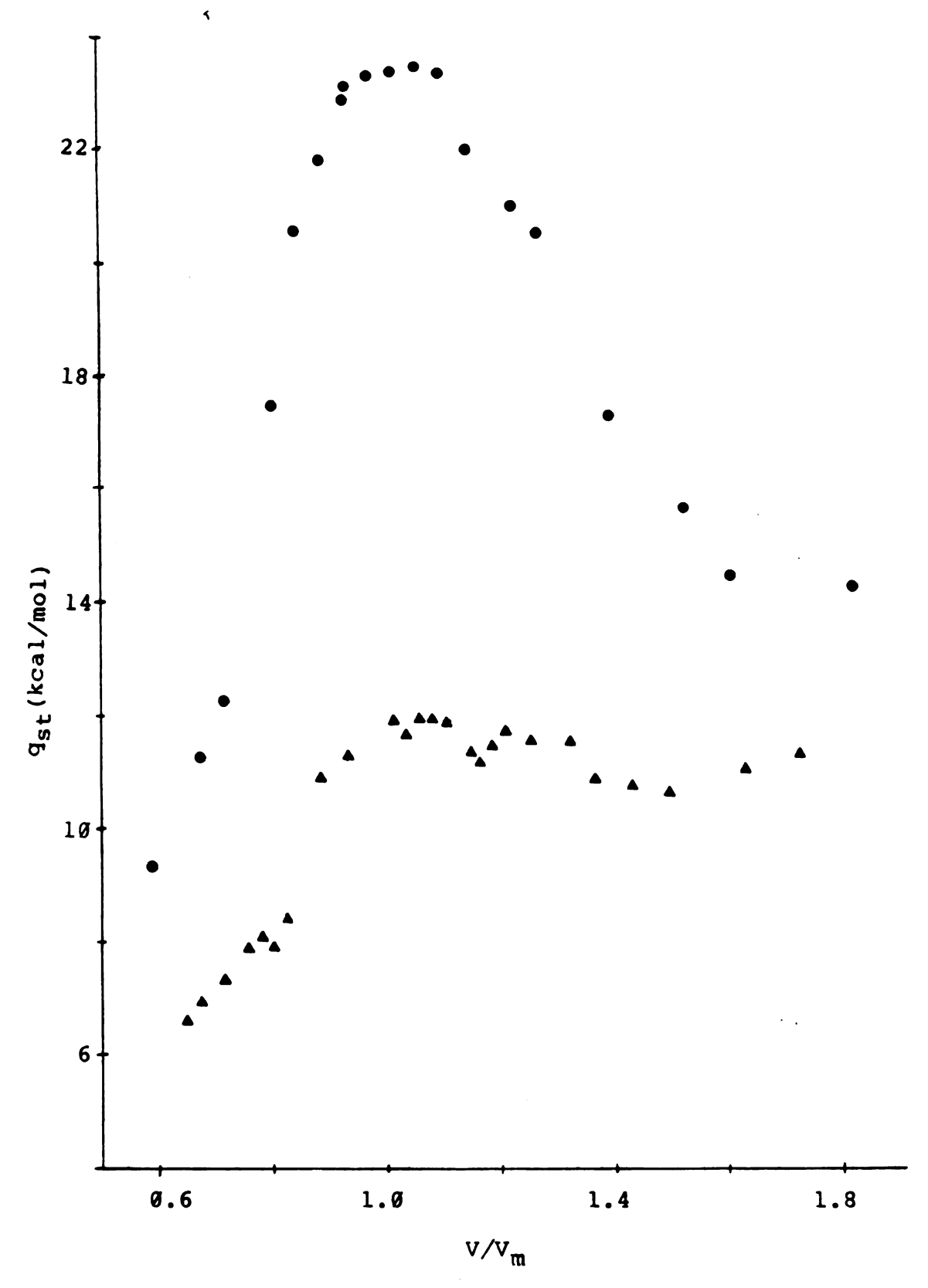


Figure 30. Heat curves, q_{st} vs. V/V_m for adsorption of 1-iodobutane onto [Zn₂Cr(OH)₆][I·nH₂O] \triangle A.D. \bullet O.D.

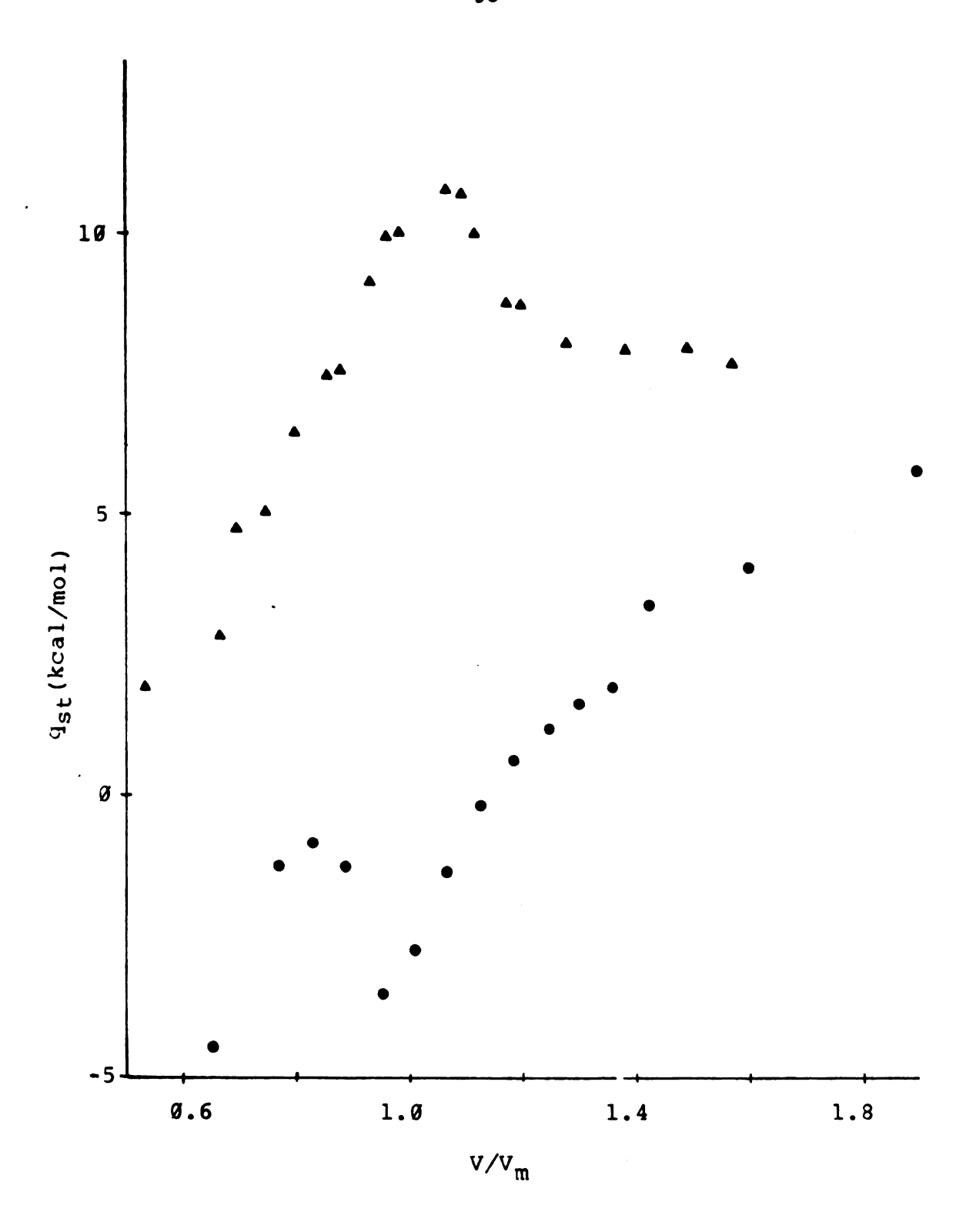


Figure 31. Heat curves, q_{st} vs. V/V_m, for adsorption of 1-bromobutane onto [Zn₂Cr(OH)₆][I·nH₂O] ▲A.D. ● O.D.

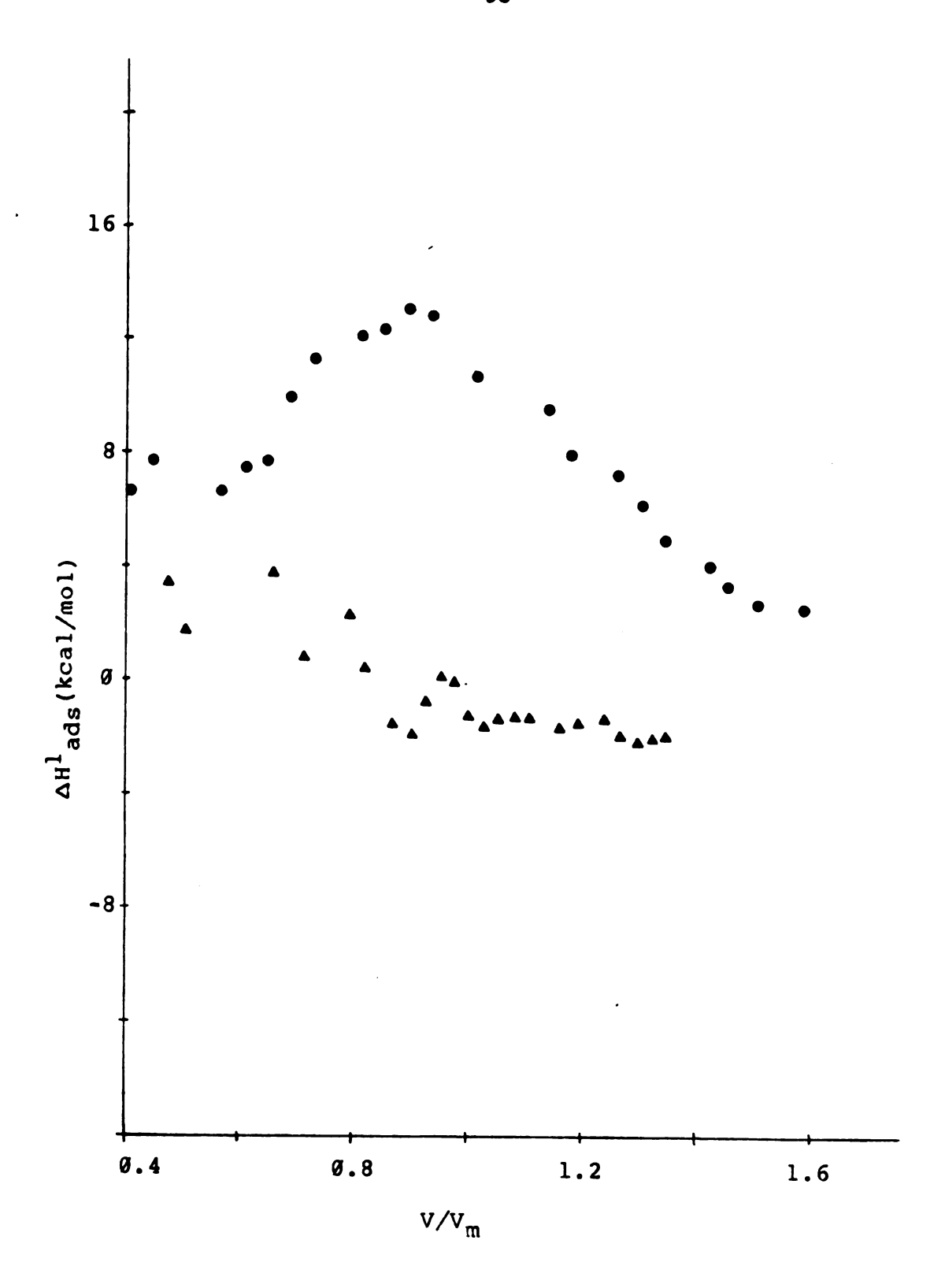


Figure 32. Plot of the enthalpy of liquid adsorption, △H¹_{ads}, vs. V/V_m for toluene adsorbed onto [Zn₂Cr(OH)₆][I·nH₂O] ▲A.D. ●O.D.

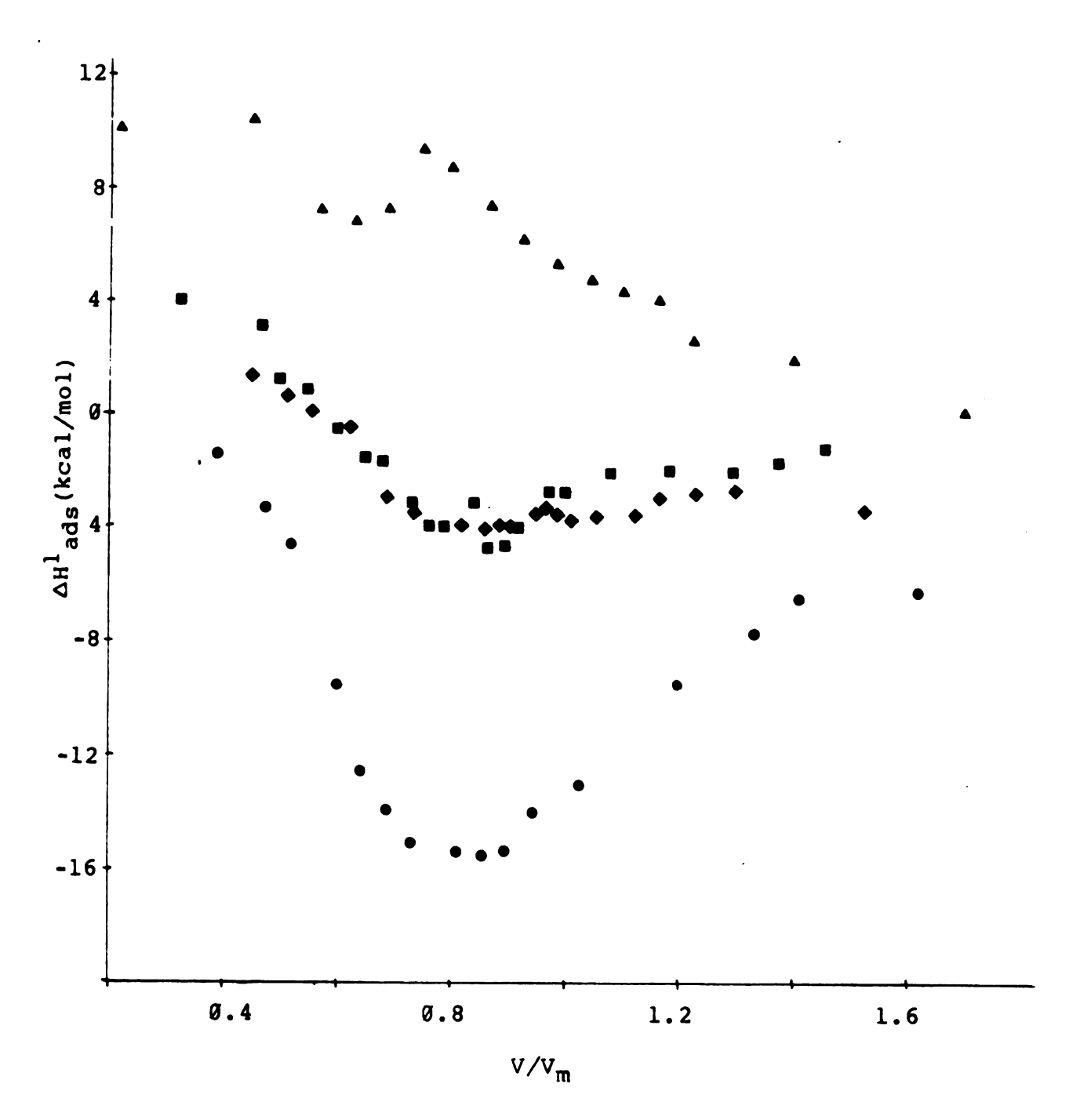


Figure 33. Plots of △H¹_{ads} vs. V/V_m for adsorption of 1-iodobutane onto [Zn₂Cr(OH)₆][I·nH₂O] ◆A.D.
• O.D.; and 1-bromobutane onto [Zn₂Cr(OH)₆]
[I·nH₂O] ■ A.D. ▲O.D.

vs. V/V_m are given in Figures 32 and 33.

From the plots it can be seen that the values of q_{st} are sometimes negative, giving a positive ΔH^g_{ads} . Even where ΔH^g_{ads} is negative, the value of ΔH^l_{ads} is sometimes positive once ΔH_{vap} is added in. For simple physical adsorption, these values are not possible. When positive values for these parameters are calculated from adsorption isotherm data, it means that an activated chemisorption is taking place rather than or along with physical adsorption.

Most often, chemisorption is thought of as formation of directed chemical bonds between a solid and an adsorbed species. The most common example of chemisorption are found in catalytic systems where simple gases such as H_2 , CO and C_2H_4 are involved. These gases can be chemisorbed by a variety of metals and oxide surfaces, either forming covalent bonds through interactions involving pi-electron systems or empty orbitals (CO, C_2H_4) , or through dissociation and bonding (H_2) . 118 , 119 Chemisorption may also involve the formation of ionic bonds, or simply dipolar interactions stronger than the van der Waals interaction responsible for simple physical adsorption. 118

Simple physical adsorption is an exoergonic process with essentially no activation energy. The process is thermodynamically controlled, so a cooler sample should always adsorb more vapor than a warmer one. A plot of the volume of toluene adsorbed onto O.D. Zn/Cr/I LDH as a function of pressure is given in Figure 34. The source of

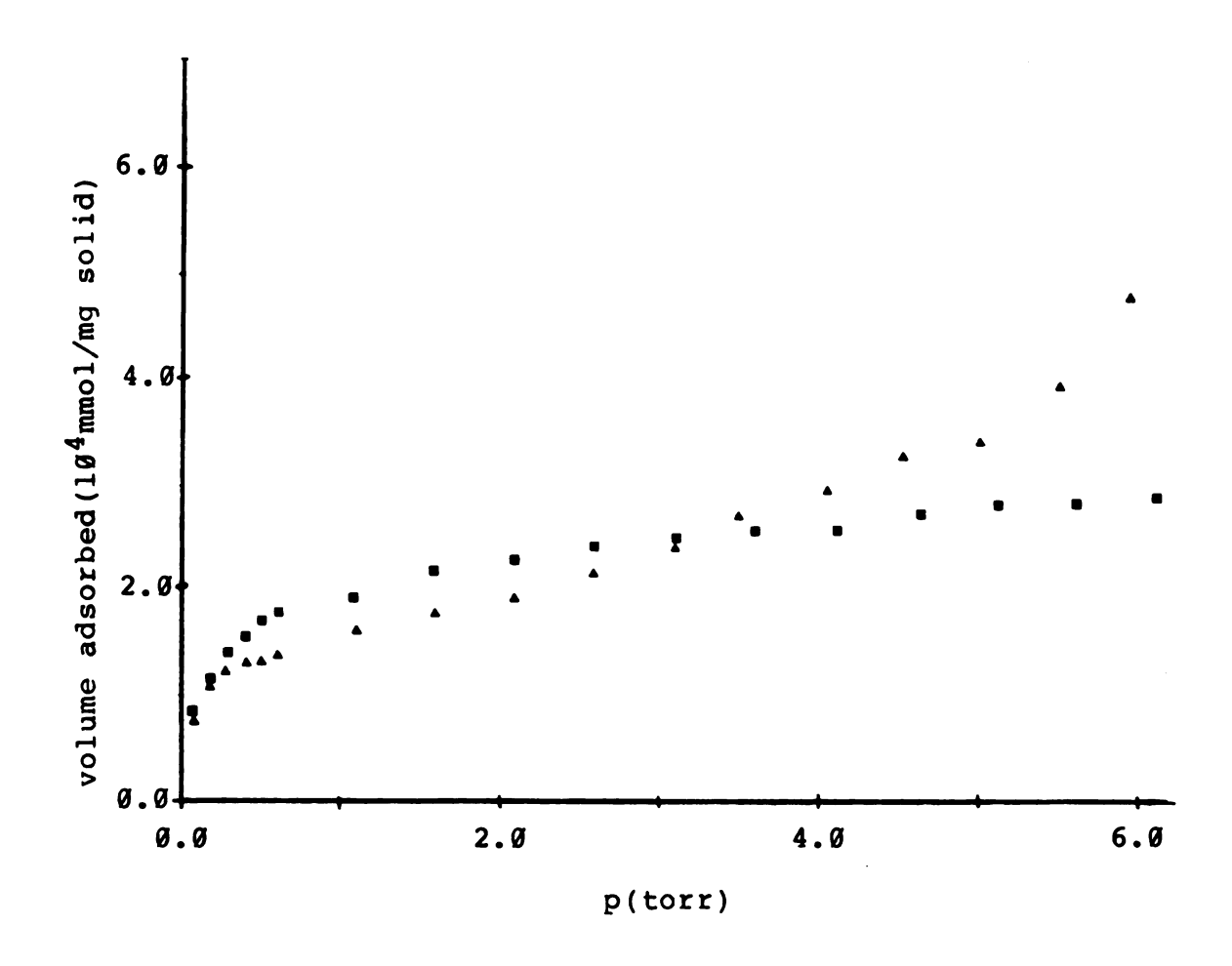


Figure 34. Adsorption of toluene onto O.D. [Zn₂Cr(OH)₆]
[I·nH₂O] as a function of pressure at ▲Ø OC
■ 22 OC.

the positive values of $\Delta \text{H}^g_{ ext{ads}}$ calculated for the adsorption of toluene onto O.D. Zn/Cr/I LDH can be seen in this plot. For the range of pressures illustrated here, the warmer LDH sample adsorbed more. Therefore, for a given value of V/V_{m} the pressure of toluene over the solid is greater for the cooler sample than for the warmer one. These values, when plugged in the Clausius-Clapeyron equation produce the positive values of AHgads. The greater adsorption at higher temperature is indicative of a chemical reaction taking place upon adsorption. In a given amount of time, a reaction taking place at a higher temperature will produce more product than one at a lower temperature. The product in this case is a chemisorbed molecule. A physical interpretation of the activation of the solid for adsorption will be suggested in a later section.

Values of q_{st} for physical adsorption are usually close to the value of ΔH_{vap} for a particular adsorbate. The values of q_{st} for 1-iodobutane on 0.D. Zn/Cr/I LDH are in the vicinity of 20 kcal/mol at V/V_m values near 1. Calculated values of q_{st} of this magnitude are usually, though not always indicative of chemisorption. The difference between this type of chemisorption and that discussed earlier is the activation barrier. So-called activated chemisorption has an activation barrier to adsorption which is surmounted by significantly more molecules at 22 °C than at 0 °C. The activation barrier for the second type of chemisorption observed, like that of

1-bromobutane on LDH, is so low that there is no significant difference between the number of interactions which occur at 0 $^{\circ}$ C and 22 $^{\circ}$ C.

The values of ΔH^1_{ads} and ΔH^9_{ads} calculated by using isotherm data are not valid in an absolute sense when activated chemisorption occurs. A true value of the heat of adsorption and chemisorption could be obtained calorimetrically were such a device available.

Some of the data from the adsorption experiments is useful as given. The curves for the adsorption of 1-bromobutane and 1-iodobutane on A.D. material, shown in Figures 26 and 27, represent physical adsorption for much of the curve. The calculated values of ΔH^1_{ads} for the two species are very close and help confirm the speculation about the deviation of the iodide substitution reactions away from first order behavior. Since the affinity of the solid for the two compounds is approximately the same, when the concentration of RI reaches a significant fraction of the RBr concentration, RI is able compete for adsorption sites on the solid. The accumulation of product on the surface would inhibit reaction and give the observed deviation from first order behavior.

The data for the alkyl halides on O.D. material is harder to interpret. The magnitude of ΔH^1_{ads} for 1-iodobutane on the O.D. material puts it in the realm of chemisorption and indicates a great affinity of the solid for the alkyl iodide. The positive value of ΔH^1_{ads} for 1-

bromobutane indicates that chemisorption is also occurring here. Some idea of the relative affinity of the solid for these molecules can be inferred from the adsorption isotherms. At room temperature, the O.D. Zn-Cr LDH adsorbed 2.05×10^{-4} mmol/mg of l-bromobutane at p/p₀ = 0.90 while 2.27×10^{-4} mmol/mg of l-iodobutane was adsorbed at a partial pressure of 0.92. These data indicate that the affinity of the solid for the two compunds was about the same.

The differences in reactivity between the A.D. and O.D. materials are harder to reconcile by using the adsorption data. The A.D. material adsorbed more of each of the adsorbates than did the O.D. material (Figures 25-27). This observation was surprising given the larger surface area of the O.D. LDH vs. the A.D. material. The so-called A.D. material which was used for adsorption studies was somewhat different from that used in the reactions. reaction material was air-dried solid scraped off a glass sheet and used in the reaction mixture without further The material referred to as "A.D." that was used in adsorption studies was outgassed at room temperature under 1x10⁻³ torr before adsorption commenced. treatment removed loosely-held surface water that would otherwise have volatilized during adsorption measurements, resulting in inaccuracies in pressure measurements. water would have condensed in the reservoir of adsorbate, causing contamination of the liquid being used. The outgassing procedure resulted in a 4.4% weight loss, corresponding to loss of 1.1 water molecules per mole of LDH out of the original 2.3.³² Of the original 2.3 waters, 0.3 were considered surface-bound, with 2.0 gallery waters. Therefore, not only surface water was removed, but also some gallery waters from near the edge of the particles. The surface of the A.D. LDH used in reactions was different from that of the "A.D." solid used for adsorption studies. The difference in surface composition may have lead to results that are hard to reconcile with observed reactivity trends. The importance of these observations will be discussed later in relation to a proposed detailed reaction mechanism.

4. Reaction and Adsorption Studies in Other Solvents.

Studies of other solvent were undertaken to elucidate the detailed mechanism of reaction and to ascertain the importance of surface properties. The O.D. solid material was used in these studies because the solid used in adsorption studies could be treated to give a material very similar to that used in the reaction mixtures. Zn/Cr/I LDH treated at 100 °C for 90 min under 1x10⁻³-1x10⁻⁴ torr experienced an average weight loss of 7.5%, corresponding to 1.9 water molecules of the original 2.3.³² This loss compares to a loss of 8.0-8.5% upon treatment at 150 °C under argon. The slight difference in composition was accepted because more severe heating in a vacuum caused partial dehydroxylation of the solid as indicated by color

change (lavender-gray to green) and weight loss.

Adsorption studies of chlorobenzene, n-octane and carbon tetrachloride were undertaken in the same manner as in the experiments just described. As before, fresh samples were used for each isotherm. The isotherms were obtained and from these plots of ΔH^1_{ads} vs. V/V_m were generated. These plots are shown in Figures 35 and 36. The heat curve of chlorobenzene is very similar to that of toluene, showing maxima and minima at the same values of partial monolayer coverage. Octane also showed activated chemisorption behavior, though judging from the magnitude of the positive value of ΔH^1_{ads} , not to as great an extent as toluene and chlorobenzene. Carbon tetrachloride showed no signs of chemisorption, based on the heat curve that was generated.

An additional experiment was performed with all the samples used for adsorption experiments. After the final point on the adsorption isotherm was recorded, the solvent source was closed off. The system containing the solid was evacuated to 1×10^{-3} torr for 5 min. The amount of adsorbate remaining on the solid after this treatment was calculated from the position of the quartz spring. The amount of adsorbate remaining on the solid after the treatment for O.D. materials at 22 °C is given in Table 18 along with their maximum measured capacities at the partial pressures given. This crude desorption experiment provides another measure of the strength of interaction between the solid

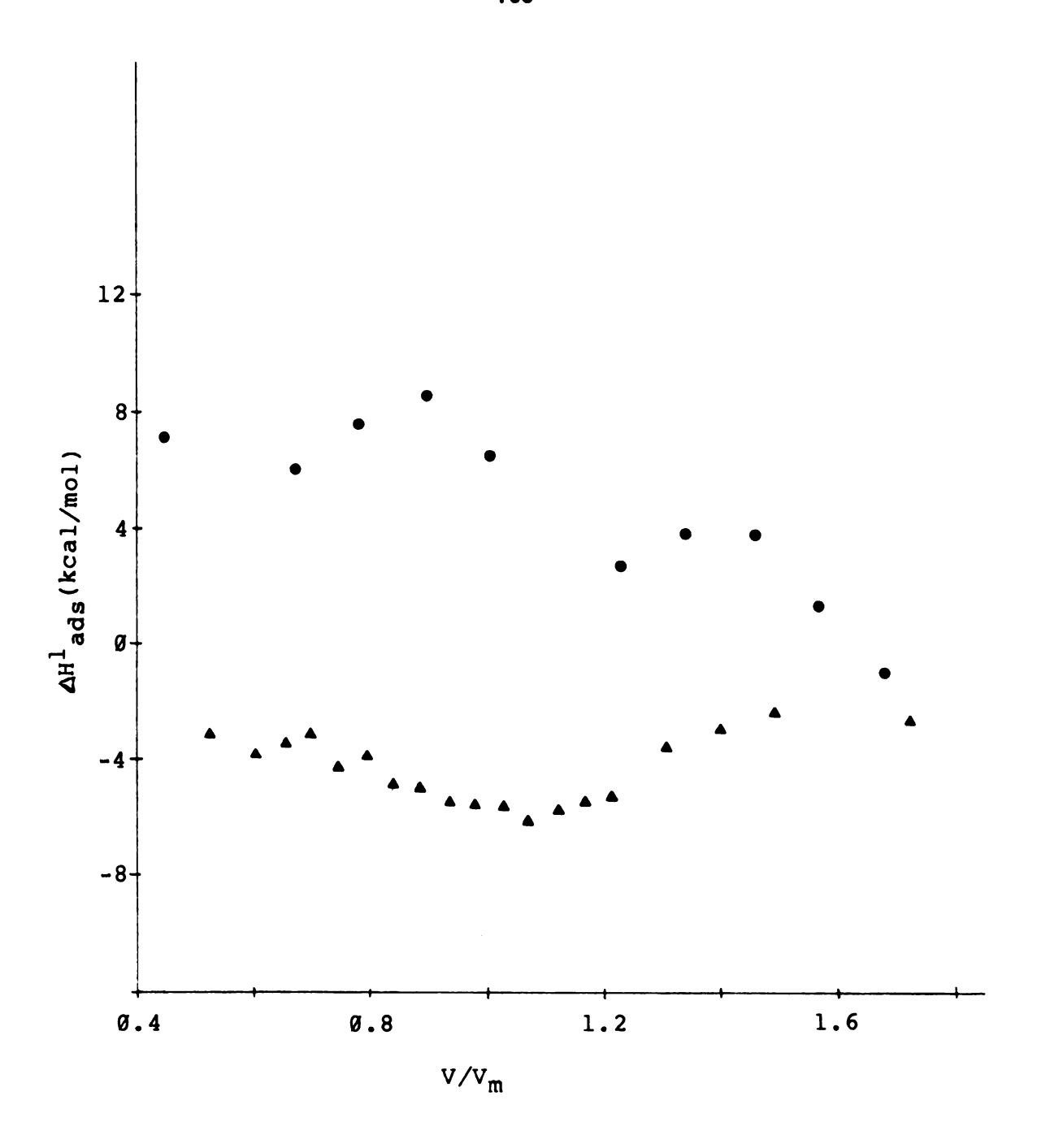


Figure 35. Plots of ΔH^1_{ads} vs. V/V_m for \bullet octane and \triangle carbon tetrachloride adsorption onto 0.D. $[Zn_2Cr(OH)_6][I^\circ nH_2O]$.

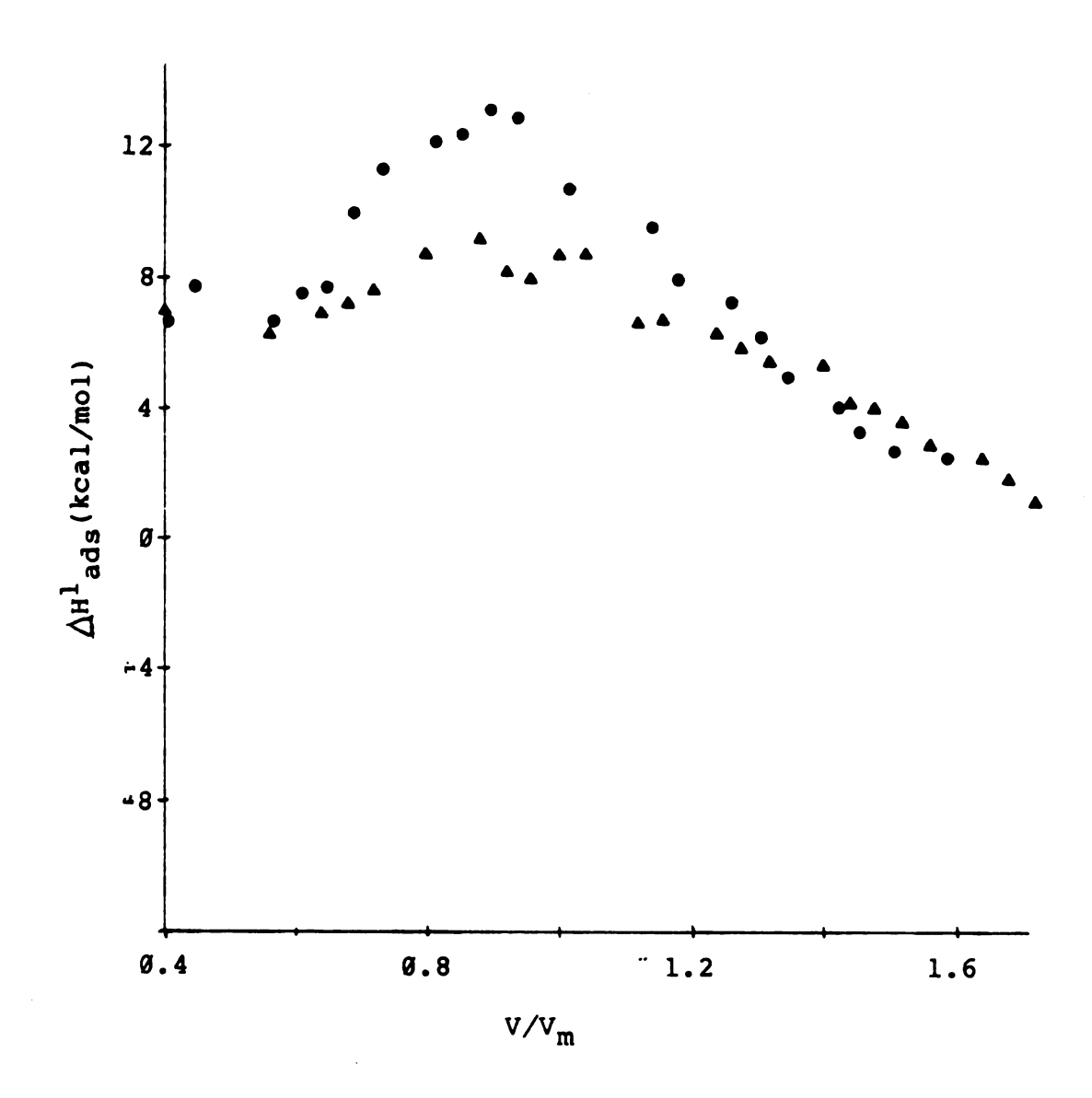


Figure 36. Plots of $\mathbb{A}H^1_{ads}$ vs. V/V_m for adsorption of $\mathbb{A}chlorobenzene$ and $\mathbb{A}chlorobenzene$ toluene onto 0.D. $[Zn_2Cr(OH)_6][I\cdot nH_2O].$

Table 18. Maximum Adsorption Capacities and Desorption Experiment Results for Various Adsorbates on O.D. $[Zn_2Cr(OH)_6][I]$.

Adsorbate (Maximum Capacity ^a 10 ⁴ mmol/mg solid)	After Desorption ^b (10 ⁴ mmol/mg solid)
toluene	4.03	1.21
laiodobutane	2.27	Ø.58
1*bromobutane	2.05	Ø.63
chlorobenzene	4.93	1.33
n+octane	2.11	Ø.13
carbon tetrachlori	de 2.41	0.05

^aAt 22°C. Value corresponds to the last point on the adsorption isotherm $(p/p_0 = \emptyset.88 + \emptyset.92)$. Evacuated for 5 min at 1×10^{-3} torr after last adsorption point.

and adsorbate. The amount of adsorbate remaining after 5 min is dependent on the rate of desorption, the more tightly held adsorbates being removed more slowly than other more loosely bound molecules. These data will be utilized in the interpretation of the reaction results to be discussed next.

Iodide substitution reactions were carried out in these solvents under the same conditions used for the reactions in toluene. 1-Bromobutane was the substrate in these reactions in which 1.00 mmol 0.D. solid and 1.00 mmol 1-bromobutane were allowed to react in 3.0 ml solvent at 90 $^{\circ}$ C. The values of k_{obs} for these reactions are listed in Table 19.

The rate constants for iodide substitutions in toluene and chlorobenzene were nearly identical. This similarity was not surprising given the similarity in adsorption isotherms and heat curves of the two adsorbates. The results

Table 19. Pseudo First Order Rate Constants for Iodide Substitution of leBromobutane with O.D. Zn/Cr/I LDH at 90°C in Various Solvents.

Solvent	104k _{obs} (s-1)b
toluene	1.32 ± 0.09
chlorobenzene n-octane	1.34 ± 0.10 10.4 ± 1.0
carbon tetrachloride	2.89 ± Ø.17

al.00 mmol 1-bromobutane; 1.00 mmol [Zn₂Cr(OH)₆][I] (O.D.); 3.0 mL solvent. b± 90% confidence limits.

of adsorption measurements of octane could also be correlated to reactivity. Evacuation after adsorption showed that a much smaller amount of octane remained on the surface than toluene $(1.31\times10^{-5}\,\mathrm{mmol}\ \mathrm{octane/mg}\ \mathrm{solid}\ \mathrm{vs}.$ 1.21×10^{-4} mmol toluene/mg solid), indicating that adsorbed octane was more easily removed. Since the octane was more easily displaced, the rate of reaction should be faster since more 1-bromobutane could be adsorbed on the surface. The reaction which did not fit the adsorption data was that carried out in carbon tetrachloride. There was less carbon tetrachloride left on the surface after evacuation than any other adsorbate $(5.06 \times 10^{-6} \, \text{mmol CCl}_A/\text{mg solid})$. This observation was consistent with the observation that no activated chemisorption was noted in the adsorption of carbon tetrachloride, indicating that there was no extra energy barrier to desorption either. The equilibrium concentration of carbon tetrachloride on the surface should have therefore been lower than that of any of the other solvents, producing a faster reaction. In fact, the rate constant for reaction in carbon tetrachloride was lower than octane and not much above toluene and chlorobenzene (Table 19). An activation energy study of these reactions was undertaken to help resolve the discrepency in adsorption and reaction results.

Iodide substitution of 1-bromobutane was carried out at several temperatures in each of the solvents. Rate constants were obtained for the initial linear portion of the reactions and Arrhenius plots prepared. The calculated values of the activation parameters for reactions in the different solvents are given in Table 20. The activation parameters for reactions in toluene and chlorobenzene were nearly identical, as expected. The values of ΔS^{\ddagger} for reactions in toluene, chlorobenzene and octane were essentially the same, perhaps indicating a similar structure in the transition state of the reaction. The activation parameter values obtained for reactions in carbon tetrachloride were different from the others. The enthalpy of activation is lower than that of the other solvents, but the entropy

Table 20. Activation Parameters for Iodide Substitution of l-Bromobutane at 90 °C by O.D. [Zn₂Cr(OH)₆][I] in Various Solvents.^a

solvent	∆H [‡] (kcal/mol)	AS* (cal/mol ^O K)	
toluene	13.1 ± 1.0	-40.6 ± 3.0	
chlorobenzene	13.1 ± 1.1	-38.7 ± 3.5	
n-octane	11.7 ± 0.9	-38.4 ± 2.9	
carbon tetrachloride	8.6 ± 0.8	-49.6 ± 3.2	

^aFrom Arrhenius plots. Reaction temperatures 50-120 °C. 1.00 mmol 1-bromobutane; 1.00 mmol LDH; 3.0 mL solvent.

of activation is more negative, indicating perhaps that more order was required in the transition state. A detailed mechanism in which these points are addressed will be suggested after a section dealing with the thermodynamics of halide exchange reactions over LDHs.

5. Thermodynamics of Reaction.

The thermodynamics of the halide exchange reactions can be examined by looking at the individual steps involved and analyzing the known data. The individual steps for solution-solid reactions, along with expressions for the enthalpy change associated with them, are given first, followed by those for gas-solid reactions.

(a)
$$RX_{(solv)} \longrightarrow RX_{(ads)}$$
 (5)

$$\Delta H_a = \Delta H^1_{ads}(RX) - \Delta H_{solv}(RX) - \Delta H^1_{ads}[(solvent)LDH(Y)]$$
 (6)

where $\Delta H^1_{ads}(RX)$ is the enthalpy of adsorption of liquid RX onto the LDH, $\Delta H_{solv}(RX)$ is the enthalpy of solvation of RX in the solvent utilized, and $\Delta H^1_{ads}[(solvent)LDH(Y)]$ is the enthalpy of adsorption of liquid solvent onto Y-substituted LDH. This model assumes that the surface of the LDH is initially saturated with solvent molecules. This saturation a likely occurrence given the excess solvent in the system and because the solvent was always added to the solid before the bromobutane.

(b)
$$RX_{(ads)} \longrightarrow RY_{(ads)}$$
 (7)

$$\Delta H_b = D_{CX} - D_{CY} + (\Delta H_{ads}^1(RY) - \Delta H_{ads}^1(RX))$$
 (8)

where D_{CX} and D_{CY} are the bond dissociation energies of carbon-X and carbon-Y bonds, respectively. The ΔH^1_{ads} terms must be added to account for any differences in the enthalpies of adsorption of the product and reactant. The conversion of the substrate is accompanied by the conversion of the LDH.

(c)
$$LDH(Y) \longrightarrow LDH(X)$$
 (9)

 $\Delta H_C = 24.2 \text{ kcal mol}^{-1} \text{ A}^{-1} [\Delta d_{001} \{\text{LDH}(X-Y)\}]$ (10) where $\Delta d_{001} \{\text{LDH}(X-Y)\} = [d_{001} \{\text{LDH}(X)\} - d_{001} \{\text{LDH}(Y)\}]$ and 24.2 kcal mol $^{-1}$ A $^{-1}$ is a calculated value for the change in enthalpy for changing the gallery height of LDHs. 118 The difference in energy for different size gallery anions results from changing the distance between the centers of positive charge in the octahedral layer and the anions. The final step in the reaction sequence is the desorption

(d)
$$RY_{(ads)} \longrightarrow RY_{(solv)}$$
 (11)

$$\Delta H_{d} = -\Delta H^{l}_{ads}(RY) + \Delta H_{solv}(RY) + \Delta H^{l}_{ads}[(solvent)LDH(X)] . \qquad (12)$$

of product and solvation in the reaction mixture.

Totalling the enthalpy terms for reaction in the solution phase gives

$$\Delta H_{\text{rxn}} = -\Delta H_{\text{solv}}(RX) + D_{\text{CX}} - D_{\text{CY}} + 24.2 [\Delta d_{\emptyset\emptyset1} \{ \text{LDH}(X-Y) \}]$$

$$+ \Delta H_{\text{solv}}(RY) + \{ \Delta H^{1}_{\text{ads}} [(\text{solvent}) \text{LDH}(X)] - \Delta H^{1}_{\text{ads}} [(\text{solvent}) \text{LDH}(Y)] \}$$
(13)

For gas-solid reactions, steps (b) and (c) are the same as those for solution phase. The initial steps and final steps are slightly different.

$$(a') \quad RX_{(q)} \longrightarrow RX_{(ads)}$$
 (14)

$$\Delta H_{a} = \Delta H^{g}_{ads}(RX) = -\Delta H_{vap}(RX) + \Delta H^{1}_{ads}(RX)$$
 (15)

$$(d') \quad RY_{(ads)} \longrightarrow \quad RY_{(v)}$$
 (16)

$$\Delta H_{d'} = -\Delta H_{ads}^g(RY) = \Delta H_{vap}(RY) - \Delta H_{ads}^1(RY)$$
 (17)

The sum of the enthalpies for vapor phase reaction is

$$\Delta H_{rxn'} = -\Delta H_{vap}(RX) + D_{CX} - D_{CY} + 24.2 [\Delta d_{00}[LDH(X-Y)]] + \Delta H_{vap}(RY)$$
 (18)

If the enthalpies of solvation of RX and RY are assumed to be equal, and the enthalpies of solvent adsorption onto LDH(X) and LDH(Y) are close to each other, the expression for the solution-solid reaction reduces to the middle terms concerning the bond strengths and energy change of the LDH. For the gas-solid reactions a similar value of the enthalpies of vaporization can be assumed. Eliminating those two terms gives the same expression as for the solution-solid reaction, namely

$$\Delta^{H}_{rxn} = D_{CX} - D_{CY} + 24.2 [\Delta d_{001} \{LDH(X-Y)\}]$$
 (19)

The values of $(D_{CX} - D_{CY})$ and 24.2[$\Delta d_{\emptyset\emptyset1}$ {LDH(X-Y)}] for some of the reactions studied are listed in Table 21. The importance of the thermodynamics in relation to the

Table 21. Values of D_{CX} - D_{CY} and 24.2 $d_{\emptyset\emptyset]}$ for Various Alkyl Halide Exchange Reactions RX + LDH(Y) \longrightarrow RY + LDH(X).

R X	Y-	DCX - DCY	24.2Ad ₀₀₁ (X-Y)	Total
RBr	· C1	-10.2	2.7	-7.5
RBr	I	17.0	-11.0	6.0
RBr	F	-48.0	7.2	-40.8

^aAll values in kcal/mol.

bBased on bond dissociation energies from reference .

proposed detailed mechanism will be discussed next.

5. Proposed Detailed Mechanism.

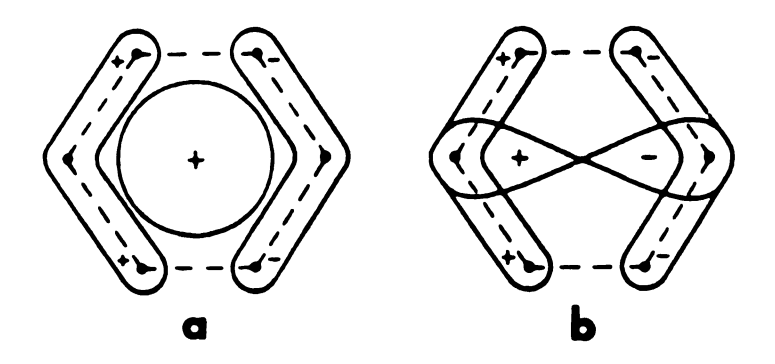
A detailed mechanism of the reactions under study can be proposed which is consistent with the results obtained from the present study. The simple mechanism proposed in Scheme 2 will be presented in light of all the data collected and discussed in some detail.

The first step of the reaction is adsorption of the reactant alkyl halide. This adsorption occurs after displacement of a solvent molecule from the surface in solution-solid reactions, but occurs unhindered in gassolid reactions. The next step of the reaction is nucleophilic attack by a gallery ion. After this step, the product alkyl halide is either retained on the solid or replaced by solvent or by reactant alkyl halide.

One of the questions surrounding the first step of the reaction concerns the nature of the adsorption of solvent and alkyl halide. The interaction of various adsorbates with hydroxyl surfaces has been studied in detail. 121,122 IR data obtained from the study of substances adsorbed on porous Vycor glass indicate that even nonpolar molecules such as alkanes interact with hydroxyl groups, shifting the O-H stretching frequency to lower energy. The magnitude of the O-H band shift is a direct indication of the strength of interaction between the adsorbate and the hydroxyl group. The results indicated that, for a series of similar compounds, such as a aromatic compounds or alkanes, the

adsorbate with the lowest ionization potential caused the greatest shift in the hydroxyl band, indicating the strongest interaction. Detailed data of this type cannot be obtained for LDHs due to the presense of broad, overlapping bands in the hydroxyl stretch region. The data from the other studies can be applied to LDHs.

The data in the published reports indicate that n-octane should bind more strongly than carbon tetrachloride, 121 is borne out in the present study since more octane than carbon tetrachloride remained on the surface of the solid after desorption at 1×10^{-3} torr. Toluene is bound more tightly than either alkanes or carbon tetrachloride as would be expected from its lower ionization potential [8.82 eV vs. $11.47(CCl_A)$; 9.90 eV(octane)].⁶² One of the pi orbitals is also of the proper symmetry to overlap the sigma bonding orbital on the hydroxyl H-atom (Figure 37). Chlorobenzene should bind in the same manner, but the interaction will be slightly weaker due to its slightly larger ionization energy (9.07 eV).62 The adsorption of the two aromatic species was similar according to the adsorption data from the present study. There are few data available on the adsorption of alkyl halides on hydroxyl groups, but the polar halide group should provide a site for binding to hydroxyls. The ionization potentials for the two alkyl halides of interest indicate that 1-iodobutane should bind more strongly than 1-bromobutane (ionization potentials: 10.13 eV C_4H_9Br ; 9.21 eV C_4H_9I).



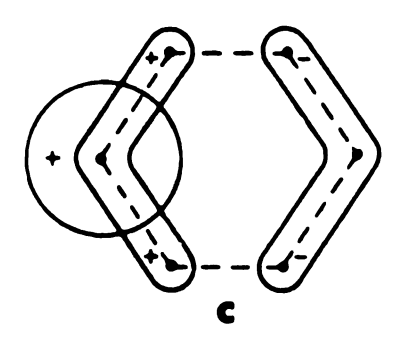


Figure 37. Possible bonding interactions of hydroxyl group orbitals with an aromatic system. (a). $e_{2g} + \sigma_{OH}^{\dagger} - \text{no net overlap; (b). } e_{2g} + H_{2p} - \\ p\text{-orbital too high in energy; (c). 0.5 } e_{2g} + \\ \sigma_{OH}^{\dagger} - \text{probable interaction.}$

The entire surface of LDHs is covered with hydroxyl groups, including the exterior basal planes, the edges of the particles and the surface of the hydroxide layers within the galleries. In the LDH samples that were adsorbents in the present study, surface water and some gallery water, probably from near the edges of the particles, had been removed prior to the adsorption studies. The removal of water allows the hydroxyl groups to interact with adsor-It seems likely that adsorption takes place not only on the exterior surface of the LDHs but also within the galleries. Not only are the gallery hydroxyl groups available for interaction, but the net positive charge of the octahedral layers is concentrated in the galleries by the presence of 2 charged layers. Polar groups, such as the halide groups of the reactant and product molecules, would be attracted to the positive charge and would bind through ionic-dipole type interactions. Adsorption of the halide group of a reactant alkyl halide is probably necessary for reaction to occur. The results of the experiments will be discussed with that assumption in mind.

(a). Under solution-solid conditions, iodide substitution of alkyl bromides occurs at a much greater rate than chlorinations even though chloride substitution is thermodynamically favored over iodide substitution (Table 21). Under gas-solid reaction conditions in the temperature range of 90 °C to 150 °C, chloride substitution and iodide substitution of 1-bromobutane by LDH gallery anions give

similar conversions (Tables 16 and 17). Fluoride substitution of vapor phase 1-bromobutane does not occur at 150 °C, however. The pattern of reactivity is related to the gallery height, the free space between the octahedral layers, of the LDHs involved. This pattern is consistent with the assertion that the reactant bromide group must insert into the gallery in order for reaction to take place. The O.D. iodide-exchanged LDH has a gallery height of 3.4 Å (d_{001} - 4.8 Å, the approximate thickness of a brucite sheet). The chloride exchanged form has a gallery height of 2.7 Å; the fluoride LDH, 2.5 Å. The diameter of the bromo group of 1-bromobutane lies somewhere between the non-polar diameter of 2.28 Å and the ionic diameter of 3.90 Å.⁵⁹ Assuming an intermediate value of 3.0 Å for the bromo group diameter, the gallery heights of the chloride and fluoride LDHs would have to expand to allow the bromo group to enter. The iodide gallery would admit the bromo group without further expansion. If the estimate of 3.0 Å is a reasonable one for the bromo group diameter, the energy required to expand a chloride gallery to accomodate bromo group is approximately 7 kcal/mol (24.2 kcal mol⁻¹ Å⁻¹ X 0.3 Å). In order to expand the fluoride lattice the required 0.5 Å, approximately 12 kcal/mol is required. value of ΔH^g ads for 1-bromobutane is 6-7 kcal/mol more exothermic at reaction temperatures than ΔH^{1}_{ads} . The difference is ΔH_{Vap} of 1-bromobutane which is liberated when the vapor condenses on the solid prior to adsorption.

extra energy given off upon vapor phase adsorption is enough to activate the chloride-substituted LDH in the gassolid reactions. Recall that chloride substitution did not proceed at an appreciable rate under solution-solid conditions. The extra energy of adsorption is not enough to activate the fluoride substitution reaction since it is not enough to expand the fluoride gallery enough to allow insertion of the bromide group.

There is a parallel between these observations and the behavior of LDHs in gallery anion replacement reactions in aqueous solution. When the reactions are carried out, the platelets of LDHs do not separate and disperse as do those of smectite clays under going exchange. 25 The anion exchange reactions apparently involve the adsorption of the exchange anion to the edge of the platelet, incorporation into the gallery and expulsion of the starting anion from the gallery. The new anion is then mixed into the interior of the gallery, away from the edge of the platelet. When the exchange anion is larger that the anion present in the galleries, exchange is accomplished only by use of a large excess of anion and high temperatures. 31,32 These conditions are apparently necessary to overcome the activation energy of exchange, the expansion of the gallery to accomodate the larger anions. Exchange of smaller anions and multiply-charged anions into LDHs is more easily accomplished, the reactions proceeding rapidly at room temperature with moderate concentrations of anion in solution.

- (b). The values of the entropy of activation for reactions over the solid material are more negative than those for reactions in homogenous solution. The ordering of the system for reactions is greater than that in solution. Not only are two particles required to come together to make the reaction proceed, but the arrangement of molecules needed to for the reaction on the solid is more specific than that required in solution. The arrangement must allow the halide group of the alkyl halide to be partially extracted while the gallery anion moves to replace it.
- (c). The values of ΔH^{\sharp} calculated for reactions over the solid are of the same order of magnitude as those of homogenous reactions, but are consistently lower. This observation reflects the assisted bond-breaking of the C-X bond in the gallery region. Part of the ΔH^{\sharp} of a nucleophilic substitution reaction goes into breaking the bond between the attacked carbon and the leaving group. When the bond is weakened by interaction with another species the barrier to breakage is lowered.

When ΔH^{\sharp} and ΔS^{\sharp} are combined to give ΔG^{\sharp} values for solution-solid iodide substitutions and the homogenous reactions listed in Table 15, the values are lower for homogenous reactions than for solution-solid reactions. The advantages of a lower enthalpy of activation on an LDH are overshadowed by the entropic changes of the solid

system.

There is another element in the activation energy. The gallery nucleophile is located in a potential energy well from which it must move to react. Reactions that used an excess of RBr showed that approximately 90% of the intercalated iodide was available for reaction. That the reaction rate depended only on the fraction of iodide remaining and not its location in the solid (i.e., the distance from the end of the gallery) suggested that the barrier to gallery diffusion was surpassed at 90 °C. Aqueous anion exchange reactions that occur without particle delamination support the supposition that the barrier to movement is relatively low. This discussion is also related to the next point to be considered.

(d). When 1-bromobutane was adsorbed onto O.D. [Zn₂Cr(OH)₆][I] at 22 ^OC, normal adsorption behavior was observed. When the same experiment was tried with A.D. material, a reaction occurred in which the weight of the material decreased. Analysis of the adsorbate revealed that 1-iodobutane had been formed in the vacuum line and had condensed in the reservoir of 1-bromobutane that was open to the vacuum line. That reaction occurred on the A.D. solid and not on the O.D. solid is at first surprising since the O.D. material was more reactive in solution studies. The treatment of the samples must be kept in mind, however. Before adsorption, the so-called A.D. material was equilibrated at a pressure of 1x10⁻³ torr.

This treatment caused a weight loss of approximately 4.4%, enough to remove the surface water and a small amount of gallery water. In the adsorption studies, the difference between the samples examined was mainly a difference in gallery water and not surface water. The solids used in reaction studies were different in surface and gallery composition.

The differences in behavior of materials used in adsorption studies was related to the gallery properties. The dag spacing of an A.D. iodide-exchanged Zn-Cr LDH is 8.34 Å vs. 8.21 Å for an O.D. sample. Assuming an octahedral layer thickness of 4.8 Å, the gallery heights of the O.D. and A.D. samples are 3.4 and 3.5 Å, respectively. The diameter of the iodide ion is 4.32 Å, larger than the gallery height. The octahedral layers somehow distort to fit more tightly around the gallery anions. The electron cloud of the anions could also be distorted to decrease the distance between charge centers in their respective layers. If the anions are located over a metal center in the octahedral layer, the three hydroxyl groups could conceivably distort to allow closer approach of anion. The gallery water of A.D. samples apparently props the layers apart to some extent since the gallery height of an A.D. sample is greater than that of an O.D. sample. The propping action of the water molecules is not the same as a column holding up a roof of a building. The water functions more as a dielectric. The oxygen of water compensates for some of the positive charge of the octahedral layers, decreasing the amount of distortion that the iodide undergoes. Because of the distortion of the anions, they are in physical "wells" in addition to the potential energy wells caused by electrostatic attraction. In order for reaction between a gallery anion and an alkyl halide to occur, the anion must come out of its physical well, i.e., either the anion must further distort or the gallery height must expand. Either process requires energy. In the reaction that occurred in the vacuum line, the A.D. sample had a gallery height that was 0.13 Å larger than the O.D. sample. The difference, which corresponds to a difference of 3.1 kcal/mol, was enough to inhibit reaction on the O.D. material while it was permitted on the A.D. material.

A question that remains concerns the nature of the activation step in the species that exhibit activatied chemisorption. The activation barrier for chemisorption involves some rearrangement of the adsorbent to enable the interaction to occur. Examination of the ΔH^1_{ads} curve for toluene indicates that activated chemisorption occurred in the early stages of adsorption on A.D. LDH (Figure 32). The extent of chemisorption was much greater for O.D. LDH. Since the adsorption interaction presumably takes place through hydroxyl groups, the activation step at least partially involves preparing the hydroxyl groups for binding by adsorbate. The preparation may involve breaking hydrogen bonds that exist between particles. Since hydrogen

bonds are weak interactions, a larger number of them could conceivably be broken at 22 °C than at 0 °C. The greater extent of activated chemisorption on 0.D. samples indicates that, compared to the A.D. material, a greater number of the hydroxyl groups are unavailable at 0 °C than at 22 °C. There could be more hydrogen bonding between particles in 0.D. LDHs, or adsorption into the galleries could require an activation in 0.D. solids not required for A.D. material. This difference in activation required for chemisorption, when examined in terms of gallery heights, is additional evidence for adsorption into galleries by adsorbates.

The absence of chemisorptive behavior of carbon tetrachloride also suggests that adsorption into the galleries takes place. Carbon tetrachloride is unique among the adsorbates studied because it is the only one too large to fit into the gallery an iodide-exchanged LDH. The strength of interaction between carbon tetrachloride and hydroxides is predicted to be the weakest of the adsorbates examined. Since the interaction of carbon tetrachloride is only slightly weaker than that of octane, according to reports, some chemisorption behavior might have been predicted for carbon tetrachloride. These data can be interpreted as evidence for chemisorption into the galleries since carbon tetrachloride alone doesn't chemisorb onto O.D. LDH.

In the discussion of differences in reaction rates and activation parameters in different solvents, the greater

rate in octane has been attributed to greater access of reactant alkyl bromide to the galleries. However, if a greater number of collisions alone were responsible for the increased reaction rate, the value of ASf for reactions in octane should have been less negative than that for reactions in toluene and chlorobenzene. The value of ΔS^* is derived from the A parameter of the Arrhenius expression and is a reflection of the frequency of reactions leading to reaction. Instead, the ΔS^* values for the 3 solvents are the same (Table 19). The reactions in octane have a smaller value of ΔH^{\dagger} than those in toluene. The value of AH in carbon tetrachloride is even smaller than for toluene. These values point to the importance of a step discussed in relation to the first step of the proposed reaction mechanism. Recall that a solvent molecule must be desorbed in order for a reactant molecule to adsorb. the adsorption was excergonic, the solid loses energy when the solvent molecule is desorbed. The amount of energy the solid loses is proportionate to the strength of interaction between the solid and the adsorbate. Therefore, the solid loses more energy in desorbing toluene and chlorobenzene than in desorbing octane. Desorbing carbon tetrachloride requires the least energy since it interacts more weakly than the other solvents. The energy that is lost by the solid is energy that could have gone into the activation of the iodide substitution reaction. Therefore, since less additional energy is required to activate the reaction, the

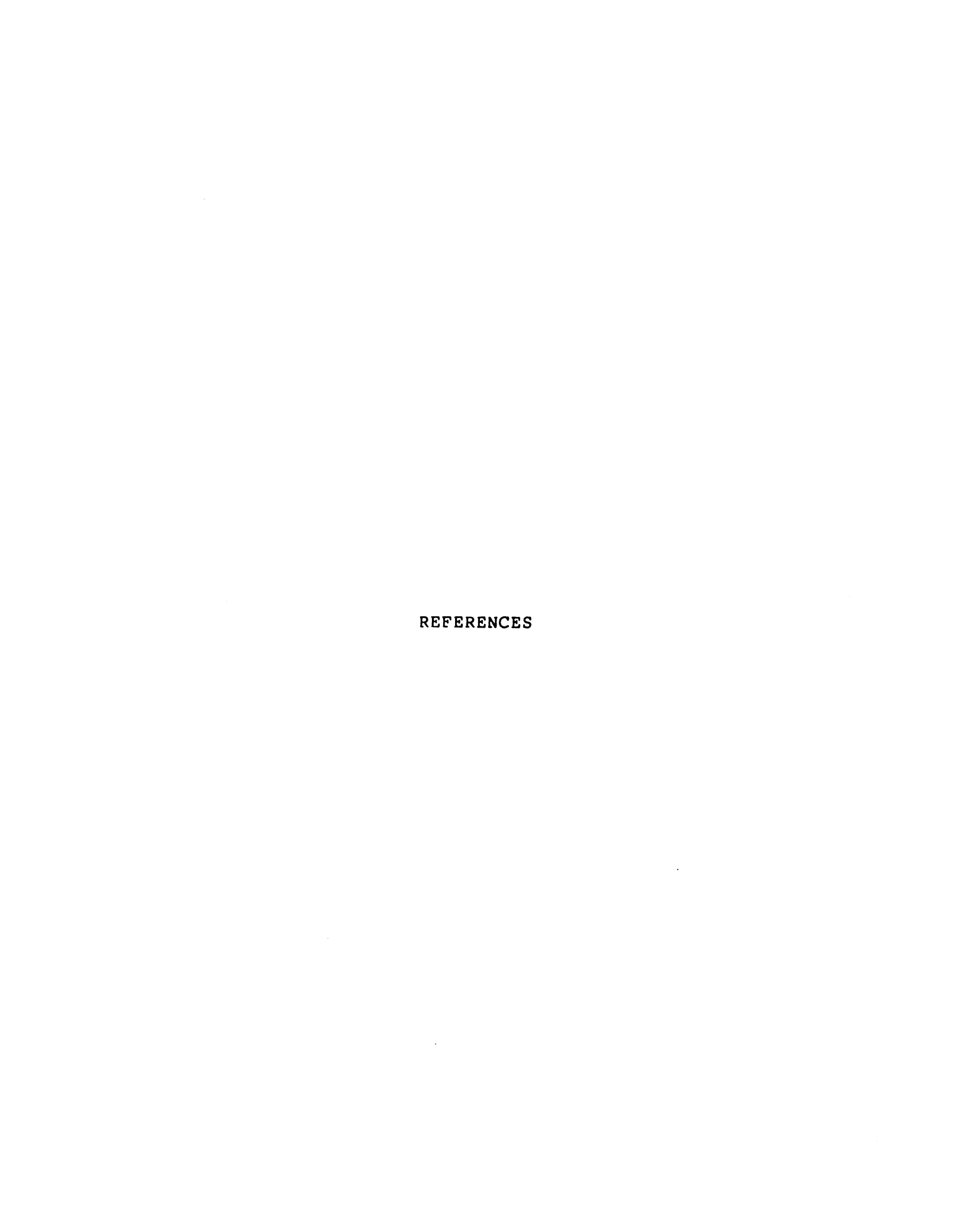
solvent system which causes the smallest loss of energy upon desorption should have the smallest value of ΔH^{\ddagger} .

The above explanation accounts for the enthalpies of activation observed in various solvents. It does not explain the anomalous entropy of activation of the carbon tetrachloride system. One would predict that the reaction would proceed faster in carbon tetrachloride since the energy lost upon desorption of the solvent would be smaller than for any other solvent. The entropy of activation is approximately 10 cal/mol OK more negative than for the other solvents, indicating a smaller effective collision frequency factor. My proposal is that too much alkyl bromide is adsorbed for the reaction to proceed efficiently. The concentration of alkyl bromide in the gallery is very large because of a large amount of adsorption. The bromide groups from the molecules are very close to one another. When the C-Br bond is activated by interaction with the hydroxyl groups of the gallery, reaction with a nearby activated bromide group becomes the preferred reaction under the crowded conditions. Therefore, even though the solid is activated to a greater extent than in the other solvents, reaction of one alkyl bromide with a nearby molecule becomes important enough to inhibit formation of iodated products. The collision frequency between iodide and alkyl bromide is thereby smaller, resulting in a rate smaller than was predicted.

Conclusions.

- (1). The swelling behavior of alkylsulfate-inter-calated Zn-Cr LDH has been reproduced in Ca-Al and Li-Al LDHs. The swelling is a general property of LDHs.
- (2). Intercalation of the disulfate radical spin probe into LDHs does not occur because of interactions between the -SO₃ groups and the hydroxyl groups of LDHs. This interaction is similar to that observed between dodecyl-sulfate ions and hydroxide surfaces.
- (3). The structure of an unaged Li-Al LDH formed by coprecipitation is variable. The Li⁺ may be removed from the structure by extended washings, leaving mixed Al(OH)₃ phases. The initial structure of the fresh precipitate is probably intercalated gibbsite analagous to that of a compound formed by reaction of a LiX solution and gibbsite. 110
- (4). Iodide intercalates of Zn-Cr LDH are active in nucleophilic displacement reactions of alkyl bromides. LDHs from which the water have been removed react 3-4 times faster than air-dried materials. The reactions occur in various organic solvents, but do not occur in the presence of water. The rate of reaction is dependent on the nature of the solvent utilized. The solvents affect the surface properties of the solid and influence the adsorption of alkyl bromides. Desorption of the solvent molecules, a prelude to reaction, affects the energy content of the solid and the activation energy of reaction. A mechanism

is proposed in which the bromide group is inserted into the LDH gallery to undergo reaction. Activation of the molecule is aided by the electrostatic attraction of the positive layers and the partially negative bromide group. anomalous activation parameters of reactions in CCl₄ solvent are explained on the basis of a solvent intercalation model which decreases the enthalpic requirements of reaction, but increase the entropic requirements. Chlorination reactions do not occur in solution phase because the bromide group of the alkyl halides is larger than the gallery height of the chloride intercalate. released upon adsorption of the bromide from solution is not sufficient to expand the gallery enough to allow penetration of the bromide group, a prerequisite for reaction. In the vapor phase, the reaction does proceed because the added heat of vaporization is sufficient to activate the reaction.



REFERENCES

- 1. Allmann, R. Chimia 1976, 24, 99.
- 2. Miyata, S.; Kumura, T. Chem. Lett. 1973, 843.
- 3. Beck, C.W. Amer. Mineral. 1956, 35, 985.
- 4. Wells, A.F. Acta Cryst. 1951, 4, 200.
- 5. Ghose, S. Acta Crystall. 1964, 17, 1051.
- 6. Brasseur, H. Z. Krystall., 1932, 82, 195.
- 7. Pastor-Rodriguez, J.; Taylor, H.F.W. Mineral. Mag. 1971, 38, 286.
- 8. Nickel, E.H.; Clarke, R.M. Amer. Miner. 1976, 61, 366.
- 9. Taylor, H.F.W. Mineral. Mag. 1973, 39, 377.
- 10. Frondel, C. Amer. Miner. 1941 26, 295.
- 11. Allmann, R.; Lohse, H.-H. N. Jahrb. Mineral. Monats. 1966, 161.
- 12. Ingram, L.; Taylor, H.F.W. <u>Mineral. Mag.</u> 1967, <u>36</u>, 465.
- 13. Allmann, R. Acta Cryst. 1968, B24, 972.
- 14. Turriziani, R. "The Chemistry of Cements"; Taylor, H.F.W., ed.; Academic Press, New York, 1964, 233, and references within.
- 15. Lerch, W.; Ashton, F.W.; Bogue, R.H. J. Research Natl. Bur. Standards 1929, 2, 715.
- 16. Feitknecht, W.; Buser, H. Helv. Chim. Acta 1951, 34, 128.
- 17. Feitknecht, W.; Buser, H. <u>Helv. Chim. Acta</u> 1942, <u>25</u>, 106.
- 18. Feitknecht, W. Z. Angew. Chem. 1936, 49, 24.
- 19. Feitknecht, W. Helv. Chim. Acta 1938, 21, 766.

- 20. Ross, G.J.; Kodoma, H. Amer. Mineral. 1967, 52, 1036.
- 21. Kuzel, H.-J. N. Jahrb. Mineral. Monats. 1965, 193.
- 22. Kuzel, H.-J. N. Jahrb. Mineral. Monats. 1966, 193.
- 23. Ahmed, S.J.; Taylor, H.F.W. Nature 1967, 215, 622.
- 24. Allmann, R. N. Jahrb. Mineral. Monats. 1968, 140.
- 25. Grim, R.E. "Clay Mineralogy", 2nd ed., McGraw-Hill, New York, 1968.
- 26. Mascolo, G.; Marino, O. Mineral. Mag. 1980, 43, 619.
- 27. Hunsaker, V.E.; Pratt, P.F. <u>Soil Sci. Soc. Amer. Proc.</u> 1976, <u>34</u>, 813.
- 28. Schalscha, E.B.; Pratt, P.F.; Gonzalez, C. Soil Sci. Soc. Amer. Proc. 1972, 36, 752.
- 29. Kinniburgh, D.G.; Jackson, M.L.; Syers, J.K. <u>Soil Sci.</u> <u>Soc. Amer. Proc.</u> **1976**, <u>40</u>, 796.
- 30. Taylor, R.M. Clay Minerals 1984, 19, 591.
- 31. Boehm, H.P.; Steinle, J.; Vieweger, C. Angew. Chem. Int. Ed. Eng. 1977, 16, 265.
- 32. Lal, M.; Howe, A.T. <u>J. Solid State Chem.</u> 1981, <u>39</u>, 337.
- 33. Morrison, S.R.; Bonelle, J.-P. <u>J. Catal.</u>, **1972**, <u>25</u>, 416.
- 34. Courty, P.; Marcilly, C. "Preparation of Catalysts III"; Poncelet, G.; Grange, P.; Jacobs, P.A., eds., Elsevier, Amsterdam, 1983, 485.
- 35. Feitknecht, W.; Buser, H.W. <u>Helv. Chim. Acta</u> **1949**, <u>32</u>, 224.
- 36. Feitknecht, W. Fortschr. Chem. Forsch., 1953, 2, 670.
- 37. Feitknecht, W.; Buser, H.W. Chimia 1951, 4, 261.
- 38. Feitknecht, W.; Gerber, M. <u>Helv. Chim. Acta</u> **1942**, <u>25</u>, 121.
- 39. Feitknecht, W. Helv. Chim. Acta 1942, 25, 555.
- 40. Feitknecht, W.; Held, F. <u>Helv. Chim. Acta</u> 1944, <u>27</u>, 1498.

- 41. Miyata, S.; Kumura, T.; Shimada, M. Ger. Offen. 2,061,094; Chem. Abstr. 1971, 75:153442u.
- 42. Miyata, S.; Kumura, T.; Shimada, M. Ger. Offen. 2,061,114; Chem. Abstr. 1971, 75:119620r.
- 43. Miyata, S.; Kumura, T.; Shimada, M. Ger. Offen. 2,061,136; Chem. Abstr. 1971, 75:131249j.
- 44. Miyata, S.; Kumura, T.; Shimada, M. Ger. Offen. 2,061,156; Chem. Abstr. 1971, 75:119619x.
- 45. Miyata, S.; Kumura, T.; Shimada, M. Japan Kokai 72 42,493; Chem. Abstr. 1973, 78:55527p.
- 46. Miyata, S.; Kumura, T.; Nosu, T. Japan Kokai 73 29,477; Chem. Abstr. 1974, 80:85256n.
- 47. Miyata, S.; Kumura, T. Japan Kokai 73 29,478; Chem. Abstr. 1974, 80:85257p.
- 48. Gastuche, M.C.; Brown, G.; Mortland, M.M. <u>Clay Miner.</u> 1967, 7, 177.
- 49. Brown, G.; Gastuche, M.C. Clay Miner. 1967, 7, 193.
- 50. Brindley, G.W.; Kikkawa, S. Amer. Mineral., 1979, 64, 836.
- 51. Miyata, S. Clays Clay Miner. 1975, 23, 369.
- 52. Miyata, S.; Okada, A. Clays Clay Miner. 1977, 25, 14.
- 53. Miyata, S.; Hirose, T. <u>Clays Clay Miner.</u> 1978, <u>26</u>, 441.
- 54. Miyata, S. Clays Clay Miner. 1980, 28, 50.
- 55. Hashi, K.; Kikkawa, S.; Koizumi, M. Clays Clay Miner. 1983, 31, 152.
- 56. Kruissink, E.C.; Alzamora, L.E.; Orr, S.; Doesburg, E.B.M.; van Reijen, L.L.; Ross, J.R.H.; van Veen, G. "Preparation of Catalysts II"; Delmon, B.; Grange, P.; Jacobs, P.A.; Poncelet, G., eds, Elsevier, Amsterdam, 1979, 143.
- 57. Kruissink, E.C.; van Reijen, L.L.; Ross, J.R.H. J. Chem. Soc., Faraday Trans. I 1981, 77, 649.
- 58. Puxley, D.C.; Kitchener, I.J.; Komodromos, C.; Parkyns, N.D. "Preparation of Catalysts III"; Poncelet, G.; Grange, P.; Jacobs, P.A., eds, Elsevier, Amsterdam, 1983, 237.

- 59. Huheey, J.E. "Inorganic Chemistry", 2nd ed.; Harper and Row, New York, 1978, 70.
- 60. Rouxhet, P.G.; Taylor, H.F.W. Chimia 1969, 23, 480.
- 61. Butler, F.G.; Dent-Glasser, L.S.; Taylor, H.F.W. <u>J.</u> Amer. Ceram. Soc. **1959**, <u>42</u>, 121.
- 62. "Handbook of Chemistry and Physics", 58th ed., Weast, R.C., ed., CRC Press, Cleveland, 1977.
- 63. Dosch, W.; zur Strassen, H. Zement-Kalk-Gips 1967, 20, 392.
- 64. Miyata, S.; Takata, M.; Okada, A. Ger. Offen. 2,222,473; Chem. Abstr. 1974, 81:54438q.
- 65. Miyata, S.; Kuroda, M. U.S. Patent 4,299,759.
- 66. Miyata, S.; Kuroda, M. Ger. Offen. 2,950,489; Chem. Abstr. 19XX, 93:96250a.
- 67. Ross, J.R.H. "Specialist Periodical Reports.
 Catalysis"; Royal Society of Chemistry, London, 1985,
 7, 1, and references within.
- 68. Alzamora, L.E., Ross, J.R.H.; Kruissink, E.C.; van Reijen, L.L. <u>J. Chem. Soc., Faraday Trans. I</u> 1981, 77, 665.
- 69. Busetto, C; Del Piero, G.; Manara, G. J. Catal. 1984, 85, 260, and references within.
- 70. Reichle, W.T. U.S. Patent 4,458,026.
- 71. Reichle, W.T. J. Catal. 1985, 94, 547.
- 72. McKillop, A.; Young, D.W. Synthesis 1979, 401.
- 73. Akelah, A.; Sherrington, D.C. Chem. Rev. 1981, 81, 557.
- 74. McKillop, A.; Young, D.W. synthesis 1979, 481.
- 75. Whitehurst, D.D. Chemtech 1986, 44.
- 76. Helfferich, F. "Ion Exchange"; McGraw-Hill, New York, 1962.
- 77. Gordon, M.; DePamphilis, M.L.; Griffin, C.E. <u>J. Org.</u> <u>Chem.</u> 1963, 28, 698.
- 78. Borders, C.L.; MacDonell, D.L.; Chambers, J.L. <u>J. Org.</u> <u>Chem.</u> 1972, <u>37</u>, 3549.

- 79. Cainelli, G.; Manescalchi, F.; Panunzio, M. Synthesis 1976, 472.
- 80. Miller, J.M.; So, K.H.; Clark, H. <u>J. Chem. Soc., Chem. Comm.</u> 1978, 466.
- 81. Hodge, P.; Sherrington, D.C. "Polymer-Supported Reactions in Organic Synthesis"; Wiley, New York, 1986, 92.
- 82. Cainelli, G.; Manescalchi, F. Synthesis 1979, 141.
- 83. Gelbard, G.; Colonna, S. Synthesis 1977, 113.
- 84. Cainelli, G.; Manescalchi, F. Synthesis 1975, 723.
- 85. Shimo, K.; Wakamatsu, S. J. Org. Chem. 1963, 28, 504.
- 86. Manescalchi, F.; Orena, M.; Savoia, D. Synthesis 1979, 445.
- 87. Regen, S.L. J. Amer. Chem. Soc. 1975, 95, 5956.
- 88. Regen, S.L. Angew. Chem. Int. Ed. Eng. 1979, 18, 421, and references within.
- 89. Starks, C.M. J. Amer. Chem. Soc. 1971, 93, 195.
- 90. Starks, C.M.; Liotta, C. "Phase Transfer Catalysis: Principles and Techniques"; Academic Press, New York, 1978.
- 91. Dehmlow, E.V. Angew. Chem. Int. Ed. Eng. 1977, 16, 493, and references within.
- 92. Tundo, P.; Venturello, P. <u>J. Amer. Chem. Soc.</u> **1979**, <u>101</u>, 6606.
- 93. Tundo, P.; Venturello, P.; Angeletti, E. <u>J. Amer.</u> Chem. Soc. 1982, <u>104</u>, 6551.
- 94. Kadkhodayan, A.; Pinnavaia, T.J. <u>J. Mol. Catal.</u> 1983 21, 109.
- 95. Cinquini, M.; Colonna, S.; Montanari, F.; Tundo, P. J. Chem. Soc. Chem. Comm. 1976, 392.
- 96. Halasz, I.; Vogtel, P. Angew. Chem. Int. Ed. Eng., 1986, 19, 24.
- 97. Tundo, P. J. Chem. Soc. Chem. Comm. 1977, 641.
- 98. Monsef-Mirzai, P.; McWhinnie, W.R. <u>Inorg. Chim. Acta</u> 1981, <u>52</u>, 211.

- 99. Kadkhodayan, A., Ph.D. Thesis, Michigan State University, 1983.
- 100. "Powder X-ray Diffraction File, Inorganic Phases", JCPDS-International Centre for Diffraction Data, Swarthmore, PA, 1983.
- 101. Serna, C.J.; Rendon, J.L.; Iglesias, J.E. <u>Clays Clay</u> <u>Miner.</u> 1982, 30, 180.
- 102. Landau, S.D., Ph.D. Thesis, Michigan State University, 1984.
- 103. McBain, J.W.; Bakr, A.M. <u>J. Amer. Chem. Soc.</u> **1926**, 48, 690.
- 104. Yoon, R.H.; Salman, T. in "Colloid and Interface Science, Vol. III", Kuker, M., ed; Academic Press, New York, 1976, 233.
- 105. Clementz, D.M.; Pinnavaia, T.J.; Mortland, M.M. <u>J.</u> Phys. Chem. **1973**, 77, 196.
- 106. McBride, M.B.; Pinnavaia, T.J.; Mortland, M.M. <u>Am.</u> <u>Mineral.</u> 1975, <u>60</u>, 66.
- 107. McBride, M.B. J. Phys. Chem. 1976, 80, 196.
- 108. Quayle, W.H.; Pinnavaia, T.J. <u>Inorg. Chem.</u> **1979**, <u>18</u>, 10.
- 109. Sachs, F.; LaTorre, R. <u>Biophys. Journal</u> **1974**, <u>14</u>, 316.
- 110. Burba, J.L. III, U.S. Patent 4,348,295.
- 111. Pinnavaia, T.J., private communication.
- 112. Atkins, P.W. "Physical Chemistry", W.H. Freeman, San Francisco, 1978.
- 113. Hine, J.; Thomas, C.H.; Ehrenson, S.J. <u>J. Amer. Chem.</u> Soc. **1955**, 77, 3886.
- 114. Evans, A.G.; Hamann, S.D. <u>Trans. Farad. Soc.</u> 1951, 47, 25.
- 115. Young, D.M.; Crowell, A.D. "Physical Adsorption of Gases", Butterworths, London, 1962, and references within.
- 116. Joyner, L.G.; Emmett, P.H. <u>J. Amer. Chem. Soc.</u> 1948, <u>70</u>, 2353.

- 117. Emmett, P.H.; Brunauer, S. <u>J. Amer. Chem. Soc.</u> **1937**, 59, 1553.
- 118. Houtepen, C.J.M.; Stein, H.N. <u>J. Coll. Int. Sci.</u> 1976, 56, 370.
- 119. Clark, A. "The Chemisorptive Bond", Academic Press, New York, 1974.
- 120. Hayward, D.O.; Trapnell, B.M.W. "Chemisorption", 2nd ed., Butterworths, Washington, D.C., 1964, and references within.
- 121. Cusumano, J.A.; Low, M.J.D. J. Catal. 1971, 23, 214.
- 122. Little, L.H.; Kiselev, A.V.; Lygin, V.I. "Infrared Spectra of Adsorbed Species", Academic Press, London, 1966.